

Research Article

Technoeconomic Analysis of a Wind Power Generation System and Wind Resource Mapping Using GIS Tools: The Case of Twelve Locations in the Commune of Evodoula, Cameroon

Vincent De Paul Igor Essouma Koung ^{1,2}, Francis Daniel Menga,³ Beguide Bonoma,^{4,5} Jean Luc Nsouandele,⁶ and Ruben Martin Mouangue ^{7,8}

¹Department of Physics, Faculty of Sciences, University of Yaounde I, P.O. Box 812, Yaounde, Cameroon

²Laboratory of Energy and Environmental, University of Yaounde I, Yaounde, Cameroon

³National Committee for Development of Technologies, Ministry of Scientific Research and Innovation, P.O. Box 1457, Yaounde, Cameroon

⁴Department of Physics, Higher Teacher's Training College, University of Yaounde I, P.O. Box 47, Yaounde, Cameroon

⁵Laboratory of Applied Physics, University of Yaounde I, Yaounde, Cameroon

⁶Department of Renewable Energy, National Advanced School of Engineering of Maroua, University of Maroua, P.O. Box 46, Maroua, Cameroon

⁷Department of Energy Engineering, University Institute of Technology, University of Ngaoundere, P.O. Box 455, Ngaoundere, Cameroon

⁸Laboratory of Analysis of Simulation and Testing, University of Ngaoundere, Ngaoundere, Cameroon

Correspondence should be addressed to Vincent De Paul Igor Essouma Koung; v_essouma@yahoo.com

Received 28 April 2023; Revised 8 January 2024; Accepted 30 January 2024; Published 2 April 2024

Academic Editor: Ayman Al-Quraan

Copyright © 2024 Vincent De Paul Igor Essouma Koung et al. This is an open access article distributed under the Creative Commons Attribution License, which permits unrestricted use, distribution, and reproduction in any medium, provided the original work is properly cited.

This paper performs a technoeconomic analysis of the wind power potential and evaluates the cost of wind power generation in Evodoula, comparing two methods, the conventional method and the uncertainty method based on a comparative spatiotemporal approach using the geographic information system (GIS) software tool. This study is based on satellite wind data measured at 10 m above ground level (AGL) over a 40-year period (1980-2019), by the meteorological service NASA (National Aeronautics and Space Administration)/Goddard Space Flight Center (GSFC). The main objectives are to obtain an appropriate design for a proven optimal location and to assess the viability of wind power at Evodoula. For this type of study, there is little literature available. The optimization of an onshore wind farm and deployment in the wind energy development interest area (ZIDEE) is carried out to obtain a minimum and parsimonious discounted cost production unitary (CPU) of the electricity produced. The results showed that in Okok, a location with a large energy deficit, an onshore wind farm with an electricity generation capacity of 12.5 MW with 5 NORDEX N100-2.5MW wind turbines would have a total energy production (TEP) of about 64.0254825 TWh and a selling price of electricity that would be 0.0034 CAD\$/kWh, which is very low compared to the utility price (about 98% cheaper). The total cost of the wind farm would be about \$11 million, with a net present cost of about \$218 million. The annual profit generated by the wind farm would be over \$6 billion. The return on investment (ROI) of the project is estimated at 2880.882%. The constructed onshore wind farm would avoid CO₂ emission at over 11 MtCO_{2,eq}/year as the energy generated is from the atmosphere. The wind farm would realize an average annual cash flow estimated at nearly \$30 million after 20 years of operation. These savings would allow the installation of CO₂ capture systems in conventional power plants. In addition, the analysis of uncertainties and risks was identified and quantified to estimate the confidence levels of the project development results. The risks have been assessed, and we recommend that the total uncertainty of the project is around 15%. The energy values in P_{75} and P_{90} are 10.08% and 19.22%, respectively, lower than the energy value in P_{50} of 11.60 GWh/An. Finally, the main policy recommendations for an inclusive design process are highlighted. The contribution of this study is to assist policy makers in making appropriate decisions in the development and implementation of energy and environmental policy in Cameroon and in many continental areas.

1. Introduction

Energy, a pole to animate economic attractiveness, is an indispensable factor for a new economic dynamic. Energy in Cameroon is characterized by an insufficient supply of electrical energy. Thus, it is difficult to meet the demand for energy throughout the territory. We note here that the most vulnerable are those who live in rural areas or isolated sites or a large number of individuals are devoid of any energy supply. However, we note that the existence of potential deposits of natural gas, hydroelectric energy, and other renewable energy sources (solar, hydraulic, wind, biomass, and geothermal) is very important. One of Cameroon's current concerns is the development of new energy sources to offset the country's current energy deficit. Consequently, the move towards full integration in Cameroon of renewable energies is increasingly being considered with the aim of optimizing considerably and sustainably its producible. Seen through this lens, the energy challenges in terms of the cost of electricity production are important in several countries in the world, including Saudi Arabia, Turkey, Ethiopia, Pakistan, Kuwait, Egypt, and Cameroon, in particular. According to some recent studies presented by [1–3], it is clear that Cameroon also has vast renewable resource potential, including the prevalence of wind energy, for electricity generation. Therefore, it is useful to do an assessment of wind energy prospects for the country. Although a number of initiatives are already underway to assess the potential use of wind energy locally, a number of work remain to be done, including in light of recent technological developments. An assessment of wind energy involves a consolidated analysis of the potential wind resources of a specific location. This starts by understanding the general wind patterns of the area and moves towards the collection and analysis of wind speed data. However, due to the lack of a reliable and accurate Cameroonian wind atlas, further studies on the evaluation of wind energy in Cameroon are necessary and continue to this day. The results of the study presented by [4, 5] estimate that Cameroon has good wind potential. Indeed, in many studies, it has been mentioned that in Cameroon, there are many potential suitable sites that have a very good wind potential, which makes it possible to consider the installation of wind farms in the country. Recently, many research teams around the world have studied different methods of energy efficiency and explored robust techniques to effectively predict wind energy production and energy costs [6]. In their work, entitled estimation and technoeconomic analysis of the wind potential in northern Cameroon, an evaluation and a technoeconomic study were carried out in this article in three cities of Cameroon on the wind potential. The results showed that the cost per kilowatt-hour of electricity produced varies by city, a cost of \$0.347 in Ngaoundere, \$0.305 in Garoua, and \$0.297 in Maroua, with corresponding energy production of at least 31536 MWh annually and 11510.640 GWh over 20 years, 29541 MWh annually and 10782.465 GWh over 20 years, and 21376 MWh annually and 7802.240 GWh over 20 years in the cities of Maroua, Garoua, and Ngaoundere, respectively. Installing six NORDEX-type wind turbines will help

solve the energy deficit problem in Northern Cameroon, which has a good wind speed. The authors concluded that the NORDEX (N43/600) wind turbine with a height of 60 m is better than the other five. Kidmo et al. [7] proposed a study on wind energy for electricity generation in the far north region of Cameroon. In this article, 28-year (1985–2013) wind speed data measured at 10 m above ground level (AGL) are analyzed statistically using the Weibull distribution. The results showed that the exposed peaks in the range of 100 to 300 m AGL fall into class 3 or higher of the International Wind Classification System and are considered suitable for most wind turbine applications (WT). An evaluation of the performance of five commercial WT (50 to 2000 kW) for electricity generation is then carried out by calculating their respective capacity, power, and energy factors. The authors concluded that among the WTs explored, YDF-1500-87 (1500 kW) appears to be the attractive option, with the highest capacity factor and lowest energy cost. In addition, COE is observed to be lower during the dry season than during the rainy season, which begins in late July and ends around mid-October. On average, the energy costs using the P-15-50 are 40.55 and 53.12 XAF/kWh, respectively, around the boroughs of Kousseri and Maroua. As for YDF-1500-87, the costs per kilowatt-hour of electricity produced are 25.53 and 33.99 XAF/kWh around the boroughs of Kousseri and Maroua, in that order. In another similar study [8], the potential of wind energy at the top of exposed ridges in the mountains surrounding the city of Maroua was assessed. In this work, 28 years of wind data, measured at 10 m above ground level (AGL), from the Maroua weather station are used. The aim of this study is to estimate the cost of wind electricity using six types of wind turbines (50 to 2000 kW). The results showed that the hill-tops in the range of 150 to 350 m AGL in increments of 50 falls into class 3 or higher of the International Wind Classification System and are considered suitable for exceptional wind applications. A comparative technical and economic assessment of the wind turbines at the top of the considered hills has been taken into account. The results showed that the lowest costs per kilowatt-hour are achieved using the YDF-1500-87 turbine (1500 kW), while the highest costs are provided by P-25-100 (90 kW). The lowest costs (USD) per kilowatt-hour of electricity produced range from a minimum of 0.0294 at the top of the hills at 350 m AGL to a maximum of 0.0366 at the top of the hills at 150 m AGL, with corresponding energy production of 6125 and 4932 MWh, respectively. In addition, the corresponding capacity factor values are 38.05% at 150 m AGL peaks and 47.26% at 350 m AGL peaks. In addition, Enercon E82-2000 wind turbines (2000 kW) provide the lowest cost of wind power and are recommended for large communities. The average P-15-50 (50 kW) wind turbine, despite the best coefficient factors (39.29% and 48.85% at 150 m and 350 m AGL peaks, in that order), generates electricity at a higher average cost per kilowatt-hour of 0.0557 USD and 0.0440 at 150 m and 350 m AGL, respectively. The P-15-50 is considered a more advantageous option for off-grid electrification of small, remote communities [2]. In the technical and economic potential of the development

of electric wind pumping systems in the Northern region of Cameroon, a performance of the selected wind turbines is examined as well as the costs of wind electricity. Four wind turbines (WT), represented by WT1, WT2, WT3, and WT4, with a nominal capacity of 20 kW and a 30 m tower, for the eight sites were considered to simulate output power and energy output. The results showed that the Figuil site shows the best combination of CF and energy cost, regardless of the WT used followed by the Basheo and Pitoa sites. The Poli site has the worst CF and COE. For the Figuil site, the CF is equal to 15.14% and the COE is 93.82 XAF/kWh using WT1. For WT2, CF and COE are 11.15% and 139.54 XAF/kWh, respectively, while for WT3, the corresponding values are 7.11% and 246.57 XAF/kWh, in that order. WT4 has the worst performance, with a CF of 5.82% and a COE of 301.05 XAF/kWh. The authors concluded that the selection of the WT for low-wind sites would require a combination of the wind resource at the WT site and WT features such as interlocking and nominal wind speeds to take full advantage of energy and water costs produced. A similar study was conducted by [3] to analyze the potential use of wind electric pumping for water distribution in off-grid locations in the North Region Cameroon (NRoC), using ground measured data as well as data derived from long-term satellites. The results showed that the capacity factor (CF) and energy cost (COE) values use WT1, WT2, WT3, WT4, and WT5, for the eight sites selected. The Figuil site shows the best combination of CF and COE, regardless of the WT used, followed by the Basheo and Pitoa sites. The Poli site has the worst CF and COE. For the Figuil site, the CF is equal to 26.52% and the COE is 49.05 XAF/kWh using WT1. WT5 shows the worst performance, with a CF of 7.11% and a COE of 420.17 XAF/kWh. The authors concluded that WT5 has the worst performance among the WT. Gaddada and Kodicherla [9] studied the potential for wind energy and estimated the costs of wind energy conversion systems (WECS) for electricity generation in the eight selected locations in the Tigray Region (Ethiopia). In this study, three commercial wind turbines, namely, POLARIS P15-50, POLARIS P50-500, and VESTAS V110-2.0, were selected as large-scale wind energy conversion systems (WECS) for the technical and economic evaluation of electricity production in eight selected locations in the Tigray Region of Ethiopia. The results showed that the highest capacity factor is obtained at 7.873% using VESTAS V110-2.0 at Mekele, while the lowest at 0.002% using POLARIS P15-50 at Shire. The average minimum cost per kilowatt-hour obtained in Mekele was \$0.0011/kWh with VESTAS V110-2.0, while the highest average cost was \$7.3148/kWh with POLARIS P15-50 in Shire. Further, the authors suggested that Atsbi, Chercher, Mekele, and Senkata were the most cost-effective for electrical and mechanical applications than the cost of hydropower in the country. Gungor et al. [10] analyzed wind potential and Weibull parameter estimation methods: a case study in Turkey. In the present study, the authors investigated the suitability of four different numerical methods for predicting Weibull distribution parameters using wind speed information from Izmir in Turkey. In addition, an economic analysis

to represent the probability of installing wind turbines between 800 and 4200 kW on the site was also carried out. The results demonstrate that the standard deviation-mean wind speed method is the most appropriate. In addition, the estimated cost of wind electricity was calculated at 0.0111 USD/kWh obtained with the Enercon E-82 E2 model wind turbine. Annual energy production ranged from 3354.2651 MWh with Enercon E-48 model wind turbine to 20519.9378 MWh with the Enercon E-126 EP4 model wind turbine. Adnan et al. [11] conducted a technoeconomic analysis for wind power generation: a case study from Pakistan. In this feasibility study, wind resource assessment (WRA) of Umerkot and Sujawal districts located in Sindh provinces of Pakistan was analyzed by analyzing average wind speeds, estimated Weibull parameters, calculation power, and energy densities for different heights of selected wind turbines. In this work, wind speed data for 2016 and 2018 (with a resolution of 10 min), the highest values of power and energy densities for Sujawal are 414.18 W/m² and 3628.22 kWh/m²/An, and for Umerkot, these values are 303.86 W/m² and 2661.81 kWh/m²/An. The results indicated that the use of NORDEX N90/2500 wind turbines is very beneficial for Umerkot and Sujawal. The associated energy costs are \$0.074/kWh and \$0.056/kWh, respectively, and the payback period is estimated at around 7 years with a project life of 20 years. The authors concluded that the Umerkot and Sujawal sites are suitable for power generation. Kaboli and Nazmabadi [12] investigated a research study based on a technoeconomic analysis of the feasibility of implementing wind power generation in Kuwait with power generation of 105 MW based on 50 wind turbines. The study focused on three main axes of analysis and numerical modeling using the RETScreen software tool. The results are used to estimate that the price of energy would be \$0.053/kWh for a power generation capacity of 105 MWh based on an initial cost of \$168 million and an O&M of 5 million dollars for 214,000 MWh of electricity exported to the grid. Abdelrahman et al. [13] examined a technoeconomic analysis to develop the first wind farm in the Egyptian western desert at Elkharga Oasis. This paper presents a comprehensive analysis of the characteristics of wind potential at Elkharga Oasis in Egypt, based on a real wind measurement campaign taken by a meteorological mast at two levels in height of 10 and 25 m, respectively. The results showed that the LCOE of the V162 turbine has the lowest value, ranging from \$28.1517 to \$28.4104/MWh, depending on the turbine distancing. However, the V110 had the highest LCOE range of \$33.99 to \$34.2861/MWh. The authors concluded, based on these results and discussions, that the best wind turbines at the Elkharga site can be ranked in decent order as V162, V150, and V110. Although there are a number of studies in the open literature that have discussed the wind potential of certain (regions) areas in Cameroon [1–8, 14–19], as these studies have shown different results, the determination, modification, proposal, and development of optimal and optimized methods for technoeconomic assessments of wind potential and the cost of energy produced are continuing. However, a technoeconomic analysis combined with the development of wind resource maps, in the occurrence of

maps of wind speed, energy produced, and cost of production generated using GIS software (geographic information system) by following an applied geographic approach, is necessary. This software, which was developed by Environmental Systems Research Institute, Inc. (Esri), is a widely used tool for wind site characterization. Over the past two decades, a number of works have been carried out to assess the wind potential in several regions of the world. GIS-based studies include Feng et al. [20], Baseer et al. [21], Xu et al. [22], Atici et al. [23], Latinopoulos and Kechagia [24], Siyal et al. [25], Omिताomu et al. [26], Ali et al. [27], Van Haaren and Fthenakis [28], Sliz-Szkliniarz and Vogt [29], Hossain et al. [30], Janke [31], Aydin et al. [32], and Baban and Parry [33]. A recent study on detailed economic analysis was conducted to investigate the feasibility of offshore wind power in the Persian Gulf region using uncertainty analysis and GIS [34]. The authors used a Monte Carlo simulation which was used for the long-term simulation of the wind field and wind turbine production. The performance of this simulation remains to be demonstrated, as it strongly depends on a number of tests to be carried out to identify the appropriate analysis method. Other work has dealt with the characterization of sites by statistical analysis methods [35–38]. Or it is noted that studies on the technoeconomic analysis of a wind energy production system and the mapping of wind resources using GIS software tools are little known. That said, in order to show this incompleteness in the knowledge of wind potential assessment, technoeconomic analysis, environmental impact study, financial analysis, mapping of wind resources, uncertainties, and risks of a wind project, this complete research work proposed on this paper highlights the interest of the combinations of horizontal and vertical interpolation techniques for the applications of wind resource mapping using GIS software tools for which certain wind potentials extractable technically exploitable are unknown or difficult to measure directly on ideal sites. We develop a new method for modeling, optimizing, and simulating a parameterized power performance model of a wind power generation system through a semiempirical approach. This model has the advantage of making it possible to study the performance of an electricity production system both hourly and monthly. In addition, we propose a new modified energy factor method (MEPFM), on the one hand, to correctly estimate the wind power density available on the twelve locations considered in the EEZ at Evodoula. On the other hand, the impact of the adjusted (interpolated) power per unit of exploitable surface as a function of a modulation factor “ a ” (which can be considered as an indicator of wind site performance) with regard to the results which are then adjusted to a GIS using an optimal 2D horizontal spatial interpolation method weighted by the inverse of the distance (IDW) for an evaluation of the energy produced annually and the unit cost of electricity production generated by the twelve sites considered as a function of conventional methods and uncertainty is shown. Therefore, the translation of this research into practical application must consider wind power estimation to assess the performance and efficiency of wind power generation by collecting, analyzing, and modeling satellite data, reanalyses of long-term wind speeds,

installed annual generation capacity, operation of wind turbines, and wind energy production. An environmental impact study to assess the environmental benefits of implementing wind energy, the economic and technical aspects of wind energy installation, has never been presented collectively. The main objectives of the current research are to evaluate the onshore wind energy production combined with the evaluation of the production cost of the generated wind electricity using the present value of costs (PVC) method at the assistance of five models of wind turbines (1650 to 5600 kW) for the twelve locations selected, namely, Evodoula, Etok, Ekol, Ayos, Okok, Nkolkougda, Ngobo, Ntouda, Nkolmeyos II, Nkotabel, Nkolabang, and Nloundou. The article offered five different wind turbine models of VESTAS V162-5.6MW, VESTAS V150-5.6MW, VESTAS V82-1.65MW, NORDEX N100-2.5MW, and NORDEX N90-2.5MW with their different data characteristic techniques. These wind turbines can be installed at heights of 59 m, 75 m, 80 m, 100 m, 105 m, 108 m, 119 m, 125 m, 148 m, 149 m, and 166 m. The working document drawn up is a real decision-making tool and will serve as a reference for developing countries with similar renewable resources for the production of electricity suitable for the sites studied. The main contributions of this paper are therefore summarized below:

- (i) Estimates of the Weibull distribution parameters for the selected locations
- (ii) Estimates of wind power density and wind energy density for selected locations
- (iii) Recommendation of wind turbines for the selected locations
- (iv) Recommendation of a height of interest of 100 m for installation and ideal layout configuration of wind turbines adapted to the proven optimal location
- (v) Assessments of the annual wind energy production and estimates of the production cost of the electricity produced for the selected sites
- (vi) Selection of the most practical wind turbine determined on the basis of the scalable adaptability performance factor “ a ” and the wind turbine that produces the lowest cost of energy produced
- (vii) Calculation of the recovery of greenhouse gas (GHG) savings from the onshore wind farm in the proven optimal location
- (viii) Estimation of the financial return of the onshore wind farm of 12.5 MW composed of five wind turbines of the model chosen over 20 years on the aggregated surfaces at the proven optimal location
- (ix) Establish the mapping of wind speeds a 100 m below the ground (AGL) over the entire study period of the EEZ in Evodoula

- (x) Establish maps of annual energy production and cost production unitary based on conventional and uncertainty methods

Thus, in order to ensure the success of the wind power program, it is essential to carry out technoeconomic studies beforehand. This is the subject of the study presented on this paper, where as an example, we considered twelve locations in the exclusive economic zone (EEZ) of Evoudoula. With the evolution of wind technology and better management of all influencing factors, the cost of electrical energy produced by the exploitation of wind energy has dropped significantly in recent years in Cameroon. Compared to other sources (conventional and unconventional) of electricity production, electrical energy of wind origin is the most competitive, particularly when this energy is produced from onshore facilities and when operating conditions are favorable. But how much does the kilowatt-hour of electricity produced by a wind farm cost?

2. Presentation of the Study Area and the Data Used

2.1. Presentation of the Study Area. The commune of Evoudoula is located between 451662.66266328277-460933.39732 332056 North latitude and 740544.9642155031-759031.228 8344726 East longitude and covers an area of approximately 250 km². Evoudoula belongs to the formation known as the central plateau, and the rainfall is between 1300 mm and 1500 mm, and we note the existence of four seasons of unequal duration, namely, a short dry season (from May to mid-August), a long season of rain (mid-August to mid-November), a long dry season (from December to mid-March), and a short rainy season (from March to May), thus allowing two cycles of winds per year. It belongs to the humid equatorial zone; the temperatures here oscillate between 22°C and 32°C. On the pedological level, there is a great variety of soils based on structure and texture. The soils are mostly ferralitic, sandy-clayey, and hydromorphs in the lowlands found in places. The relief is very rugged, with high hills especially in the northern part of the town where rocky outcrops are encountered in most roads. The vegetation is that of the equatorial forest, degraded by the overexploitation of the soil to take into account the roughness. Table 1 presents the different details (metric coordinates, height, measurement period, data size, temporal resolution, actual altitude, and characteristic) of the twelve locations in the EEZ of Evoudoula presented at Figure 1.

2.2. Data Used. In this article, the choice fell on MERRA-2 reanalysis data produced by the National Aeronautics and Space Administration (NASA)/Goddard Space Flight Center (GSFC), because MERRA-2 has temporal and grid resolutions, respectively, of 1 hour and 0.5° × 0.625° in longitude and latitude which were used as the source of wind speed and direction data. Satellite data wind speed and direction in monthly format of the twelve locations in the EEZ of the municipality from Evoudoula are taken from NASA's open source database. These average monthly wind and

direction data have been recorded in the long term at a height of 10 m from the ground in the EEZ over a period of 40 years (quadridécadal) from January 01, 1980, to December 31, 2019. The data are available since 1980 and updated monthly. The zonal and southern wind components of MERRA-2 were processed at 10 m above the ground [39]. This is how these wind data were downloaded, preprocessed, and analyzed to perform a detailed analysis of the wind speed data of the twelve locations in the EEZ of Evoudoula on the one hand and to select an accurate method that gives a more accurate estimate of the Weibull distribution parameters (K and C) on the other hand. From the parameters of this distribution, the spatial distribution of the wind potential is then determined.

3. Materials and Methods

3.1. Materials. In this section, the materials used are presented below:

- (i) The downloaded raw meteorological data is saved as a CSV file and further processed with the Microsoft Excel 2016 program by clicking "upload to CSV." The raw data was downloaded and then statistically analyzed every twelve months of the year with the Excel software from the 2016 office pack
- (ii) Excel software from the 2016 pack records the monthly data for the entire site under study. Mean monthly data of winds and numerical directions are acquired from NASA from the MERRA-2 weather model over a period of 40 years (1980 to 2019) of the twelve selected locations in the EEZ under study (Table 1) of the municipality of Evoudoula. These data were collected and then statistically processed on a four-decade scale (period of 40 years). This data was analyzed for the twelve site-specific locations of the study area by the embedded Weibull spatial distribution "LOI.WEIBULL" in Excel 2016 through data statistics, monthly that have been calculated for each parameter to be established. Thus, the Excel 2016 software made it possible to draw our various curves
- (iii) The location map of my study area (Figure 1) is made using global geographical coordinates of UTM WGS 84 projection spatial reference in decimal degrees and then transformed into metric coordinates to establish a cartography of the site under study produced using the QGIS 3.8 software, which made it possible to vectorize the municipality of Evoudoula as well as its neighboring boundaries
- (iv) In addition, the QGIS 3.8 software made it possible to draw up the 2D topographic map of the municipality of Evoudoula and its surroundings (Figure 2), as well as the 3D topographic map of the municipality of Evoudoula (Figure 3)
- (v) The spatial analyst extension package ArcGIS 10.4.1 enabled the elaboration of mapping in terms of

TABLE 1: The details of the twelve locations selected in the EEZ of the commune of Evoudoula.

Locations	Metric coordinates (UTM WGS84)		Height (m)	NASA measurement period	Data size	Temporal resolution	Actual altitude (m)	Characteristic of the location
	Latitude UTM: Y (m)	Longitude UTM: X (m)						
Evoudoula	452607.098067673	744537.521317534	10 m above the ground	1 January 1980 to 31 December 2019	40 years	Monthly	589 m above sea level	Plain (medium altitude zone)
Ekol	454182.891094454	751878.244465815	10 m above the ground	1 January 1980 to 31 December 2019	40 years	Monthly	519 m above sea level	Plain (medium altitude zone)
Etok	452459.799885314	740132.704592087	10 m above the ground	1 January 1980 to 31 December 2019	40 years	Monthly	496 m above sea level	Plain (medium altitude zone)
Ayos	451956.998809024	753100.53509488	10 m above the ground	1 January 1980 to 31 December 2019	40 years	Monthly	560 m above sea level	Hill (high altitude area)
Okok	457317.584751385	749322.663855856	10 m above the ground	1 January 1980 to 31 December 2019	40 years	Monthly	504 m above sea level	Plain (low altitude area)
Nkolkougda	452662.378091507	746206.470127518	10 m above the ground	1 January 1980 to 31 December 2019	40 years	Monthly	533 m above sea level	Plain (medium altitude zone)
Ngobo	457409.03077657	747472.822646267	10 m above the ground	1 January 1980 to 31 December 2019	40 years	Monthly	501 m above sea level	Plain (low altitude area)
Ntouda	460288.012024404	745955.598386086	10 m above the ground	1 January 1980 to 31 December 2019	40 years	Monthly	503 m above sea level	Plain (low altitude area)
Nkolmeyos II	459653.393852223	738640.855404364	10 m above the ground	1 January 1980 to 31 December 2019	40 years	Monthly	476 m above sea level	Plain (low altitude area)
Nkotabel	456097.566936127	745583.793999193	10 m above the ground	1 January 1980 to 31 December 2019	40 years	Monthly	484 m above sea level	Plain (medium altitude zone)
Nkolabang	454133.234684029	738473.047031469	10 m above the ground	1 January 1980 to 31 December 2019	40 years	Monthly	476 m above sea level	Plain (low altitude area)
Nloudou	457309.11952975	736082.806740775	10 m above the ground	1 January 1980 to 31 December 2019	40 years	Monthly	519 m above sea level	Plain (low altitude area)

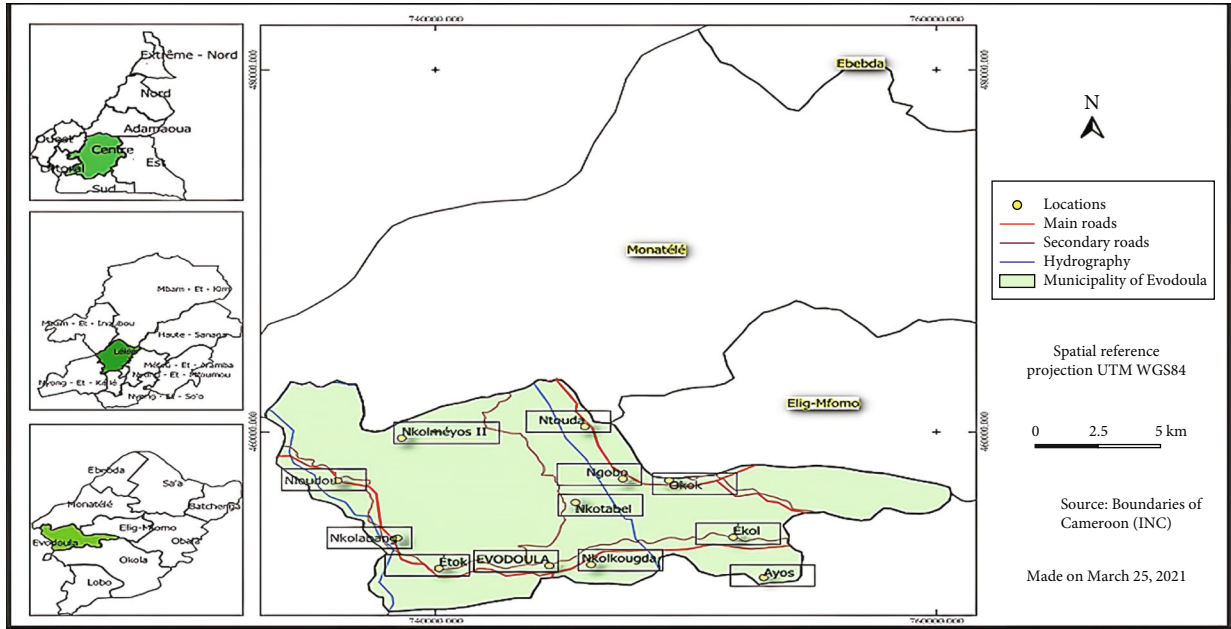


FIGURE 1: Map of the municipality of Evodoula and location of the locations selected with a view to delimit the EEZ on the one hand and the optimal selection of a place name for the location of the future onshore wind farm on the other hand.

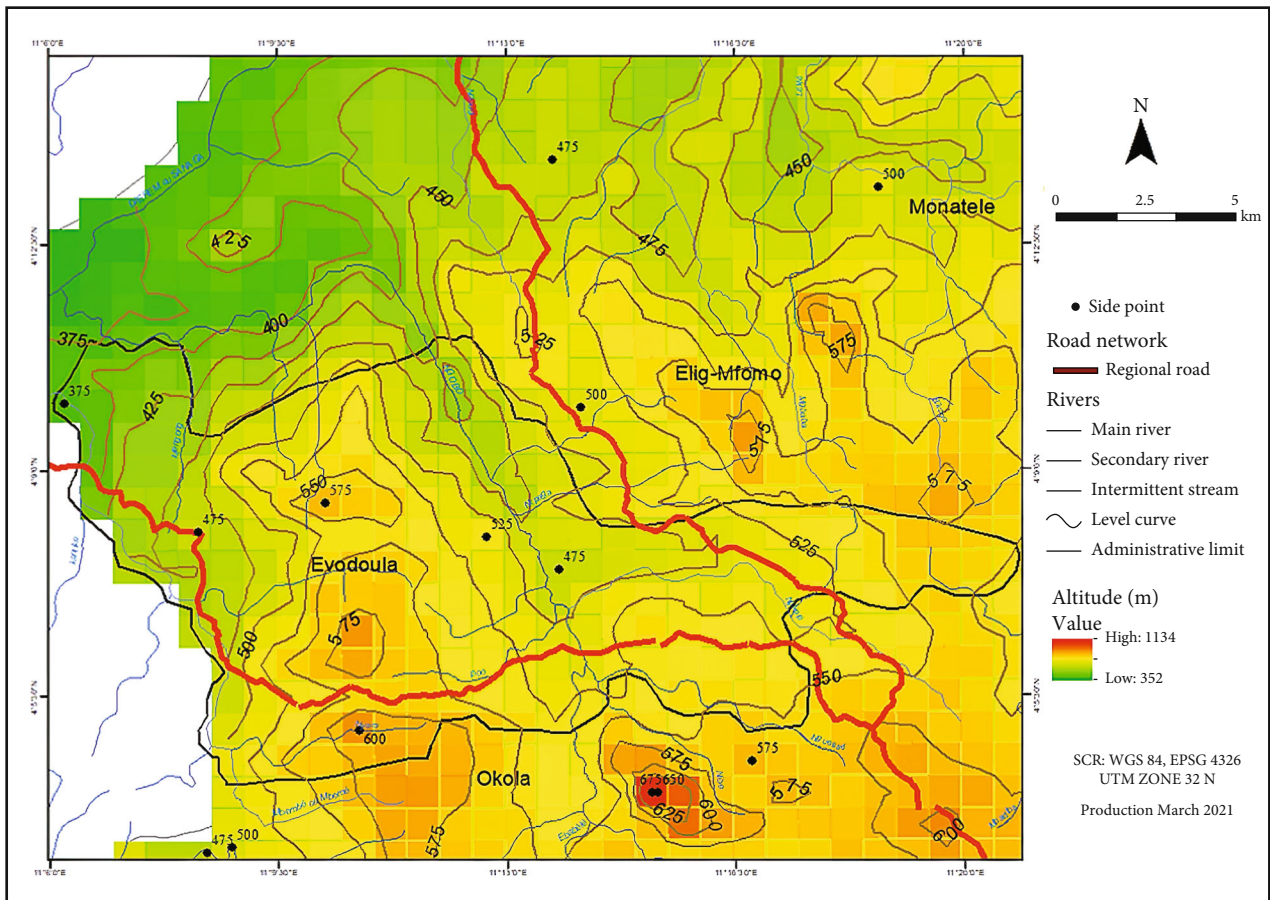


FIGURE 2: 2D topographic map of the municipality of Evodoula and periphery. On the map, the level curves at 25 m and the different altitudes of the plan area are highlighted, and then, a cartographic dressing is created on the map.

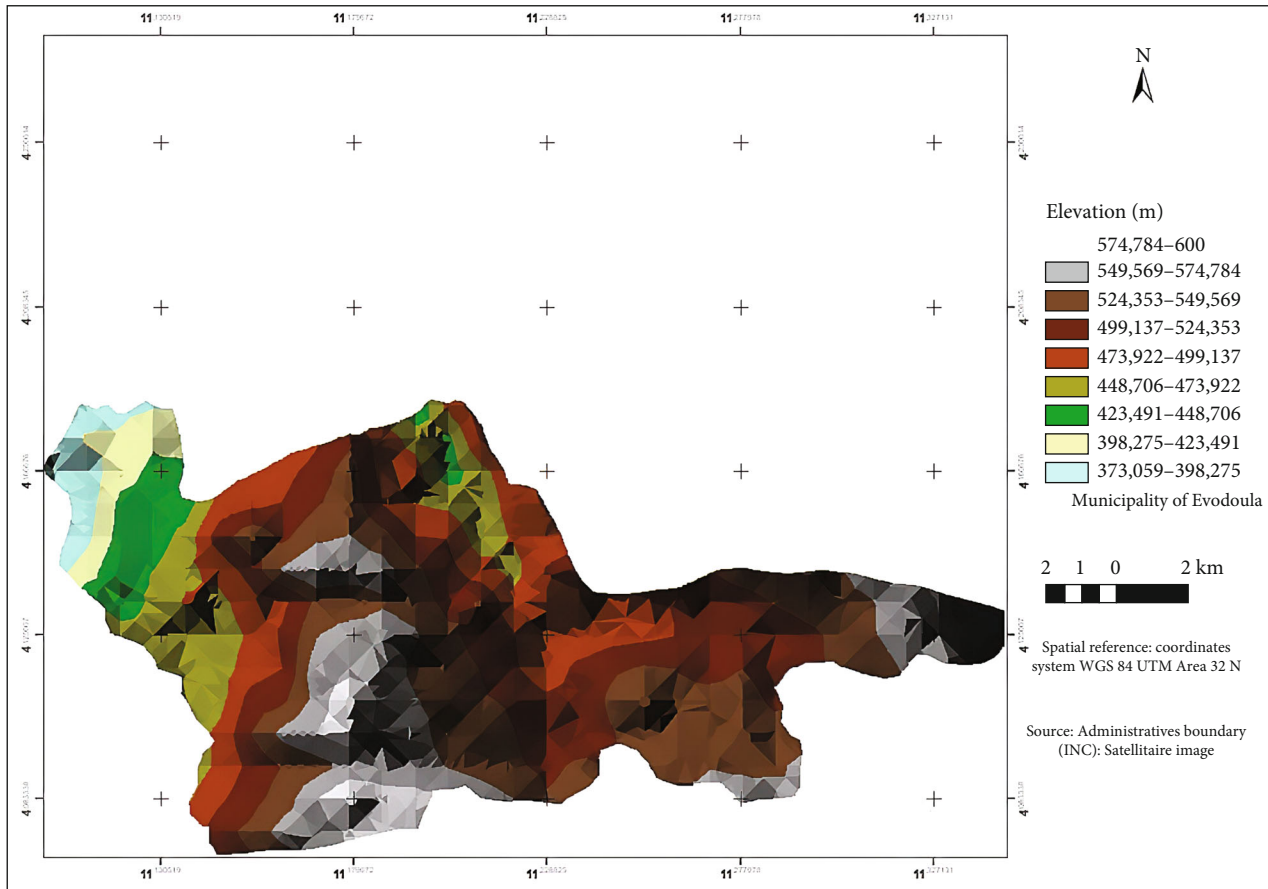


FIGURE 3: 3D topographic map of the municipality of Evodoula. On the map, the different real altitudes of the study area are highlighted. Elevations change with gray level.

wind speed, annual energy production, and cost production unitary in Evodoula EEZ at 100 m above ground level (AGL)

- (vi) Plotting the wind rose using wind direction data from the twelve locations in the EEZ of Evodoula 100 m above ground level (AGL) has been performed using Excel 2016 software

3.2. Detailed Research Methodology Adopted in This Work and Scope of the Study. The methodology developed to assess wind potentials is a set of sequential steps that incorporate the characteristics theoretical, geographic, technical, economic, and environmental aspects of the EEZ of Evodoula as well as the constraints of using wind energy. The following actions were carried out: initially, the optimal potential localities conducive to the installation of wind turbines were studied according to a comparison of the defined multicriteria analyses (conventional and uncertainty) reflecting a spatiotemporal approach combined with the use of a geographic information system (GIS). Second, the wind speed data sets measured by NASA weather service satellites were extrapolated vertically and interpolated horizontally to derive the surface of aggregated wind speed data at the rotor hub blade height. Moreover, the number of hours at full load or number of production hours at rated power (Nhepn) over

the entire study period (1980-2019) was estimated for five turbines of different powers on the basis of the distribution parameters of Weibull probability and power curves. Next, the layer of locations available for the construction of a wind farm was overlaid with a grid wrap on the layer of the number of hours of production at nominal power to determine the technical potential of wind energy in the location-say case studies. Finally, to assess the economic viability, the cost production unitary of electricity in the grid was estimated. The steps are shown in (Figure 4): (1) the evaluation methodology begins with measuring the wind for selected locations, (2) preprocessing of wind speeds and wind direction using Excel 2016 software, and (3) statistical description of wind speed data. The relationship between the wind at the hub of the wind turbine and the power delivered by the wind turbine is given by the power curve (see Section 3.3.9). But the problem is that the measurements are not taken exactly at the level of the hub of the future wind turbines, which is why the calculation of the wind potential begins with several stages of extrapolation of the initial wind measurements to ideal heights or heights of interest:

- (i) (4) The vertical extrapolation takes into account the fact that the measurement mast is generally lower in height than that of the hub of the wind turbines (see Section 3.3.3)

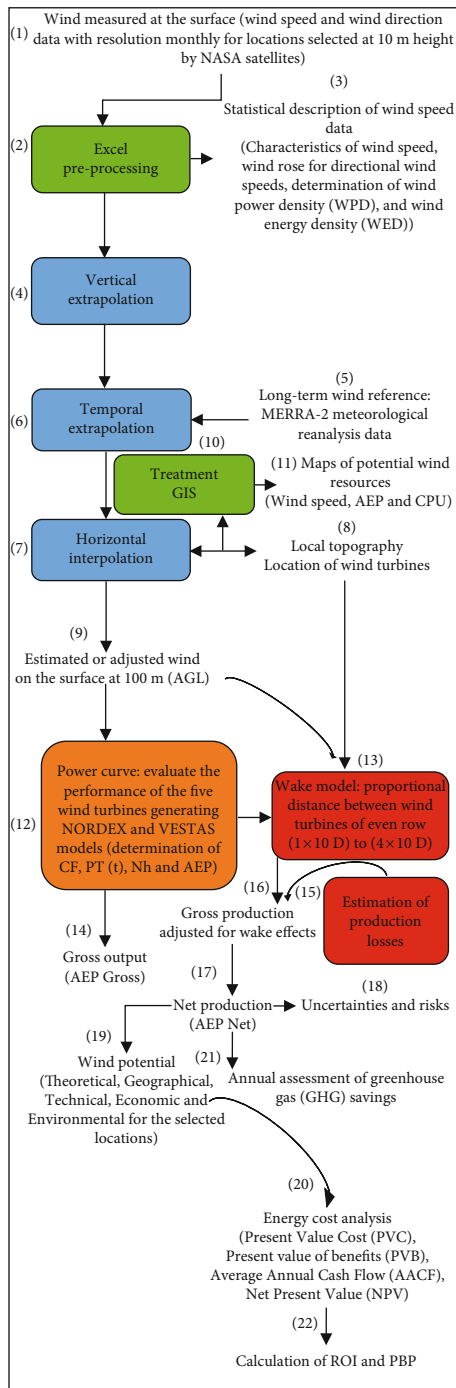


FIGURE 4: Synoptic diagram of the flowchart chain of research methodology for the assessment of wind potential. In green, the stages of preprocessing of the measured wind and GIS processing; in blue, the stages of extrapolation of the measured wind; in orange, the calculation of production from the wind thus estimated; in red, the stages to take into account the losses to be withdrawn from gross output.

(ii) (6) Temporal extrapolation makes it possible to take into account the fact that the measurements, which are carried out over a period of approximately one year, are not necessarily representative of an average

year, because of the interannual variability of the wind. (5) To do this, we use another set of wind data, available over a large number of years for a location close to the site, called the “long-term reference”

(iii) (7) The horizontal interpolation makes it possible to take into account the fact that the wind turbines will not be placed at the exact location of the mast but at a few tens or hundreds of meters. (8) For this, we rely on the topography of the site, and (10) the GIS processing according to the analysis approach is based on a spatial and ecological policy. (11) The locations of future wind turbines in the farm are shown in Section 3.3.5

During these wind extrapolation steps, the Weibull distribution is very often used to model the wind speed statistics (see Section 3.3.1). (9) This gives an estimated or adjusted wind at the right height, in the right places, taking into account the interannual variability of the wind. (12) The power curve of the wind turbines then makes it possible to calculate the gross production for this wind (see Section 3.3.10). (14) From this gross production, we must subtract the losses to obtain the net production. The first losses to be removed are the losses due to wake effects in a wind farm (13), that is to say the reduction of the wind arriving at a wind turbine due to the presence of other wind turbines upstream of the flow. These losses are linked to the geometry of the wind farm, to the wind statistics (with great importance of the direction), and to the power curve of the wind turbines. (15) The other losses or loss factors are linked to the production activity and are systematically estimated by standard error percentages. (16) Gross production adjusted for wake effects is applied to the wake model and estimated production losses. (17) The net output obtained by the calculations is taken as the median of the possible outcomes and is called P_{50} . (18) The risk in the economic sense is evaluated by the uncertainties on this value of the potential (see Section 3.3.11). The uncertainties relate to the following:

- (i) The wind (on the measurement itself and on each of the extrapolation steps)
- (ii) Estimation of production losses (detailed above)

They are estimated, globally or for each stage, by percentages (generally standard). (19) The evaluation of the multifaceted wind potentials is sought to be calculated. (20) The analysis of the energy costs is to be determined. (21) Evaluation of the reduction in greenhouse gas (GHG) savings is to be advocated. (22) ROI and PBP are indicators that measure the profitability and payback time of a project, respectively. The corrected power law model is used to determine wind speeds at different heights. A technical and economic evaluation was made for the aggregate production of electricity using wind turbines on the locations studied. To summarize our study, we propose an organization chart which was carried out for the aggregated production of electricity using wind mills with the studied places. The overview of the

approach of each workflow given in the (Figure 4) is to illustrate the analysis procedure of this study.

3.3. Methods

3.3.1. Modeling the Distribution of Wind Frequencies. The most widely used model for modeling the distribution of wind speeds is the Weibull probability distribution. This was chosen in this work to model the distribution of wind speeds. The choice of the Weibull function is motivated by site data spanning 40 years. The Weibull distribution parameters K and C are calculated based on this data. This noncumulative distribution (PDF) is expressed mathematically by the relation formulated with the following equation [18, 37, 38, 40–43].

$$f(V_{\text{Lat,Lon}}) = \left(\frac{K}{C}\right) \cdot \left(\frac{V_{\text{Lat,Lon}}}{C}\right)^{K-1} \cdot \exp\left[-\left(\frac{V_{\text{Lat,Lon}}}{C}\right)^K\right], V_{\text{Lat,Lon}} > 0, K > 0, C > 0, \quad (1)$$

where $V_{\text{Lat,Lon}}$ (m/s) represents the wind speed at a defined latitude and longitude, $f(V_{\text{Lat,Lon}})$ represents the probability of observation or occurrence of the wind speed $V_{\text{Lat,Lon}}$, C is the Weibull scale parameter which informs the quality wind (m/s), and K is the Weibull shape parameter which indicates the shape of the frequency distribution (dimensionless).

The corresponding cumulative distribution function (CDF) is given by the mathematical relation defined in

$$F(V_{\text{Lat,Lon}}) = \int f(V_{\text{Lat,Lon}})dV = 1 - \exp\left[-\left(\frac{V_{\text{Lat,Lon}}}{C}\right)^K\right], V_{\text{Lat,Lon}} > 0. \quad (2)$$

3.3.2. Weibull Parameter Estimation Methods. In this article, a probability distribution function is used to model the wind speed distributions in the commune of Evodoula. The sites concerned in the EEZ are Evodoula, Ekol, Etok, Ayos, Okok, Nkolkougda, Ngobo, Ntouda, Nkolmeyos II, Nkotabel, Nkolabang, and Nloundou. There are different methods available to calculate the parameters of distribution functions. Several methods are used to determine these parameters. The Weibull distribution parameters (K and C) used in this study are determined by the energy factor method, the empirical method, and the method of moments. The choice of these three methods is motivated by the knowledge of the average data of the wind speed of the site.

(1) Energy Pattern Factor Method (EPFM). The energy pattern factor method (EPFM) is related to averaged wind speed data; i.e., it can be calculated by dividing the mean of the cube of the wind speed by cubes of the mean speed wind at a known latitude and longitude and is defined by the following equation [17, 42, 44–46].

$$\text{EPFM} = \frac{1/n \sum_{i=1}^n V_{\text{Lat,Lon}_i}^3}{\left(1/n \sum_{i=1}^n V_{\text{Lat,Lon}_i}\right)^3}, \quad (3)$$

where $V_{\text{Lat,Lon}_i}$ (m/s) is the wind speed for the i^{th} observation at the defined latitude and longitude, n is the number of samples of the wind speed, and $\bar{V}_{\text{Lat,Lon}}$ (m/s) is the average monthly or annual wind speed at a defined latitude and longitude.

Once the energy pattern factor method (EPFM) is calculated using Eq. (3), the Weibull shape parameter K is estimated from Eq. (4). The Weibull scale parameter C is determined using Eq. (5).

$$K = 1 + \frac{3.69}{(\text{EPFM})^2}, \quad (4)$$

$$C = \frac{\bar{V}_{\text{Lat,Lon}}}{\Gamma(1 + 1/K)}. \quad (5)$$

3.3.3. Extrapolation of Wind Speed as a Function of Height. In order to have adequate speeds for the operation of wind turbines at different heights, the vertical extrapolation of the wind speed is necessary and takes into account the characteristics linked to the sites. The present study uses the corrected formula of Justus and Mikhael for the vertical extrapolation [17]. Equations (6)–(8) illustrate this corrected power law.

$$\hat{V}_{\text{Lat,Lon}}(z_2) = V_{\text{Lat,Lon}}(z_1) \cdot \left(\frac{Z_2}{Z_1}\right)^\alpha, \quad (6)$$

$$\alpha = \frac{1}{\ln(\bar{Z}/Z_0)} - \frac{0.0881}{1 - 0.00881 \ln(z_1/10)} \cdot \ln\left(\frac{V_{\text{Lat,Lon}}(z_1)}{6}\right), \quad (7)$$

$$\bar{Z} = \sqrt{Z_1 \cdot Z_2}, \quad (8)$$

where $V_{\text{Lat,Lon}}(z_1)$ represents the reference speed measured at 10 m from the ground at a defined latitude and longitude; $V_{\text{Lat,Lon}}(z_2)$ represents the speed calculated at values greater than 10 m from the ground at a defined latitude and longitude; Z_1 and Z_2 denote the heights at 10 m from the ground and at variable values greater than 10 m from the ground, respectively; and Z_0 is the roughness of the ground.

3.3.4. Extrapolation of Weibull Distribution Parameters. The model proposed in our study is in accordance with Eqs. (9)–(11). Using the chosen model, the following formulas are therefore used to extrapolate to the different altitudes [17]:

$$n = 0.37 - 0.088 \ln(C_{10}), \quad (9)$$

$$C_Z = C_{10} \times \left(\frac{z}{z_{10}}\right)^n, \quad (10)$$

$$K_z = \frac{K_{10}}{1 - 0.00881 \ln(Z/10)}, \quad (11)$$

where z represents the height where we would like to install the wind turbines, C_z and K_z are the corresponding parameters, and C_{10} and K_{10} are the Weibull parameters, respectively, calculated at a 10 m.

3.3.5. 2D Spatial Variability: Technical for Horizontal Spatial Interpolation of Measurements. In the present study, we considered a technical and its variants: inverse distance weighting (IDW). This method of 2D spatial interpolation assigns values to unknown points which are calculated as weighted averages of the values available to the known grid points (GIS [47]). This method is also known as distance-based interpolation and is formulated by the following mathematical relationship.

$$\widehat{V}_{\text{Lat,Lon}}(x) = \frac{\sum_{i=1}^n w_i(x)^p \cdot V_{\text{Lat,Lon}_i}}{\sum_{i=1}^n w_i(x)^p}. \quad (12)$$

Or

$$w_i(x) = \frac{1}{d(x, x_i)} \quad (13)$$

is a simple weighting function, as defined by Shepard [48], where x is the point to be interpolated, x_i is a (known) interpolation point, $V_{\text{Lat,Lon}_i}$ are the known values at a defined latitude and longitude of the function $\widehat{V}_{\text{Lat,Lon}}$ which represents the integer ratio which gives an estimate of the known value at the point of interest at a latitude and longitude at point x_i , d is a given distance from each point of interest (measurement operator) from the interpolation point x_i to the point to be interpolated x , n is the total number of known points used in the interpolation, and p is a real positive number, called the power parameter. Here, the weight of neighboring points decreases when the distance increases. Larger values of p give greater influence to values closer to the interpolated point. For $0 < p < 1$, in $\widehat{V}_{\text{Lat,Lon}}(x)$, smoothed peaks are observed around the interpolation point x_i , whereas for $p > 1$, the peak becomes sharper. The choice of p is therefore a function of the degree of smoothing desired for the interpolation, of the density and distribution of the interpolated samples, and of the maximum distance beyond which an individual sample can influence the surrounding points. As described, the interpolation function is indeterminate at the interpolation points (0/0 division). In this case, the weight will be taken as 1 for the point at distance 0 from x and 0 for all other points as defined by Duplyakin et al. [49]. In this study, the IDW method is evaluated with 2, 3, 4, 5, 6, 8, 12, and 16 points used for interpolation to assess the role that the amount of data used in interpolation plays in reducing or increasing the interpolation error.

3.3.6. Available Wind Power Density (WPD). The available average power density is defined by the available instantaneous power P reported per unit area S , which is given by the following mathematical relationship.

$$\bar{P} = \frac{P}{S} = \frac{1}{2} \cdot \rho \cdot \bar{V}^3. \quad (14)$$

Wind power density (WPD) per monthly or annual unit area of a site based on a Weibull probability density function can be expressed as follows by rearranging Eq. (14); thus, we obtain the following mathematical relation [50].

$$\text{WPD} = \bar{P} = \frac{1}{2} \cdot \rho \cdot c^3 \cdot \Gamma\left(1 + \frac{3}{K}\right), \quad (15)$$

where Γ is a function that characterizes the shape of the frequency distribution and the asymmetry of the speed frequency distribution, and it is given by the following mathematical relationship.

$$\Gamma(x) = \left(\sqrt{2\pi x}\right) \cdot (x^{x-1}) \cdot (e^{-x}) \cdot \left(1 + \frac{1}{12}x + \frac{1}{288}x^2 - \frac{139}{51840}x^3 + \dots\right), \quad (16)$$

with

$$x = 1 + \frac{3}{K}. \quad (17)$$

Much research has used the energy pattern factor method (EPFM) to calculate wind power density ([44] citing [46]). However, during our numerical simulations, we find that the profile for which we are studying did not correspond to the EPFM defined by Akdağ and Dinler [51] to Eq. (3). For the first time, we are trying to modify the EPFM, previously defined by Akdağ and Dinler [51]. Thus, the modified energy pattern factor method (MEPFM) in the present study is proposed by the mathematical relation given in the following equation.

$$\text{MK}_e = \text{MEPFM} = \frac{1}{\bar{V}_{\text{Lat,Lon}}^3} \sum_{i=1}^n V_{\text{Lat,Lon}_i}^3. \quad (18)$$

The average monthly or annual power density available at a defined latitude and longitude is established by the following mathematical relationship.

$$\text{WPD}_{\text{Lat,Lon}}(z_2) = P(v_{\text{Lat,Lon}}) = \frac{P(V_{\text{Lat,Lon}})}{S} = \frac{1}{2} \cdot \rho_{\text{Lat,Lon}} \cdot \bar{V}_{\text{Lat,Lon}}^3 \cdot \text{MK}_e. \quad (19)$$

3.3.7. Wind Energy Density Estimation (WED). The energy density of a wind turbine or wind energy density (WED) monthly or yearly at a defined latitude and longitude is a very important parameter; it makes it possible to quantify the energy produced during a time T by the wind turbines or the park. It should be noted that the time T depends on the availability factor and the load factor. It is obtained by the following equation.

$$\text{WED}_{\text{Lat,Lon}}(z_2) = \text{WPD}_{\text{Lat,Lon}} T = \frac{1}{2} \cdot \rho_{\text{Lat,Lon}} \cdot \bar{V}_{\text{Lat,Lon}}^3 \cdot \text{MK}_e. \quad (20)$$

The available wind power density and the wind energy density thus calculated depend on the metric coordinates considered in the EEZ for a height of interest of 100 m (AGL).

3.3.8. Average Air Density in the EEZ of the Study Area. The average value of the air density was estimated based solely on the altitude at 589 m in height at a place called Evodoula by Eq. (21) which approximates the standard United States atmosphere profile for air density [52]. Note that the air density calculated at this height is assumed to be constant for the calculation of the wind power density of the locations in the EEZ, because there will be no significant difference.

$$\rho_{\text{Lat,Lon}} = \rho_0 - 1.194 \times 10^{-4} \times H_m, \quad (21)$$

where H_m is the altitude of the locations in meters (see Table 1); the air density at sea level is given by $\rho_0 = 1.225 \text{ kg/m}^3$.

3.3.9. Useful Wind Power. The energy produced by a wind turbine depends on its characteristic curve. This is therefore an important element in the modeling. According to the work of Lu et al. [53], there are many models that have been developed for the simulation of the power supplied by a wind turbine. This section presents two parameterized power models (physical and modified) used in this study:

(1) Quadratic Model or Pallabazzer Model. The quadratic model is the one that generally has the lowest squared error rate and is therefore more suitable for testing the reliability of wind turbines. It differs from the linear model by the non-linear shape of the curve between the engagement speed and that for which the rated power is obtained. For this purpose, in this part, the power generated by the wind turbine is estimated by the following four equations.

$$P_i(V) = \left\{ \begin{array}{lll} 0 & \text{for } V < V_D & \text{area I} \\ P_N \frac{V^K - V_D^K}{V_N^K - V_D^K} & \text{for } V_D \leq V < V_N & \text{area II} \\ P_N & \text{for } V_N \leq V \leq V_C & \text{area III} \\ 0 & \text{for } V > V_C & \text{area IV} \end{array} \right\}, \quad (22)$$

where P_N is the rated electric power of the aerogenerator; V designates the wind speed at the height of the hub at a given instant; and V_D , V_N , and V_C denote the cut-in wind speed, rated wind speed, and cut-off wind speed of the wind generator, respectively, once the power $P_i(V)$ at the output of the wind turbine at each time step i is calculated.

The use of an adaptive power curve derived from the previous one by linear transformation equivalent to a modular factor “ a ” is calculated by

$$a = \frac{\widehat{V}_{\text{Lat,Lon}}(z_2) - \bar{V}_{\text{Lat,Lon}}(z_1)}{V_i}, \quad (23)$$

where “ a ” is the adaptive or modular factor (dimensionless), $\widehat{V}_{\text{Lat,Lon}}(z_2)$ is the average wind speed calculated by the extrapolation method between two heights z_2 and z_1 (m/s) (see Section 3.3.3), $\bar{V}_{\text{Lat,Lon}}(z_1)$ is the average wind speed at reference height (m/s), and V_i is the undisturbed free wind speed measured at hub height interpolated at each step i fixed at 1 (m/s).

(2) Quadratic Model Modified or Pallabazzer Model Modified. This adaptive power curve model generated by the wind turbine is expressed by the following four equations in given in Eq. (24), in considering adjusted wind speed V_a given in Eq. (25):

$$P_{a,i}(V_a) = \left\{ \begin{array}{lll} 0 & \text{for } V_a < V_{a,D} & \text{new area I} \\ P_N \frac{V_a^K - V_{a,D}^K}{V_{a,N}^K - V_{a,D}^K} & \text{for } V_{a,D} \leq V_a < V_{a,N} & \text{new area II} \\ P_N & \text{for } V_{a,N} \leq V_a \leq V_{a,C} & \text{new area III} \\ 0 & \text{for } V_a > V_{a,C} & \text{new area IV} \end{array} \right\}, \quad (24)$$

with

$$V_a = \frac{V_i}{a}, \quad (25)$$

where $P_{a,i}(V_a)$ is the adaptive power of the wind turbine at each time step i being calculated; we estimate the average output power P_{Useful} of a turbine. The latter is an important parameter of a wind turbine, because it determines the total energy production $PT(t)$, $V_{a,D}$, $V_{a,N}$, and $V_{a,C}$ denoting the adaptive cut-in wind speed, the adaptive rated wind speed, and the adaptive cut-off wind speed, respectively. V_a is the adjusted wind speed (m/s), and V_i is the undisturbed free wind speed at nacelle height of each wind turbine in the farm (m/s).

3.3.10. Energy Generated. The energy generated (in watt-hour) by a wind turbine is the product of the useful power recovered by the wind turbine and the operating time T (in hours). The average energy produced by a wind turbine is established by

$$E_{\text{MPSE}} = P_{\text{MPE}} \times \Delta t, \quad (26)$$

with

$$P_{\text{MPE}} = \int_0^{+\infty} P_{a,i}(V_a) \cdot f(V_{\text{Lat,Lon}}) dV_{\text{Lat,Lon}}, \quad (27)$$

where E_{MPSE} is the average energy produced at the output of the wind turbine (MWh), P_{MPE} is the average power produced by the wind turbine (W), and Δt is the operating period of the wind turbine. For this period, the maximum energy produced annually by a wind turbine is given by

$$E_{MP} = P_N \times 8760, \quad (28)$$

where P_N is the rated power and E_{MP} is the maximum energy produced (MWh).

The total power produced by the wind turbine is given by Eq. (29). This power is used to power the load. Surplus energy is used to charge the battery.

$$PT(t) = N_{wt} \times P_{a,i}(V_a), \quad (29)$$

where $PT(t)$ is the total power of wind turbines, N_{wt} is the total number of wind turbines, and $P_{a,i}(V_a)$ is the adaptive electrical power at the output of the wind turbine given by Eq. (24).

3.3.11. Uncertainties and Risks. The total uncertainty as a fraction of production is denoted as σ , and it is assumed that the distribution of productions is Gaussian with a standard deviation equal to σ . Then, the expression of P_{90} , production that we are 90% sure to exceed, is given by the following equation [54].

$$P_{90} = P_{50}(1 - 1.282\sigma), \quad (30)$$

where P_{50} is the median net output obtained and σ is the standard deviation.

3.3.12. Capacity or Load Factor of Wind Turbines. The load factor or the capacity factor, also called the utilization factor, is represented by the ratio between the electrical energy actually produced by the wind turbine over a given period and the energy it would have produced if it had operated at its rated power during the same period [55]. In the present study, to determine the load factor of wind turbines, the formula given in Eq. (31) was used.

$$CF(\%) = \frac{PT(t)}{E_{MP}}. \quad (31)$$

If we obtain a load factor of at least 25%, we can speak of the electricity production of the wind turbines [56].

3.3.13. Technoeconomic Analysis of Wind Turbines. The economic problems of wind systems are common these days. The unit cost of electricity produced by a wind turbine is affected by several factors. The economic merit of a generating wind power plant depends on local, endogenous conditions which may vary from place to place. Economic evaluation is essential while investing hugely in installing large-scale wind turbines for wind power generation. At the initial stage, the specific site analysis of the wind characteristics is carried out, and then, a selection of wind turbines is examined while considering the mechanical configuration

of the turbine adapted to the site. When the investment capital is high while evaluating the initial investment for the project, investment for essential requirements such as land, transmission lines, and power conditioning systems should also be accounted for a wind turbine. The estimation of present value cost analysis based on net present value is as described in the following section [57]. First of all, we start by defining all the necessary elements used in the present study during the construction of the economic model of the wind turbines for the twelve locations under study. The validation of the economic model is based on information such as the initial investment of the project C_I and the cost of operation and maintenance M_c , which is $m\%$ of the initial investment. In addition, D_{OM} is the discounted operating costs and maintenance costs for the lifetime n of the wind turbine for a first year. Note that the construction of an economic model of wind turbines differs from one country to another and from one site to another. These include, among others, the work of Sukkiramathi and Sessaiah [58], Mostafaeipour et al. [59], Touafio et al. [60], Moria et al. [61], and Kassem et al. [62, 63]. In addition, some authors have proposed modifications of the economic model using the PVC (present value cost) method and the CPU (cost production unitary or cost per unit) method (Said [64]).

$$D_{OM} = mC_I \left[\frac{1}{I} - \frac{1}{(1+I)^n} \right], \quad (32)$$

where the initial investment cost C_I is equal to the sum of the component costs [65, 66]. The total investment cost is

$$C_I = C_{Wt} + C_{St} + C_{En} + C_{Ci} + C_{Tr} + C_{El} + C_{Misc}, \quad (33)$$

$$C_{Wt} = C_{Spe} \times P_N, \quad (34)$$

where the parameter I is the interest rate (%), C_{Wt} is the cost of the wind turbine (\$), C_{St} is the cost of the study or 2% of C_{Wt} (\$), C_{En} (is the engineering cost or 5% of C_{Wt} (\$), C_{Ci} is the civil work and the installation cost which is 8% of C_{Wt} (\$), C_{Tr} is the cost of transport which is 2% of C_{Wt} (\$), C_{El} is the cost of the electrical connection which is 7% of C_{Wt} (\$), C_{Misc} is the miscellaneous cost which is 1% of C_{Wt} (\$), and C_{Spe} is the specific cost of the wind turbine (\$).

The net present value (NPV) of all costs including the initial investment is C_I :

$$NPV = C_I \left[1 + m \left[\frac{1}{I} - \frac{1}{(1+I)^n} \right] \right]. \quad (35)$$

For the calculation of the cost of this wind energy, one can use the method of the present value of the costs (PVC) for the estimation of the cost of production of the wind energy. Therefore, the annual operating cost of the turbine is

$$PVC = \frac{C_I}{n} \left[1 + m \left[\frac{1}{I} - \frac{1}{(1+I)^n} \right] \right]. \quad (36)$$

Wind farm efficiency is measured by AEP (annual energy production), reflecting how the wind turbine exploits the wind resource and estimating the electricity production during the lifetime of a wind turbine in 1 year given by the following relation:

$$AEP = 8760 \times P_N \times CF, \quad (37)$$

where P_N is the rated power of the turbine and CF is the factor of wind turbine load or capacity factor. Thus, the estimate of the cost production unitary of 1 kWh of wind energy produced by different wind turbines is given by the following relationship:

$$CPU(\$/kWh) = \frac{PVC}{AEP} = \frac{C_I}{8760n} \left(\frac{1}{P_N CF} \right) \left[1 + m \left[\frac{1}{I} - \frac{1}{(1+I)^n} \right] \right]. \quad (38)$$

3.3.14. Annual Greenhouse Gas (GHG) Savings. After determining the value of the expected gross (AEP Gross) and net annual energy production (AEP Net) based on a modified chosen power model (modified quadratic model) combined with a spatial interpolation technical (inverse distance weighted or (IDW)), the annual reduction in greenhouse gas (GHG) emissions could be calculated. According to statistics from the Journal Our World in Data based on the Global Carbon Project, annual carbon dioxide (CO₂) emissions based on production are measured in kilograms per kilowatt-hour of primary energy consumption. Production-based emissions are based on territorial emissions, which do not take into account emissions embedded in traded goods per kilowatt-hour from Cameroon's average national electricity generation mix over the 40-year period (1980-2019) amounted to 180.0825 g/kWh, which was used for this calculation of GHG emissions [67]. The carbon intensity of energy production is measured as the amount of carbon dioxide emitted per unit of energy production. This is measured in kilograms of CO₂ per kilowatt-hour. Equation (39) was used to calculate the reduction in GHG emissions:

$$G = \frac{180.0825 \times AEP}{1000000}, \quad (39)$$

where G is the annual reduction in emissions of (GHG) in ton equivalents (CO₂/year) and AEP is the annual energy production in kilowatt-hour per year).

The wake loss rate (WLR) takes into account the AEP Gross and the AEP Net. The WLR was calculated using the following equation.

$$WLR (\%) = \left(\frac{AEP \text{ Gross}}{AEP \text{ Net}} - 1 \right) \times 100. \quad (40)$$

Most systems require investment, and in addition to access to other funding benefits, return on investment is necessary. The return on investment (ROI) of a wind farm is considered as the rate of return, or profit taking into account the turnover generated by the profits, i.e., the present value

of the profits (PVB), and the total investment cost, i.e., the present value of the costs (PVC). In this study, the ROI was calculated with the following equation.

$$ROI (\%) = \frac{PVB - NPV}{NPV}. \quad (41)$$

Earnings generated by the wind farm are the difference between the annual gross income and the total annual expenditure. Thus, the PVB was calculated using the following equation.

$$PVB = (CPU_{\text{selling price}} - CPU_{\text{cost per kWh of the wind farm}}) \text{TEPNet}, \quad (42)$$

where TEPNet (kWh) is the net total energy produced by the wind farm.

The payback time, or payback period, indicates the number of annuities until the investment is paid. The PBP was calculated by the following equation.

$$PBP (\text{Yr}) = \frac{NPV}{\text{average annual cash flow}}. \quad (43)$$

4. Results and Discussion

4.1. Statistical and Average Characteristics of the Wind on the Twelve Locations of Evodoula

4.1.1. Monthly, Annual, and Interannual Variation of the Average Wind Speed at a Height of 100 m. The processing of the data made it possible first of all to calculate the average monthly, annual, and interannual speeds of the average wind speed at a height of 10 m from the reference ground (not represented in these graphs), simultaneously extrapolated at 100 m above ground level (AGL) using Eq. (6), and then present their evolution curve. Figure 5 shows the variations of the monthly averages of the wind speed for the twelve locations Evodoula, Etok, Ekol, Ayos, Okok, Nkolougda, Ngobo, Ntouda, Nkolmeyos II, Nkotabel, Nkolabang, and Nloundou. The analysis of this figure shows that all the twelve places have a maximum average wind speed during the period August–February and the month of March. As for the minimum, it occurs during the period of the month of November. The results obtained from the monthly average wind speeds between the localities of Evodoula show that the curves describe the same pace at an installation (or interest) height of 100 m. As can be seen, the average monthly wind speeds varied between 1.112 and 4.440 m/s. Minimum and maximum velocities occurred in November at Nloundou and August at Ayos, respectively. Figure 5 presents the monthly average variation of the monthly average wind speed of the months of the year over the 40 years of measurements during the period 1980-2019.

Figure 6 show the results of the comparison of the average annual wind speed of the twelve locations selected during the periods studied (1980-2019, 1980-1989, 1990-1999, 2000-2009, and 2010-2019). Ayos has the maximum annual average wind speed of 3.155 m/s during the period 2000-

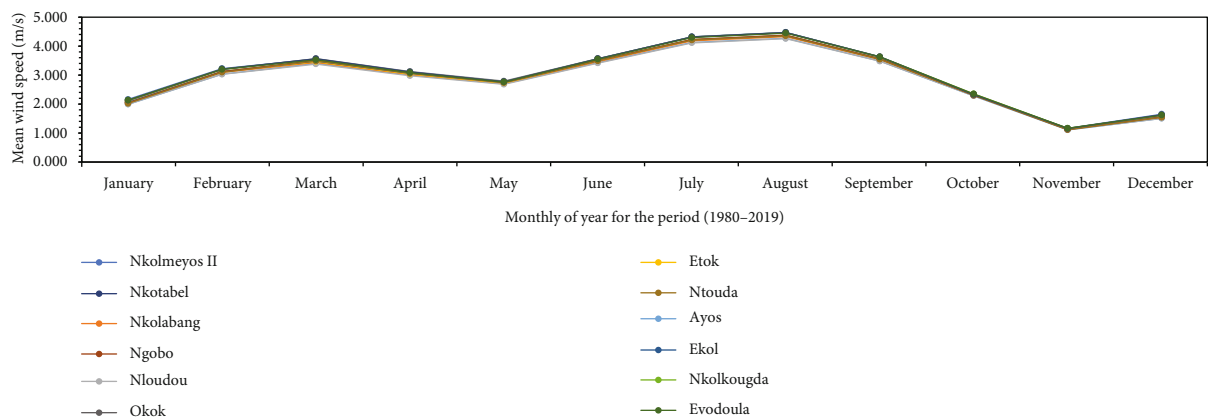


FIGURE 5: The average monthly wind speed (of multiyear winds) of the twelve locations selected during the period of 1980-2019.

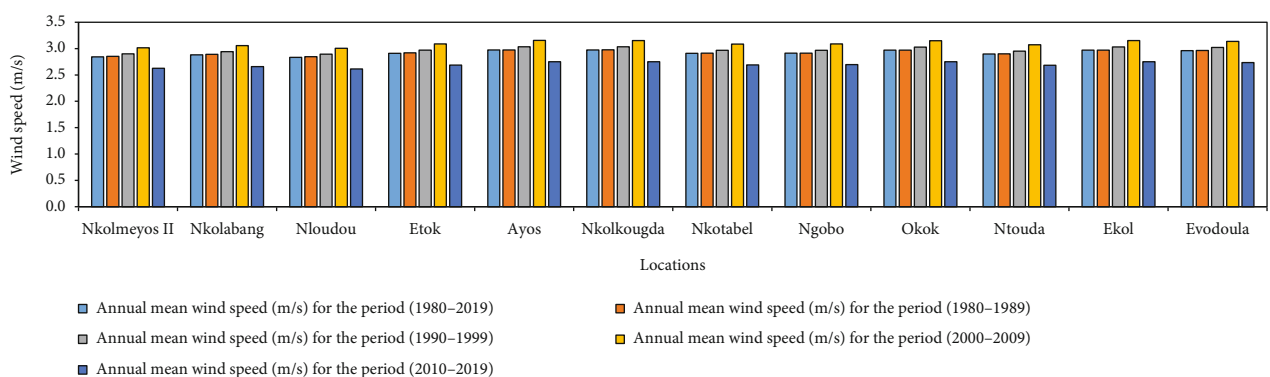


FIGURE 6: The average annual wind speed of the twelve locations selected during the periods studied (1980-2019, 1980-1989, 1990-1999, 2000-2009, and 2010-2019).

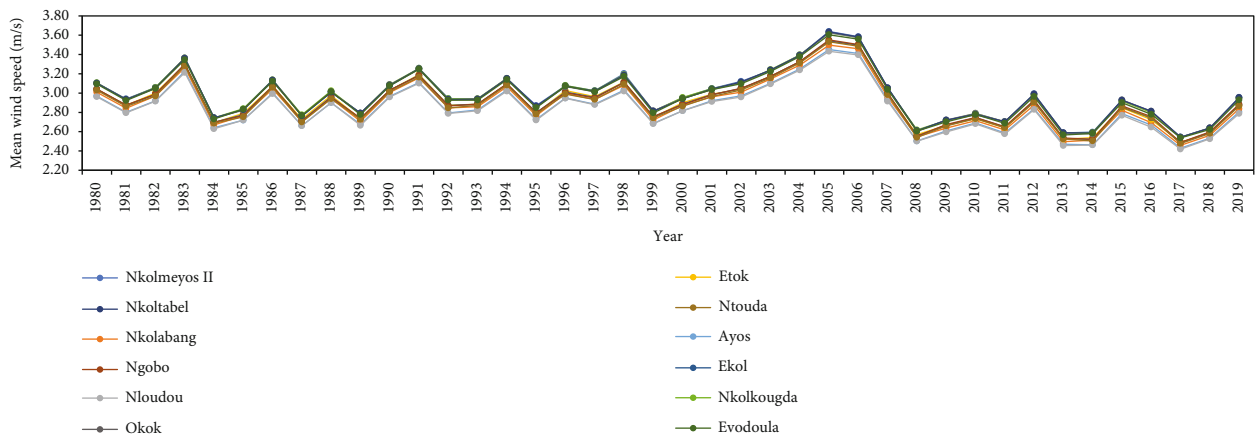
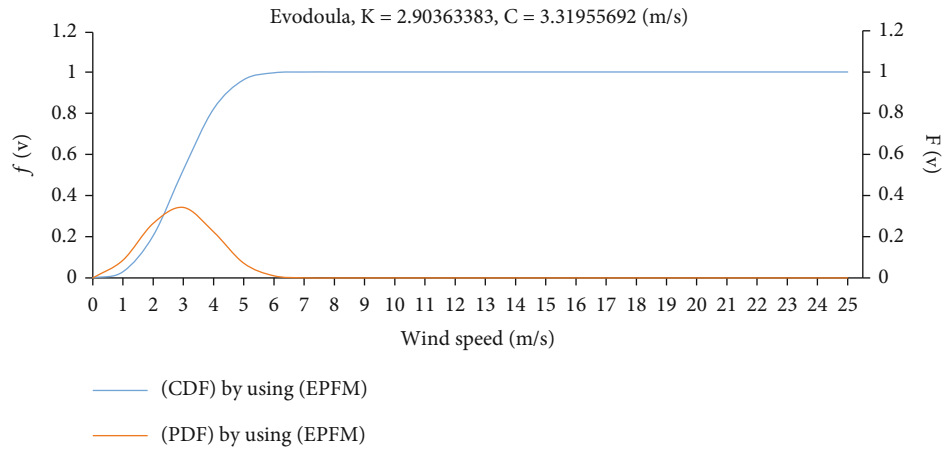


FIGURE 7: Evolution of the long-term multiyear wind speeds of the twelve locations at 100 m height for the period of 1980-2019.

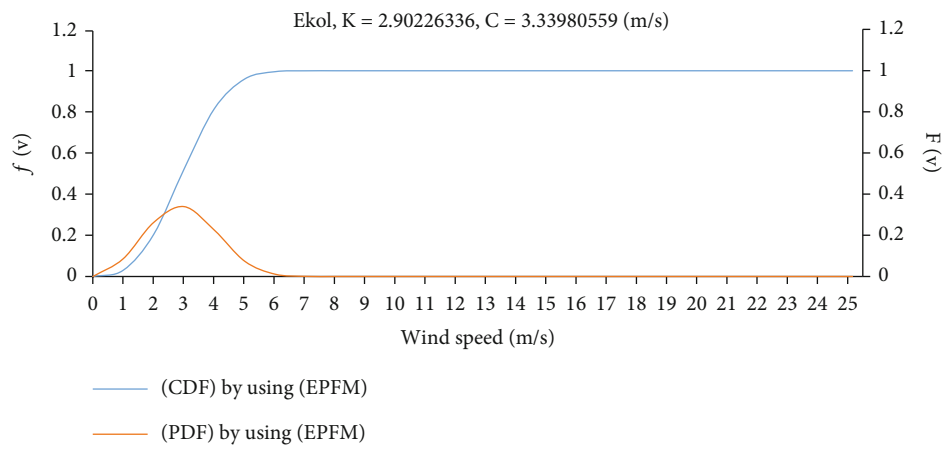
2009, followed by Ekol, Nkolkougda, Okok, Evoudoula, Ngobo, Nkotalabel, Etok, Ntouda, Nkolabang, Nkolmeyos II, and Nloundou, as shown in Figure 6. Moreover, it is observed that the annual average wind speed values in the wind speed values at Etok and Nkotalabel are the same, i.e., about 3.087 m/s during the period 1980-2019. In addition, the results of comparing the annual average wind speed values in the wind speed values at Ayos, Okok, and Ekol are approximately the

same, i.e., about 2.974, 2.972, and 2.972 m/s, respectively during the four-decade period (1980-2019) and the ten-year period (1980-1989).

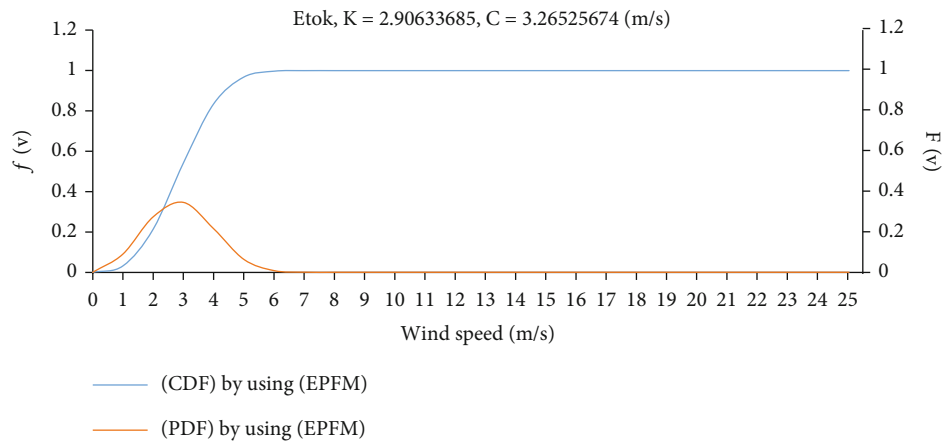
Figure 7 shows the long-term evolution of the annual average wind speed at selected locations from 1980 to 2019 at the height of 100 m above the ground. This figure shows that the behavior of the wind speeds on the locations is in an oscillatory regime and marked by a strong interannual



(a)



(b)



(c)

FIGURE 8: Continued.

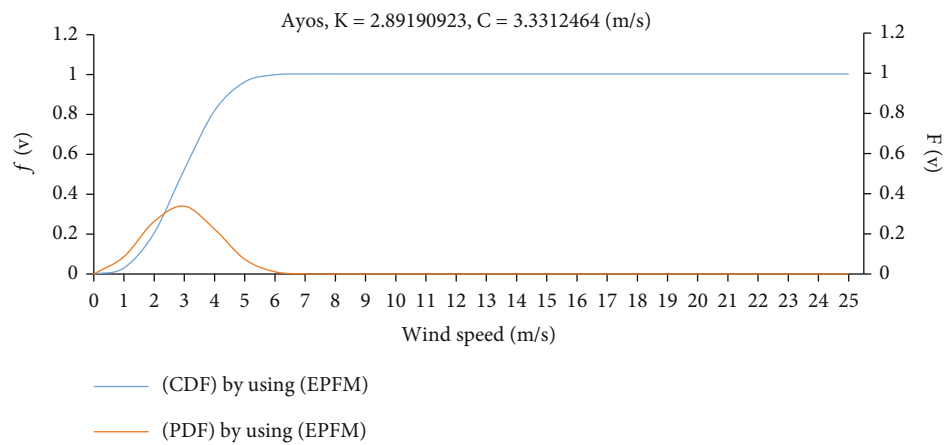
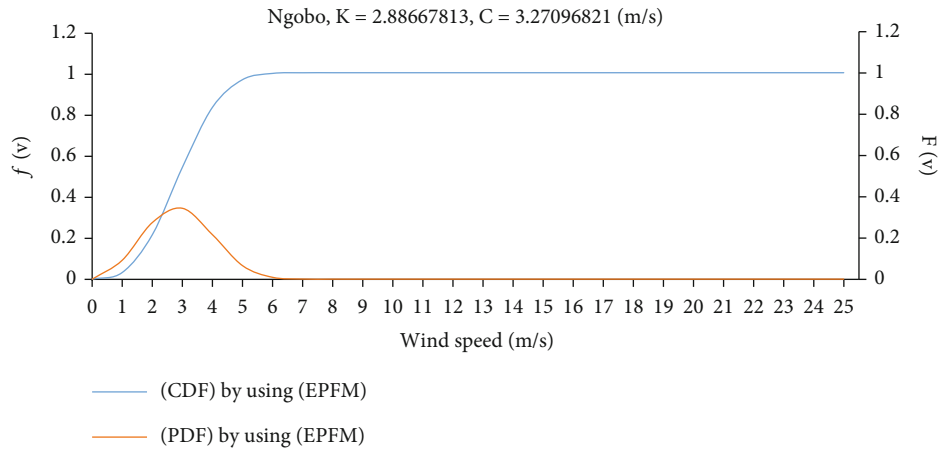
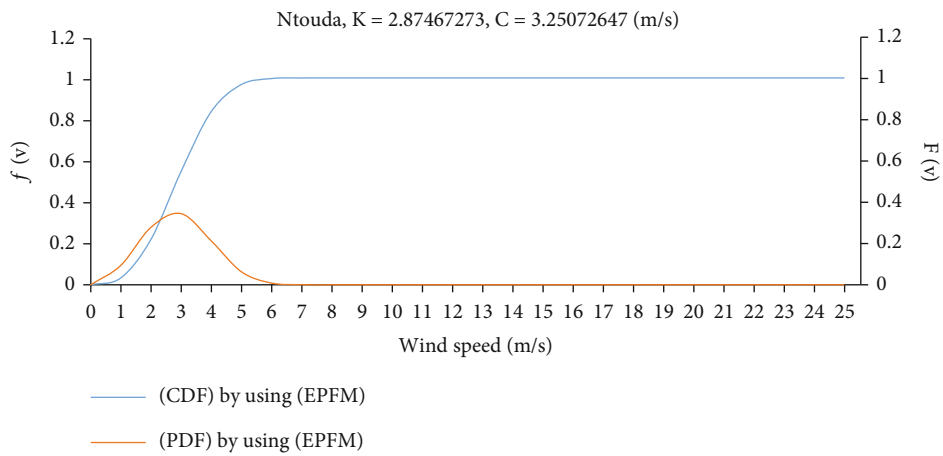


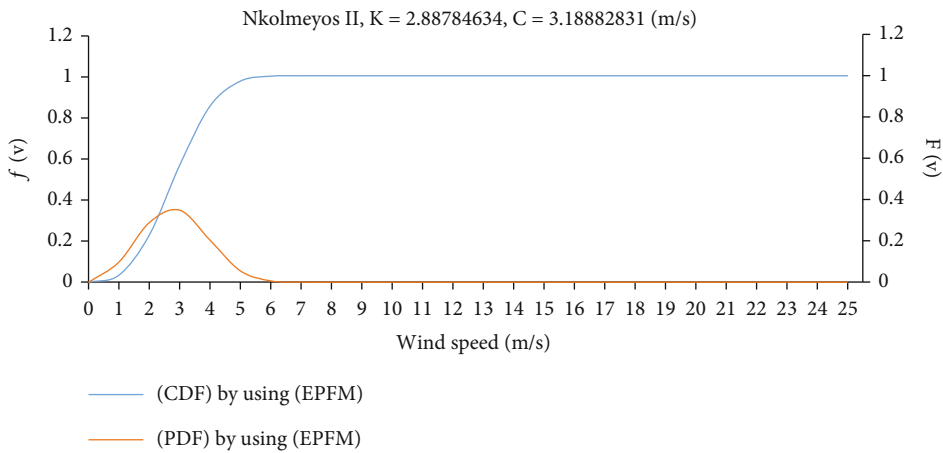
FIGURE 8: Continued.



(g)



(h)



(i)

FIGURE 8: Continued.

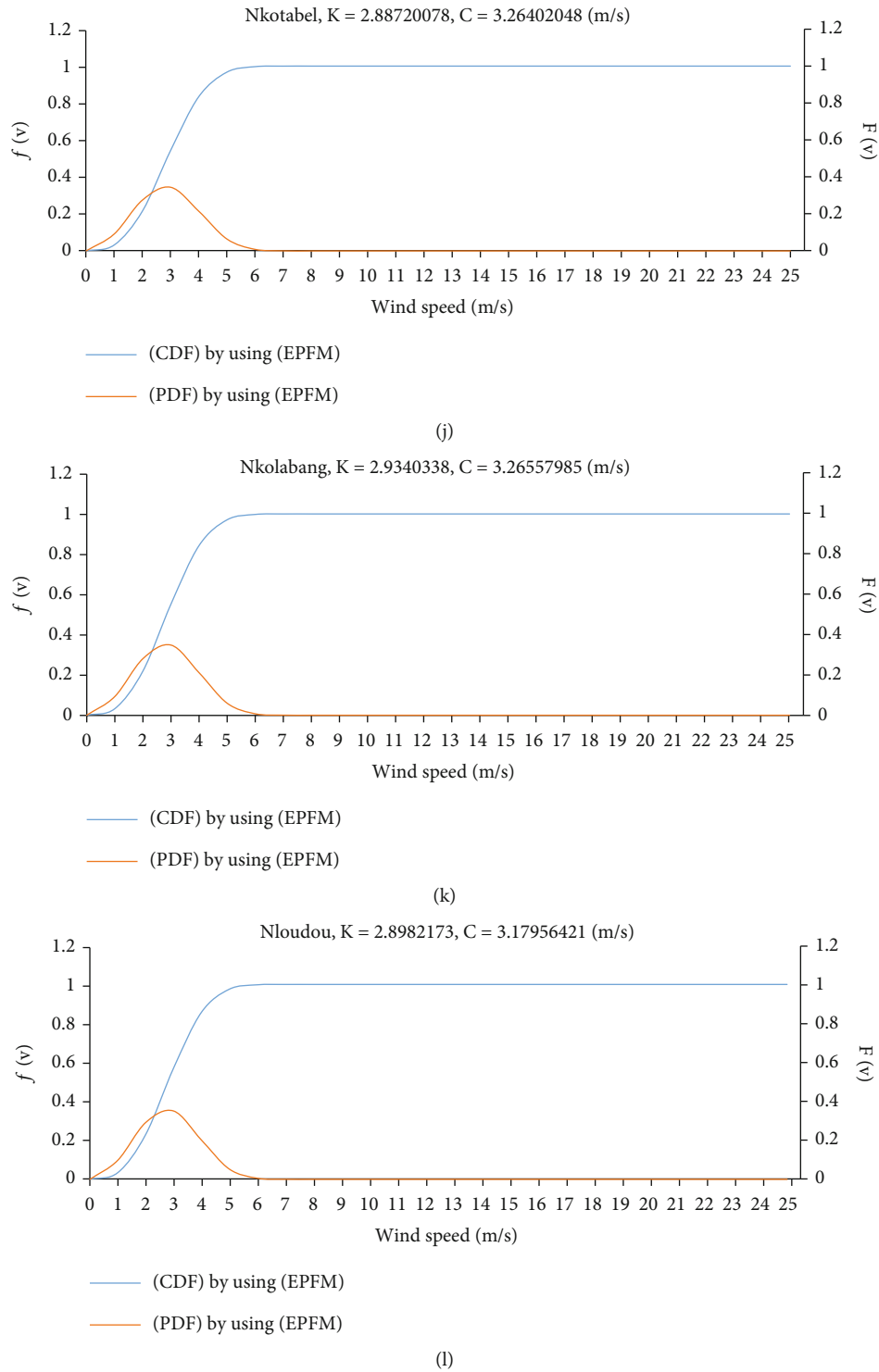


FIGURE 8: Curves of Weibull annual fits of probability distribution function (PDF) and cumulative distribution function (CDF) to wind speed data at a height of 100 m for (a) Evodoula, (b) Ekol, (c) Etok, (d) Aynos, (e) Okok, (f) Nkolkougda, (g) Ngobo, (h) Ntouda, (i) Nkolmeyos II, (j) Nkotabel, (k) Nkolabang, and (l) Nloudou.

variability of the winds on a four-decade scale. We notice that Aynos presents a maximum of average annual wind speeds during the year 2005 of 3.64 m/s, followed by Okok, Ekol, and Nkolkougda, with values being identical at 3.63 m/s. As for the minimum, it occurs during the year 2017 of

2.42 m/s in Nloudou. The standard deviation between the maximum value (2005) and the minimum value (2017) is 1.22 m/s. This justifies the reconciliation of the values obtained. Thus, the similar shape of the wind speed evolution curves is reinforced.

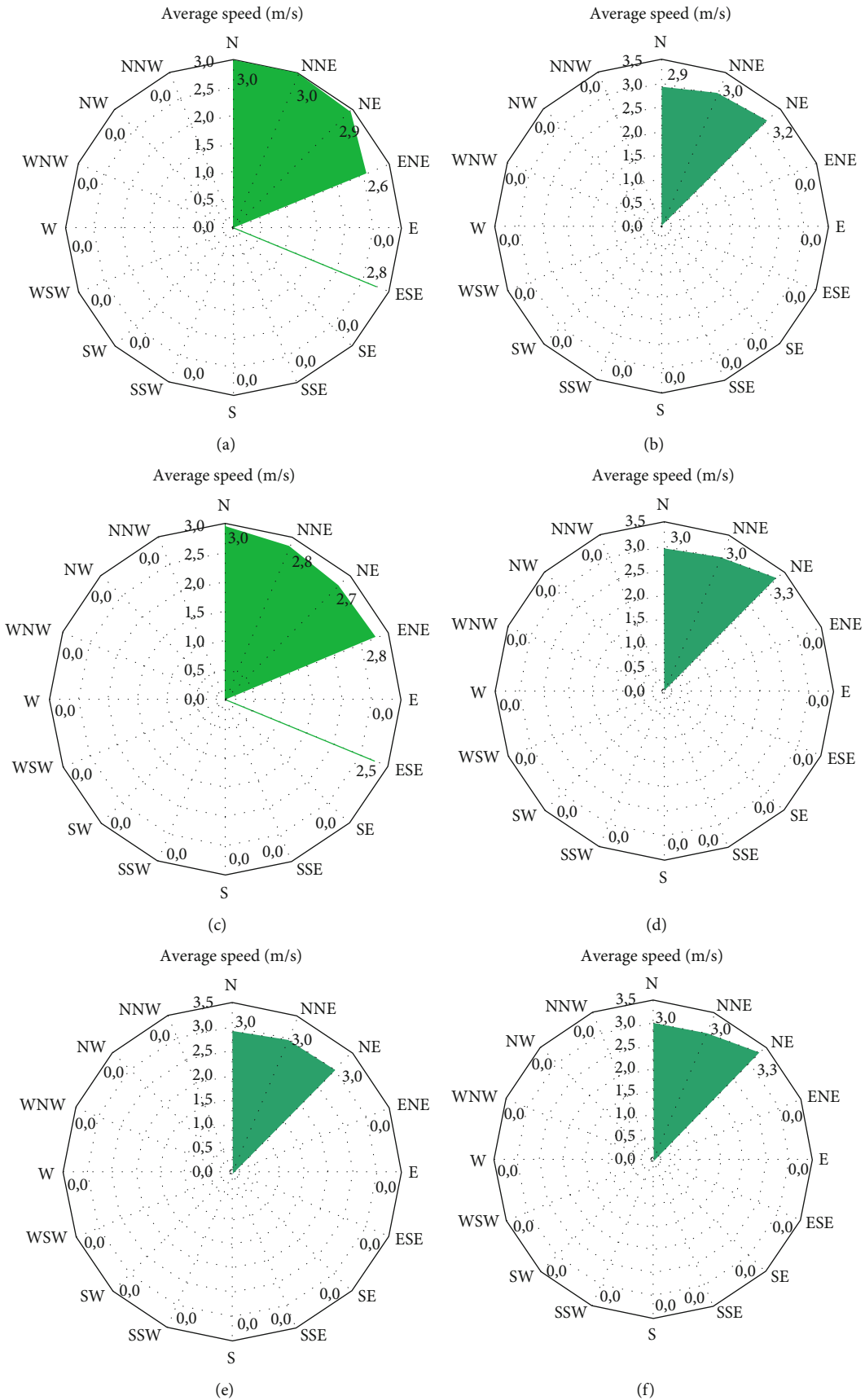


FIGURE 9: Continued.

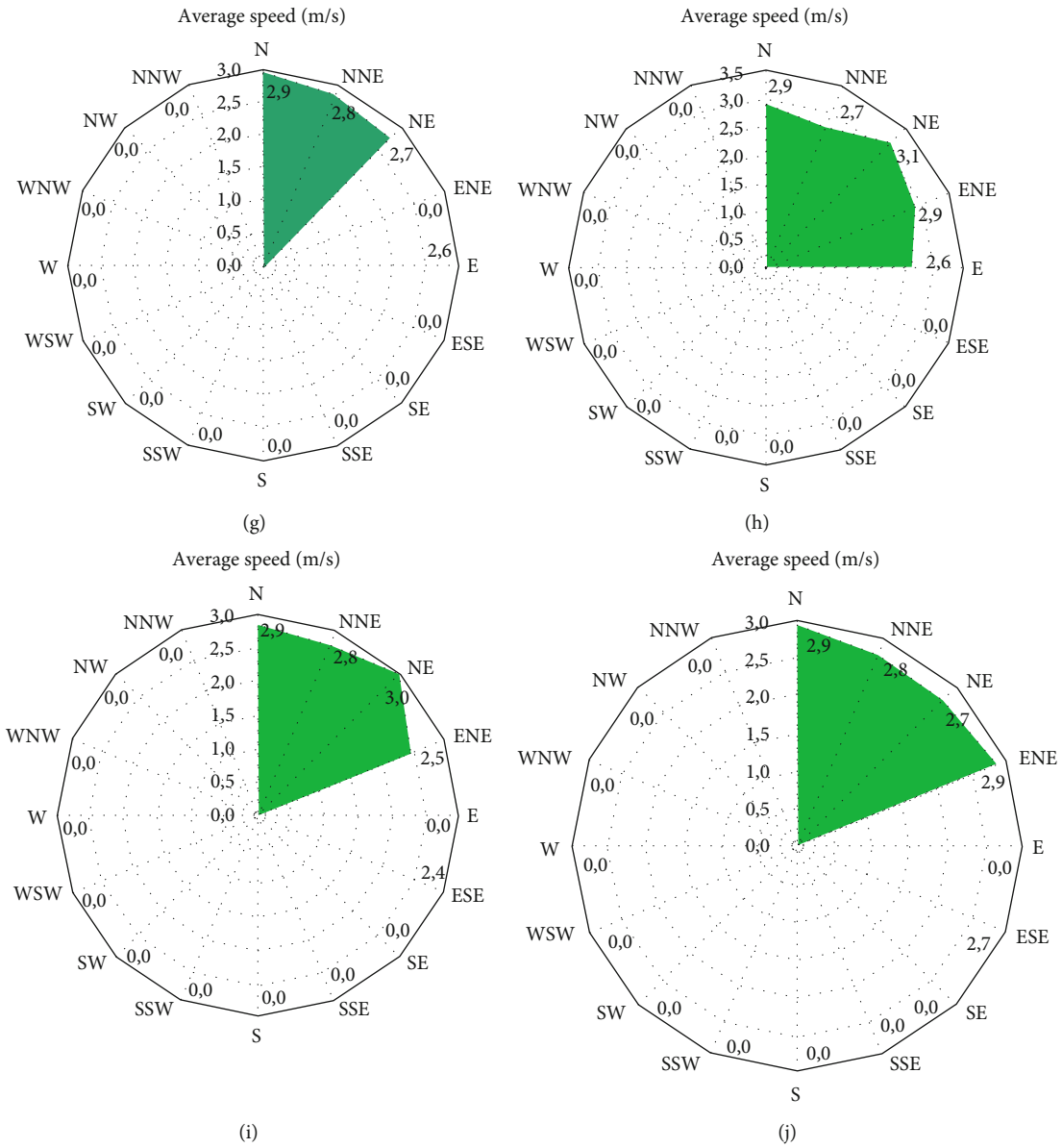


FIGURE 9: Continued.

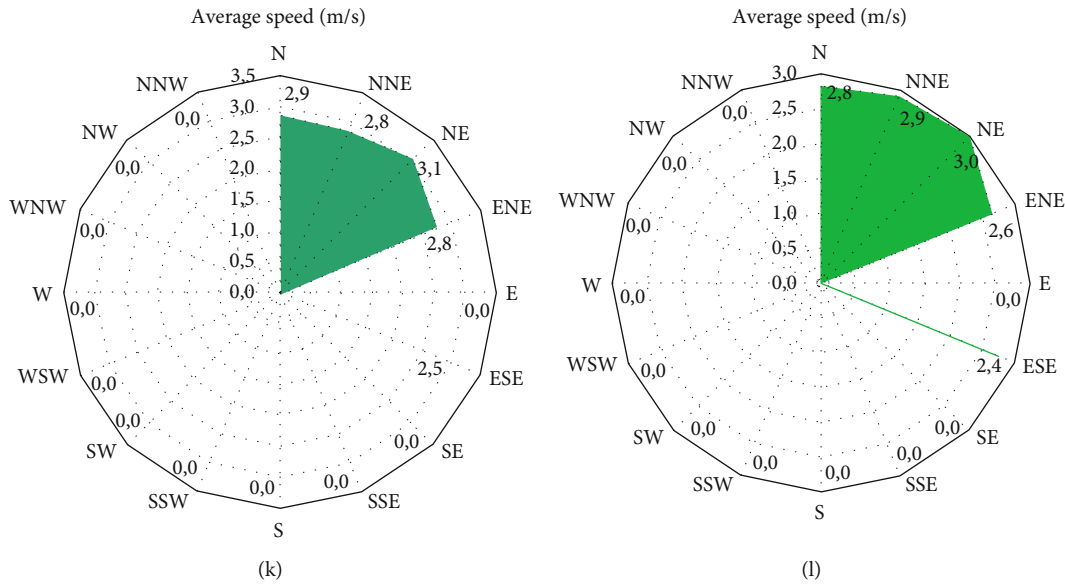


FIGURE 9: The diagram of the wind rose over the 40-year period studied (1980-2019) for (a) Evodoula, (b) Ekol, (c) Etok, (d) Ayos, (e) Okok, (f) Nkolkougda, (g) Ngobo, (h) Ntouda, (i) Nkolmeyos II, (j) Nkotabel, (k) Nkolabang, and (l) Nloundou.

4.1.2. *Variation of the Weibull Distribution.* The curves of adjustment of the statistical distribution of the annual frequencies of the wind speeds of 1980-2019 obtained from the distribution of Weibull on the places are represented in Figures 8(a)–8(l). These figures show the annual variation over the period studied from 1980 to 2019 of the Weibull distribution at a height of 100 m above the ground (AGL); thus, the curves representative of the statistical distributions of the wind speed are obtained by adjustment of the data, within the meaning of the energy pattern factor method (EPFM) and by using the Weibull model. Observation of the curves shows that the evolution of the annual distribution differs from one location to another. The results of the annual Weibull shape and scale parameters show a dissimilarity from one location to another as indicated on Figures 8(a)–8(l). Moreover, we notice that at 100 m height, 34.24%, 33.98%, 34.66%, 33.93%, 33.92%, 34.07%, 34.31%, 34.39%, 34.85%, 34.45%, 34.84%, and 35.07% of the wind speeds are greater than or equal to 3 m/s, respectively, at Evodoula, Ekol, Etok, Ayos, Okok, Nkolkougda, Ngobo, Ntouda, Nkolmeyos II, Nkotabel, Nkolabang, and Nloundou. We also notice that on the figures, the probabilities for that the wind blows in a range of speeds here for a range from 2 m/s to 3 m/s is $f(V_{Lat,Lon}(3)) - f(V_{Lat,Lon}(2)) = 34.24 - 26.5$ either 7.74% ; $f(V_{Lat,Lon}(3)) - f(V_{Lat,Lon}(2)) = 33.98 - 26.28$ either 7.7% ; $f(V_{Lat,Lon}(3)) - f(V_{Lat,Lon}(2)) = 34.66 - 27.49$ either 7.17% ; $f(V_{Lat,Lon}(3)) - f(V_{Lat,Lon}(2)) = 33.93 - 26.31$ either 7.62% ; $f(V_{Lat,Lon}(3)) - f(V_{Lat,Lon}(2)) = 33.92 - 26.3$ either 7.62% ; $f(V_{Lat,Lon}(3)) - f(V_{Lat,Lon}(2)) = 34.07 - 26.24$ either 7.83% ; $f(V_{Lat,Lon}(3)) - f(V_{Lat,Lon}(2)) = 34.31 - 27.47$ either 6.84% ; $f(V_{Lat,Lon}(3)) - f(V_{Lat,Lon}(2)) = 34.39 - 27.78$ either 6.61% ; $f(V_{Lat,Lon}(3)) - f(V_{Lat,Lon}(2)) = 34.85 - 28.94$ either 5.91% ; $f(V_{Lat,Lon}(3)) - f(V_{Lat,Lon}(2)) = 34.45 - 27.52$ either 6.93% ; $f(V_{Lat,Lon}(3)) - f(V_{Lat,Lon}(2)) = 34.84 - 28.09$ either 6.75% ; $f(V_{Lat,Lon}(3)) - f(V_{Lat,Lon}(2)) = 35.07 -$

29.13 either 5.94% and the ranges of speeds extend weakly up to 25 m/s. The analysis of Figure 6 translates the high probability for the wind speeds here (very low) ranging from 2 and 3 m/s. This means that the large wind turbines installed on these places, at a height of 100 m, can produce energy for 92.26%, 92.3%, 92.83%, 92.38%, 92.38%, 92.17%, 93.16%, 93.39%, 94.09%, 93.07%, 93.25%, and 94.06% time and operate at rated power, respectively, at Evodoula, Ekol, Etok, Ayos, Okok, Nkolkougda, Ngobo, Ntouda, Nkolmeyos II, Nkotabel, Nkolabang, and Nloundou. Figures 8(a)–8(l) show that the average annual speed on the locations is between 2 and 3 m/s (greater than or equal to the starting wind speed of most wind turbines), which allows electricity production.

4.1.3. *Wind Rose Diagrams of the Selected Locations.* The statistical study of the data allowed the determination of the wind rose which is the graphic representation of the average wind speed as a function of the direction in a polar reference. The wind rose is determined for the 40-year data set from 1980 to 2019. The wind direction was recorded for each selected location. A total of 16 directions were considered, and the average wind speeds for these directions are presented in Figure 9(a)–9(l). It is observed that the prevailing wind direction at Nkolmeyos II, Ekol, Nkolkougda, Nkolabang, Ayos, Ntouda, and Nloundou turned out to be north-east (NE) with average speed values of 3.0 m/s. For Etok and Ngobo, it was found to be north (N) with average speed values of 3.0 m/s and 2.9 m/s, respectively. Additionally, it can be seen that the wind direction with the most significant average speed was north (N) to north-east (NE) at Okok. For Evodoula, the wind direction was north (N) to north-north-east (NNE) with average speed values of 3.0 m/s. Additionally, the prevailing wind direction for Nkotabel was north (N) and east-north-east (ENE) with average speed values of 2.9 m/s.

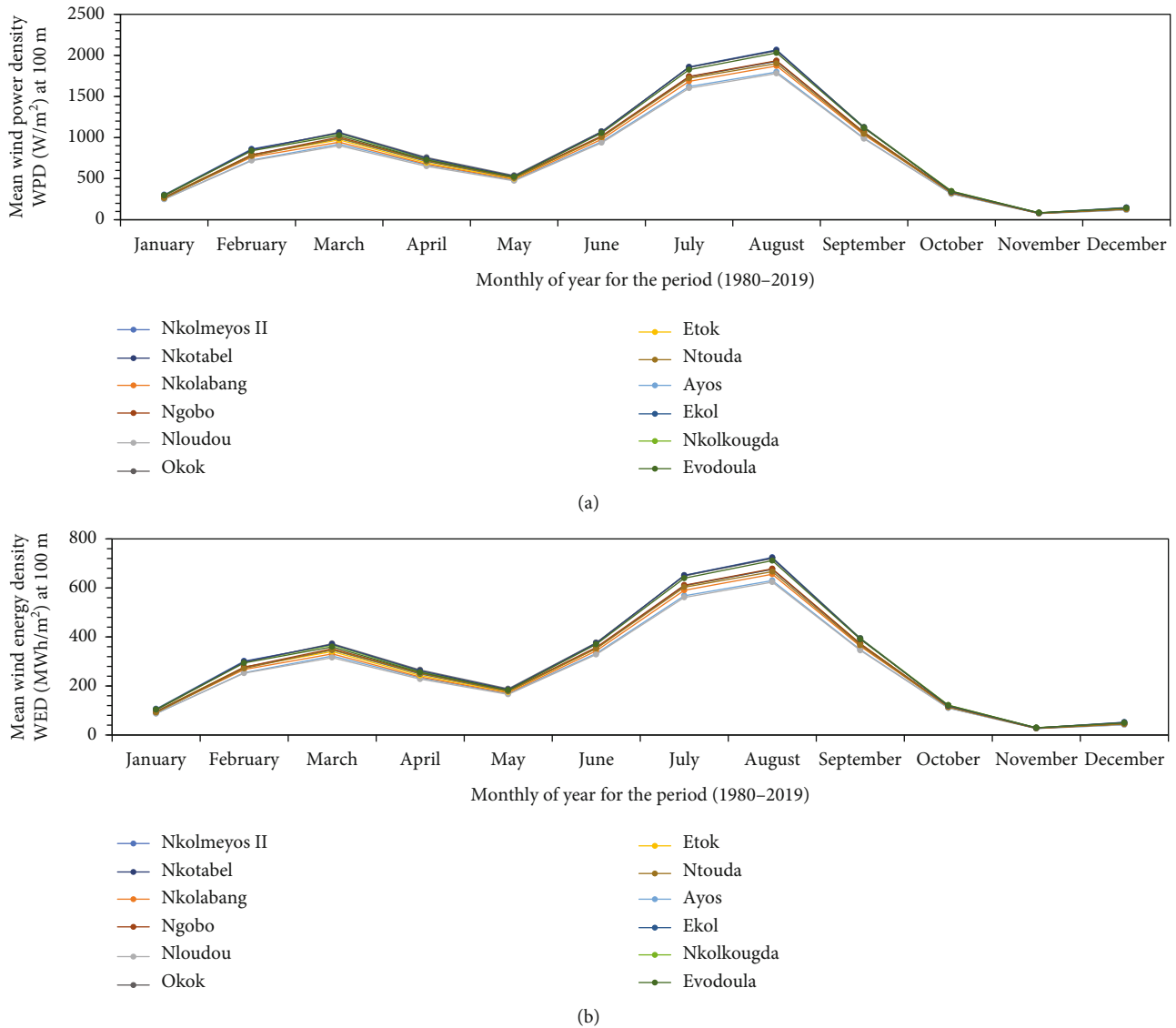


FIGURE 10: Monthly variation at 100 m height for the twelve locations selected in Evoudoula for (a) average wind power density and (b) average wind energy density.

The interest of these figures (Figures 8(a)–8(l) and 9(a)–9(l)) is to make better extrapolations in order to obtain favorable speeds for the production of electrical energy and the orientation of wind turbines on the selected locations.

4.1.4. Estimation of Monthly Average Wind Power Density (WPD) and Monthly Average Wind Energy Density (WED) at a Height of 100 m. Curves of monthly average wind power density and energy density monthly average wind turbine at a height of 100 m are illustrated in Figures 10(a)–10(b), respectively. The results obtained show that the estimation of the monthly mean wind power density from the Weibull parameters correspond closely to the different time scales. The monthly values of wind power densities and wind energy density are presented in Tables 2–5. The values of wind power densities and wind energy density were calcu-

lated at a height of 100 m from the ground using Eqs. (19) and (20), respectively. It can be seen that the monthly wind power densities are between 84.470 W/m² and 2030.065 W/m² in Evoudoula, between 82.024 W/m² and 2061.322 W/m² at Ekol, between 81.715 W/m² and 1930.587 W/m² in Etok, between 82.449 W/m² and 2067.827 W/m² in Ayos, between 82.239 W/m² and 2054.590 W/m² in Okok, between 84.321 W/m² and 2058.789 W/m² in Nkolkougda, between 76.901 W/m² and 1901.601 W/m² in Ntouda, between 77.848 W/m² and 1934.946 W/m² in Ngobo, between 26.512 W/m² and 629.918 W/m² at Nkolmeyos II, between 78.795 W/m² and 1927.960 W/m² at Nkotabel, between 79.953 W/m² and 1871.350 W/m² in Nkolabang, and between 76.164 W/m² and 1779.878 W/m² in Nloundou. Additionally, the monthly wind energy densities are in the range of 29.598 to 711.335 MWh/m² at Evoudoula, are in

TABLE 2: The results of the summary of the values according to a method (EPFM) chosen and a method (MEPFM) proposed at 100 m above ground level (AGL): summary of the values of the parameters linked to the power of the wind, namely, the parameters of Weibull (K and C), the average speed (V_m), the wind power density (WPD), and the wind energy density present in the wind (WED) for Evodoula, Ekol, and Etok.

Locations Mast height Methods	Evodoula						Ekol 100 m						Etok					
	EPFM		MEPFM		EPFM		MEPFM		EPFM		MEPFM		EPFM		MEPFM			
	K (-)	C (m/s)	V_m (m/s)	WPD (W/m^2)	WED (MWh/m^2)	K (-)	C (m/s)	V_m (m/s)	WPD (W/m^2)	WED (MWh/m^2)	K (-)	C (m/s)	V_m (m/s)	WPD (W/m^2)	WED (MWh/m^2)			
January	3.056	2.373	2.121	295.187	103.434	3.051	2.376	2.123	296.575	103.92	3.037	2.326	2.078	279.057	97.781			
February	3.860	3.509	3.174	838.993	293.983	3.837	3.526	3.188	853.813	299.176	3.858	3.440	3.112	790.598	277.026			
March	4.459	3.842	3.504	1026.326	359.625	4.453	3.879	3.538	1057.380	370.506	4.468	3.773	3.442	971.206	340.311			
April	4.074	3.378	3.065	728.312	255.200	4.061	3.406	3.090	748.051	262.117	4.091	3.325	3.017	693.227	242.907			
May	4.106	3.026	2.746	521.499	182.733	4.087	3.038	2.757	529.005	185.363	4.124	2.987	2.712	500.605	175.412			
June	4.387	3.869	3.525	1055.866	369.976	4.378	3.885	3.540	1070.260	375.019	4.395	3.809	3.471	1006.663	352.735			
July	4.540	4.668	4.262	1825.382	639.614	4.536	4.694	4.285	1856.643	650.568	4.543	4.589	4.190	1734.203	607.665			
August	4.534	4.835	4.414	2030.065	711.335	4.529	4.859	4.436	2061.322	722.287	4.537	4.755	4.342	1930.587	676.478			
September	4.435	3.946	3.598	1114.947	390.677	4.426	3.954	3.604	1122.377	393.281	4.441	3.887	3.544	1064.554	373.020			
October	3.684	2.590	2.337	345.464	121.051	3.623	2.568	2.315	339.656	119.015	3.722	2.567	2.317	334.409	117.177			
November	1.684	1.303	1.163	84.470	29.598	1.697	1.295	1.156	82.024	28.741	1.662	1.280	1.144	81.715	28.633			
December	2.726	1.812	1.612	141.337	49.524	2.713	1.830	1.628	146.205	51.230	2.701	1.768	1.572	132.241	46.337			
Annual	2.904	3.320	2.960	833.987	292.229	2.889	3.333	2.972	846.942	296.769	2.906	3.265	2.912	793.256	277.957			

TABLE 3: The results of the summary of the values according to a chosen method (EPFM) and a method (MEPFM) proposed at 100 m above ground level (AGL): summary of the values of the parameters linked to the power of the wind, namely, the Weibull parameters (K and C), the average speed (V_m), the wind power density (WPD), and the energy density wind turbine present in the wind (WED) for Ayos, Okok, and Nkolkougda.

Locations Mast height Methods	Ayos						Okok 100 m						Nkolkougda					
	EPFM		MEPFM		EPFM		MEPFM		EPFM		MEPFM		EPFM		MEPFM			
	K (-)	C (m/s)	V_m (m/s)	WPD (W/m ²)	WED (MWh/m ²)	K (-)	C (m/s)	V_m (m/s)	WPD (W/m ²)	WED (MWh/m ²)	K (-)	C (m/s)	V_m (m/s)	WPD (W/m ²)	WED (MWh/m ²)			
January	3.099	2.404	2.150	304.311	106.630	2.997	2.348	2.097	289.341	101.385	3.053	2.379	2.126	297.634	104.291			
February	3.863	3.541	3.203	861.492	301.867	3.818	3.513	3.176	846.268	296.532	3.855	3.523	3.187	849.689	297.731			
March	4.446	3.871	3.530	1051.498	368.445	4.459	3.888	3.546	1063.667	372.709	4.459	3.868	3.528	1047.438	367.022			
April	4.048	3.391	3.075	739.104	258.982	4.071	3.422	3.105	757.998	265.602	4.071	3.398	3.083	742.084	260.026			
May	4.078	3.023	2.744	522.120	182.951	4.105	3.058	2.776	538.550	188.708	4.102	3.040	2.760	529.300	185.467			
June	4.372	3.876	3.531	1063.886	372.785	4.386	3.891	3.545	1074.423	376.478	4.385	3.887	3.541	1070.910	375.247			
July	4.535	4.697	4.288	1860.113	651.784	4.537	4.691	4.283	1852.583	649.145	4.539	4.692	4.284	1854.382	649.776			
August	4.526	4.864	4.440	2067.827	724.566	4.530	4.854	4.431	2054.590	719.928	4.532	4.858	4.435	2058.789	721.400			
September	4.422	3.953	3.604	1122.434	393.301	4.429	3.955	3.606	1123.204	393.571	4.431	3.960	3.611	1127.367	395.029			
October	3.601	2.561	2.308	338.007	118.437	3.643	2.579	2.325	343.104	120.224	3.666	2.593	2.339	347.513	121.769			
November	1.717	1.304	1.163	82.449	28.890	1.681	1.290	1.152	82.239	28.817	1.692	1.305	1.165	84.321	29.546			
December	2.766	1.850	1.647	149.010	52.213	2.659	1.804	1.604	142.026	49.766	2.721	1.821	1.620	143.642	50.332			
Annual	2.884	3.332	2.974	846.854	296.738	2.883	3.332	2.971	847.333	296.905	2.899	3.334	2.973	846.089	296.47			

TABLE 4: The results of the summary of the values according to a method (EPFM) chosen and a method (MEPFM) proposed at 100 m above ground level (AGL): summary of the values of the parameters linked to the power of the wind, namely, the parameters of Weibull (K and C), the average speed (V_m), the wind power density (WPD), and the wind energy density present in the wind (WED) for Ntouda, Ngobo, and Nkolmeyos II.

Locations Mast height Methods	Ntouda						Ngobo 100 m						Nkolmeyos II					
	EPFM		MEPFM		EPFM		MEPFM		EPFM		MEPFM		EPFM		MEPFM			
	K (-)	C (m/s)	V_m (m/s)	WPD (W/m ²)	WED (MWh/m ²)	K (-)	C (m/s)	V_m (m/s)	WPD (W/m ²)	WED (MWh/m ²)	K (-)	C (m/s)	V_m (m/s)	WPD (W/m ²)	WED (MWh/m ²)			
January	2.925	2.258	2.014	261.153	91.508	2.952	2.278	2.033	266.708	93.454	2.933	2.224	1.984	249.077	87.277			
February	3.780	3.406	3.077	775.280	271.658	3.788	3.428	3.098	789.605	276.677	3.803	3.336	3.015	726.204	254.462			
March	4.467	3.800	3.466	992.237	347.680	4.469	3.816	3.481	1004.974	352.143	4.477	3.706	3.381	919.764	322.285			
April	4.095	3.362	3.051	716.198	250.956	4.091	3.373	3.061	723.717	253.591	4.110	3.282	2.980	665.585	233.221			
May	4.130	3.007	2.730	510.440	178.858	4.124	3.016	2.739	515.626	180.675	4.146	2.952	2.681	481.848	168.840			
June	4.393	3.808	3.470	1006.157	352.557	4.391	3.825	3.485	1020.063	357.430	4.400	3.735	3.404	949.115	332.570			
July	4.538	4.577	4.179	1721.005	603.040	4.540	4.597	4.197	1743.825	611.036	4.545	4.488	4.098	1621.600	568.209			
August	4.535	4.731	4.320	1901.601	666.321	4.533	4.758	4.344	1934.946	678.005	4.539	4.644	4.240	1797.711	629.918			
September	4.437	3.863	3.522	1045.648	366.395	4.437	3.882	3.540	1061.418	371.921	4.448	3.798	3.464	992.740	347.856			
October	3.690	2.536	2.289	324.243	113.615	3.678	2.544	2.295	327.751	114.844	3.743	2.515	2.271	313.747	109.937			
November	1.641	1.247	1.115	76.901	26.946	1.649	1.255	1.122	77.848	27.278	1.635	1.238	1.108	75.663	26.512			
December	2.589	1.731	1.538	127.949	44.833	2.612	1.746	1.551	130.276	45.649	2.592	1.691	1.502	119.039	41.711			
Annual	2.875	3.251	2.898	788.235	276.197	2.877	3.267	2.912	799.730	280.225	2.884	3.189	2.844	742.674	260.233			

TABLE 5: The results of the summary of the values according to a method (EPFM) chosen and a method (MEPFM) proposed at 100 m above ground level (AGL): summary of the values of the parameters linked to the power of the wind, namely, the parameters of Weibull (K and C), the average speed (V_m), the wind power density (WPD), and the wind energy density present in the wind (WED) for Nkotabel, Nkolabang, and Nloundou.

Locations Mast height Methods	Nkotabel						Nkolabang 100 m						Nloundou					
	EPFM		MEPFM		EPFM		MEPFM		EPFM		MEPFM		EPFM		MEPFM			
	K (-)	C (m/s)	V_m (m/s)	WPD (W/m ²)	WED (MWh/m ²)	K (-)	C (m/s)	V_m (m/s)	WPD (W/m ²)	WED (MWh/m ²)	K (-)	C (m/s)	V_m (m/s)	WPD (W/m ²)	WED (MWh/m ²)			
January	2.980	2.294	2.048	270.853	94.907	3.004	2.289	2.044	267.575	93.758	2.956	2.229	1.989	249.693	87.492			
February	3.815	3.430	3.101	788.315	276.226	3.847	3.397	3.073	762.747	267.266	3.822	3.328	3.009	719.361	252.064			
March	4.468	3.797	3.464	990.118	346.937	4.471	3.738	3.410	943.928	330.752	4.477	3.680	3.358	900.470	315.525			
April	4.089	3.352	3.042	710.342	248.904	4.100	3.299	2.994	676.335	236.988	4.114	3.258	2.958	650.420	227.907			
May	4.122	3.005	2.728	509.668	178.588	4.133	2.968	2.695	490.656	171.926	4.149	2.934	2.665	472.991	165.736			
June	4.394	3.816	3.478	1012.606	354.817	4.399	3.775	3.440	979.748	343.304	4.405	3.720	3.391	937.022	328.332			
July	4.539	4.593	4.194	1739.131	609.392	4.544	4.545	4.150	1684.485	590.243	4.546	4.469	4.081	1601.285	561.090			
August	4.534	4.753	4.339	1927.960	675.557	4.539	4.707	4.297	1871.350	655.721	4.542	4.629	4.227	1779.878	623.669			
September	4.438	3.881	3.539	1060.178	371.486	4.445	3.848	3.509	1032.844	361.908	4.450	3.789	3.455	985.247	345.231			
October	3.689	2.551	2.302	329.958	115.617	3.743	2.550	2.303	327.025	114.589	3.768	2.520	2.276	314.402	110.166			
November	1.654	1.262	1.128	78.795	27.610	1.658	1.270	1.135	79.953	28.016	1.643	1.243	1.112	76.164	26.688			
December	2.648	1.753	1.558	130.635	45.774	2.670	1.739	1.546	126.854	44.450	2.620	1.690	1.501	117.909	41.315			
Annual	2.887	3.264	2.910	795.713	278.818	2.905	3.233	2.883	770.292	269.91	2.898	3.180	2.835	733.737	257.101			

TABLE 6: Characteristic technical data of the V162-5.6MW, V150-5.6MW, V82-1.65MW, N100-2.5MW and N90-2.5MW wind turbines.

Characteristics of wind turbine models	VESTAS V162-5.6MW	VESTAS V150-5.6MW	VESTAS V82-1.65MW	NORDEX N90-2.5MW	NORDEX N100-2.5MW
Hub height (m)	100/119/125/148/149/166	100/105/125/148/155/166	59/100/108	80/100/120	75/100
Recommended hub height for installation (m)	100	100	100	100	100
Rated power P_N (kW)	5600	5600	1650	2500	2500
Rotor diameter (m)	162	150	82	90	100
Cut-in wind speed V_D (m/s)	3	3	2.5	3	3
Rated wind speed V_N (m/s)	Not defined	Not defined	13	14	12
Recommended rated wind speed V_N (m/s)	14	15	13	14	12
Cut-off wind speed V_C (m/s)	25	25	32	25	20

the range of 28.741 to 722.287 MWh/m² at Ekol, are in the range of 28.633 to 676.478 MWh/m² at Etok, are in the range of 28.890 to 724.566 MWh/m² at Ayos, are in the range of 28.817 to 719.928 MWh/m² at Okok, are in the range of 29.546 to 721.400 MWh/m² at Nkolkougda, are in the range of 26.946 to 666.321 MWh/m² at Ntouda, are in the range of 77.848 to 1934.946 MWh/m² in Ngobo, are within the range of 26.512 to 629,918 MWh/m² at Nkolmeyos II, are in the range of 27.610 to 675.557 MWh/m² at Nkotabel, are in the range of 28.016 to 655.721 MWh/m² at Nkolabang, and are in the range of 26.688 to 623.669 MWh/m² at Nloundou. Moreover, it is seen that the highest wind power density and wind energy density are reached in August (2067.827 W/m² and 724.566 MWh/m²), respectively, at a place called Ayos, and the lowest values are obtained in November (75.663 W/m² and 26.512 MWh/m²), respectively, at a place called Nkolmeyos II as indicated in Tables 3 and 4. From the statistical analysis of these results, it was revealed that “the EPFM corresponded better to the reanalysis data.” “This remark was reinforced by the evaluation of the performances of the distribution used,” while the technical of calculating the available wind power density and the wind energy density revealed “the MEPFM proposed by adhering to the formulation with the aim of estimating the existing wind potential on the selected locations.” The results of this study showed that for each selected location, it falls within class 1 to 8 of the International Wind Classification System, because the average annual wind speed recorded in the location Evodoula was 2.96 m/s, the corresponding annual average power density has been estimated at 833.987 W/m², and the average annual energy density was 292.229 MWh/m²; the average annual wind speed recorded in the place called Ekol was 2.972 m/s, the corresponding annual average power density has been estimated at 846.942 W/m², and the average annual energy density was 296.769 MWh/m²; the average annual wind speed recorded in the place called Etok was 2.912 m/s, the corresponding annual average power density has been estimated at 793.256 W/m², and the average annual energy density was 277.957 MWh/m²; the average annual wind speed recorded in the place called Ayos was 2.974 m/s, the corresponding annual average power density has been esti-

ated at 846.854 W/m², and the average annual energy density was 296.769 MWh/m²; the average annual wind speed recorded in the place called Okok was 2.971 m/s, the corresponding annual average power density has been estimated at 847.333 W/m², and the average annual energy density was 296.905 MWh/m²; the average annual wind speed recorded in the place called Nkolkougda was 2.973 m/s, the corresponding annual average power density has been estimated at 846.089 W/m², and the average annual energy density was 296.47 MWh/m²; the average annual wind speed recorded in the place called Ntouda was 2.898 m/s, the average power density corresponding annual was estimated at 788.235 W/m², and the average annual energy density was 276.197 MWh/m²; the average annual wind speed recorded in the place called Ngobo was 2.912 m/s, the corresponding annual average power density has been estimated at 799.730 W/m², and the average annual energy density was 280.225 MWh/m²; the average annual wind speed recorded in the place called Nkolmeyos II was 2.844 m/s, the corresponding annual average power density has been estimated at 742.674 W/m², and the average annual energy density was 260.233 MWh/m²; the average annual wind speed recorded in the place called Nkotabel was 2.910 m/s, the corresponding annual average power density has been estimated at 795.713 W/m², and the average annual energy density was 278.818 MWh/m²; the average annual wind speed recorded in the place called Nkolabang was 2.883 m/s, the corresponding annual average power density has been estimated at 770.292 W/m², and the average annual energy density was 269.91 MWh/m²; and the average annual wind speed recorded in the place called Nloundou was 2.835 m/s, the corresponding annual average power density has been estimated at 733.737 W/m², and the average annual energy density was 257.101 MWh/m².

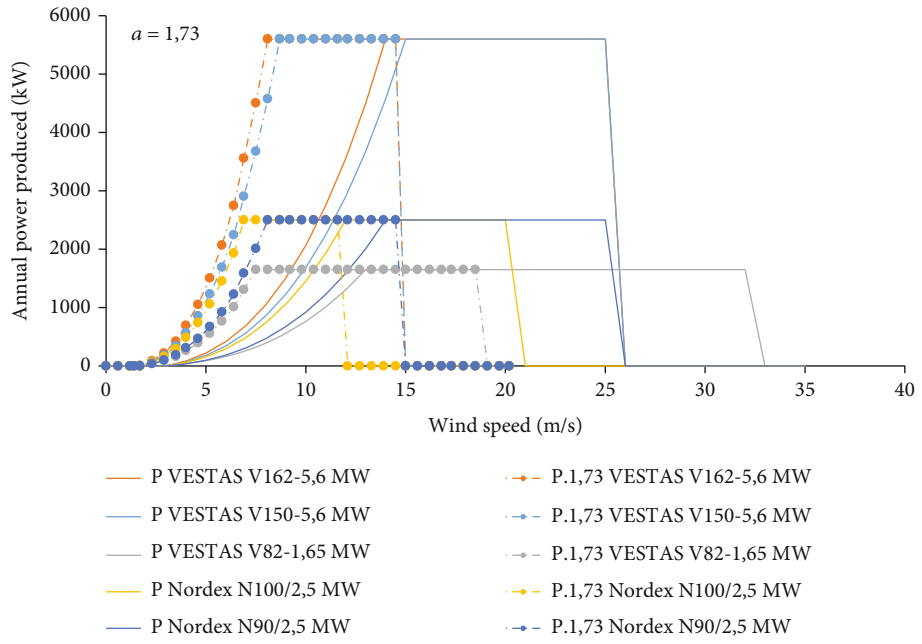
4.2. *Performance of Selected Wind Turbines and Technical Analysis of Wind Power Generation Potential.* Selected wind turbines that will satisfy the estimated annual energy for the selected location are shown in Table 6. In the present work, five different models of wind turbines, 1 of medium power and 4 of high power, were used in order to know which

model of wind turbine will produce more energy. The selection of these wind turbines was made after an overall comparison between the different models of wind turbines. In addition, the different models used for the estimation of the wind turbine output power were applied to the data of the five wind turbines (V162-5.6MW, V150-5.6MW, V82-1.65MW, N100-2.5MW, and N90-2.5MW) provided by the manufacturers. The blades are located at the level of the hub, and one must take into account the height of the mast of the wind turbine for the power calculations. In this study, to evaluate the annual performance of the five wind turbines in the selected location, the annual average output energy produced by each turbine and the annual capacity factors of the different wind turbine models were calculated using Eqs. (26)–(29) and (31).

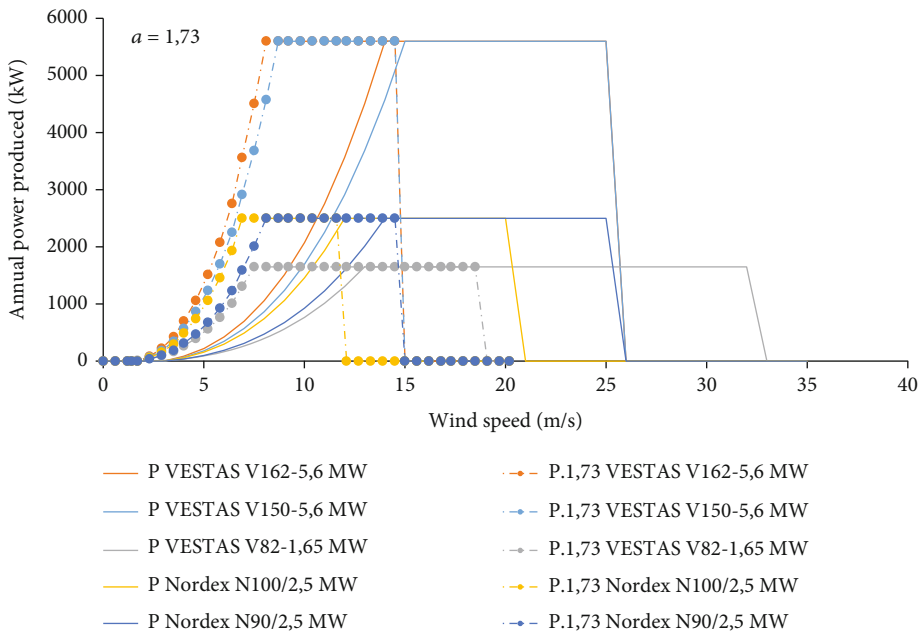
The calculation of the production requires making the assumption of a certain power curve. The problem here is that the observations are made on the surface, that is to say, at a height of 10 m where the wind is much weaker than at an altitude of 80 to 100 meters where the current wind turbines are located. So, using a classic power curve for such an altitude will lead to almost zero productions where very few speeds exceed the starting wind speed (3 or 4 m/s). To remedy this problem, one relies on the power curve explained in Section 3.3.9 using Eq. (22), for its mathematical expression explained and plotted in Figure 11, but a linear transformation equivalent to that of the first power curve is applied to it. To fill this research gap, which has an important element of review, this study demonstrates, to make a difference with other publications which may take the form of comparison and/or critique. For this, we propose a new method for optimizing a modified parameterized power model which is developed in Eq. (24). Thereafter, a calculation of the annual energy production more efficient by the use of the modulation factor “ a ” is established in Eq. (23), which represents a new methodology for a search criterion. Figure 11 illustrates the classic annual power curve of the selected wind turbines and the annual adaptive power curve derived from the previous one by equivalent linear transformation of factor a . For example, in Okok, the dotted pink curve corresponds to a scalable adaptability performance factor $a = 1.73$. This shifts the curve towards weaker winds. This value $a = 1.73$ is not insignificant, and it corresponds to an extrapolation from 10 to 100 m each step wind speed of 1 m/s assuming a corrected Mikhael power law. We will use this fixed value, or else, we will adjust a so as to have a realistic load factor. This corresponds in a way to extending the mast of the wind turbine to a height where the winds are sufficient. These figures show the power-speed characteristics of these five wind turbines selected, based on data from the manufacturers, the twelve locations selected, and the simulation results of these characteristics from the chosen modified quadratic model. In order to ensure the validation of the chosen model, we compared the values V_i of the speed of the undisturbed free wind at hub height interpolated at each step i of $1 \text{ m}\cdot\text{s}^{-1}$, with the values V_a of the speed of the adjusted wind using Eq. (25) obtained by simulation in Excel. We will present the results obtained on these figures

(see Figure 11), comparative graphs with the classic annual power curve of the wind turbines selected from the previous one by linear transformation equivalent to modulating factor “ a ” of the simulated model with the monthly data estimated at 100 m in the twelve locations considered in the EEZ of Evodoula. The curves representative of the interpolated values and those fitted by each of the models were first drawn up on the same curve, after which, we selected the one that best fits the estimated (interpolated) wind speed data at each location of the EEZ at Evodoula. However, a comparison of these two models used using the monthly data for the twelve locations at a height of 100 m represented in Figure 11 is carried out on the basis of the characteristic power speeds of wind turbines, i.e., rated power P_N , cut-in speed V_D , rated speed V_N , cut-off speed V_C , and the Weibull parameters K extrapolated from the twelve locations (as shown in Tables 2–5) at the height of the hub of the wind turbine at 100 m according to the altitude recommended in this work. We concluded that the modified quadratic model is better suited for wind turbines at this height than the quadratic model which underestimates the power and therefore the productivity (estimated production). Thus, our choice fell on the modified Pallabazzer model. This result then contradicts Pallabazzer [68] and Pallabazzer and Gabow [69]. The annual comparison results from simulations of the performance of the two models indicated a modulating factor a of between 1.67 and 1.73 over the twelve locations (see Figure 11). It can be seen that for locations Evodoula, Ekol, Okok, Nkolougda, and Ayos, an identical modulating factor $a = 1.73$ (very windy locations) was indicated, and for locations Etok, Ngobo, Ntouda, and Nkotabel, an identical modulating factor $a = 1.7$ was shown (less windy locations). However, location Nkolabang showed a different modulating factor $a = 1.69$ (little windy location), and as for locations Nloundou and Nkolmeyos II, an identical modulating factor $a = 1.67$ was shown (slightly windy locations). Therefore, we will rely on the choice made on the modified quadratic model to determine the energy produced annually, the number of production hours at rated power, the total number of hours produced annually, and the capacity or load factor which result on the twelve locations. That being said, we will deduce the choice of proven (optimal) location, so the known location is Okok.

In Table 7, we represent the values reflecting the estimate of the energy produced by the wind farms for different rated powers, the number of production hours at rated power, and the total number of hours produced annually over the data collection period of 8760×40 for the twelve locations selected for the five wind turbines. The results obtained are tabulated in this table showing the gross and net annual energy production (AEP) and the capacity factors (CF) of the wind turbines calculated using two methods, namely, the conventional method and the uncertainty method. It can be noted that the highest capacity factor of 18.4% is obtained almost identically in the locations Okok and Ayos with NORDEX N100-2.5MW as indicated in Table 7. This can be attributed to the rated speed of 12 m/s and the generation time of 19336.41849 h and

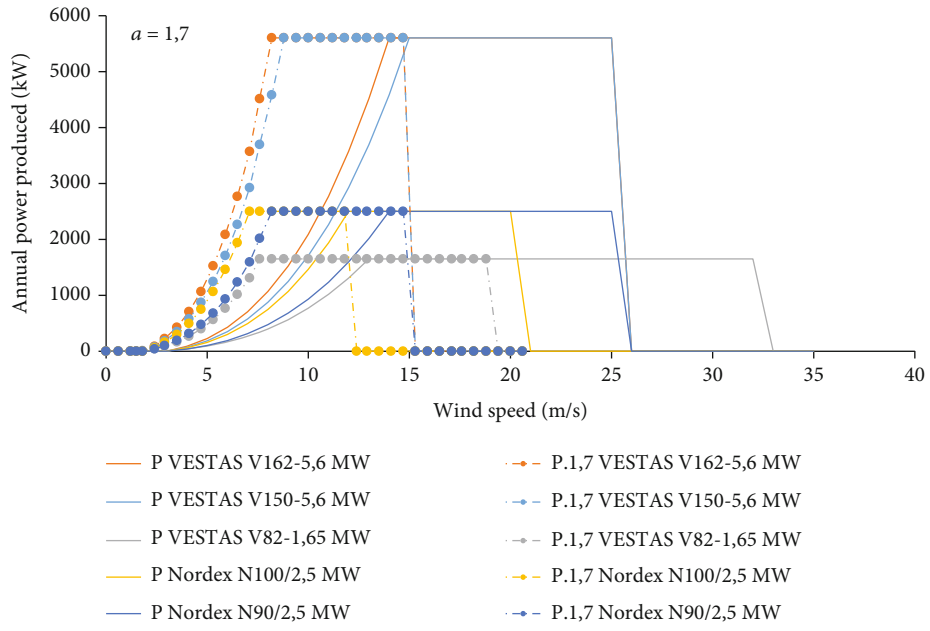


(a) Evodoula

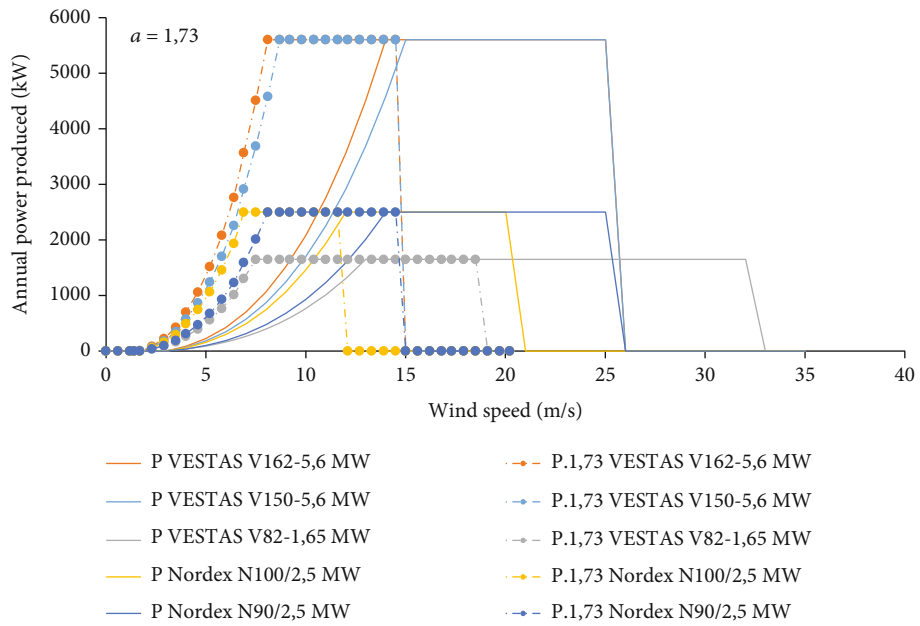


(b) Ekol

FIGURE 11: Continued.

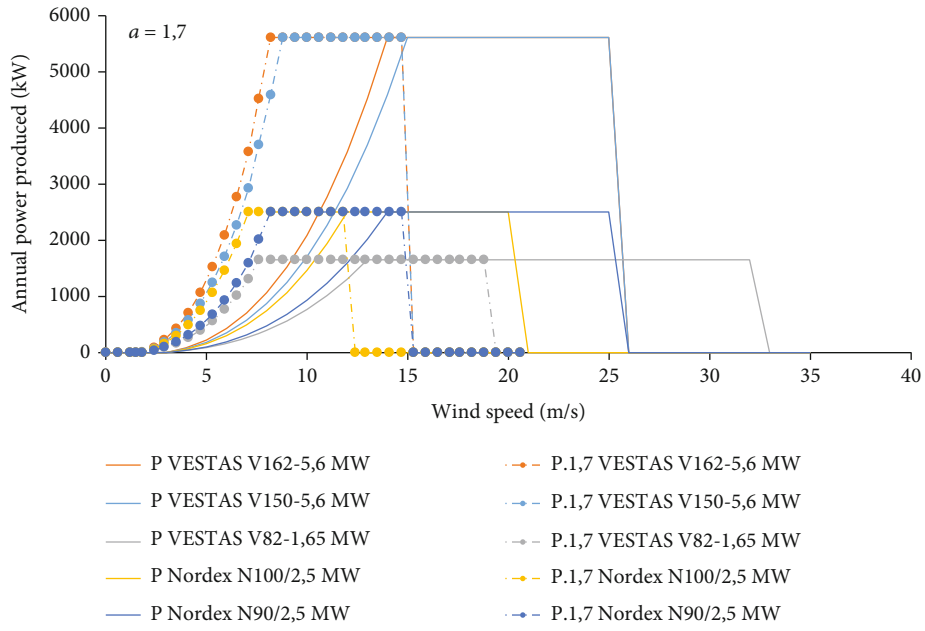


(c) Ntouda

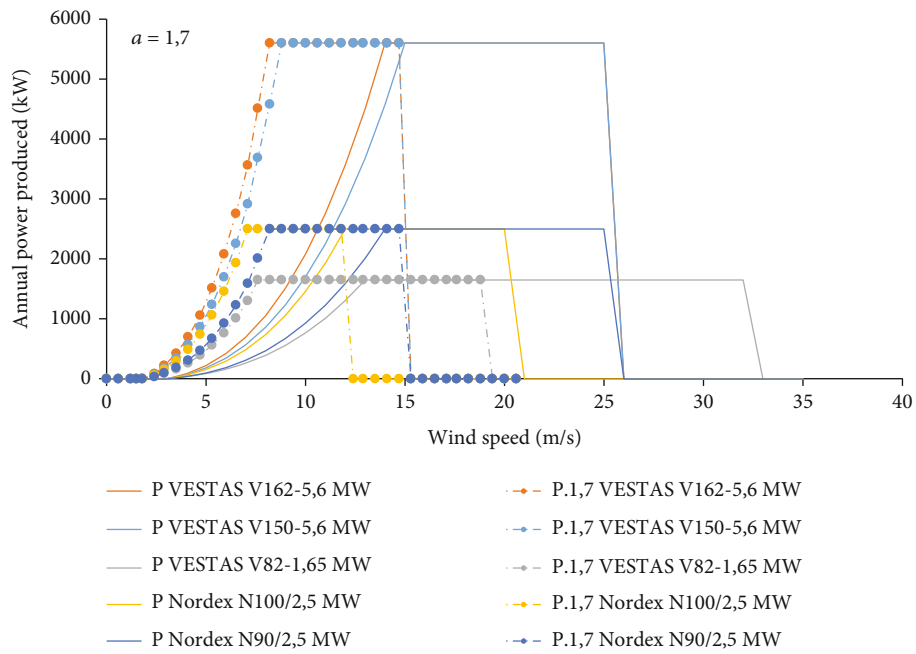


(d) Okok

FIGURE 11: Continued.

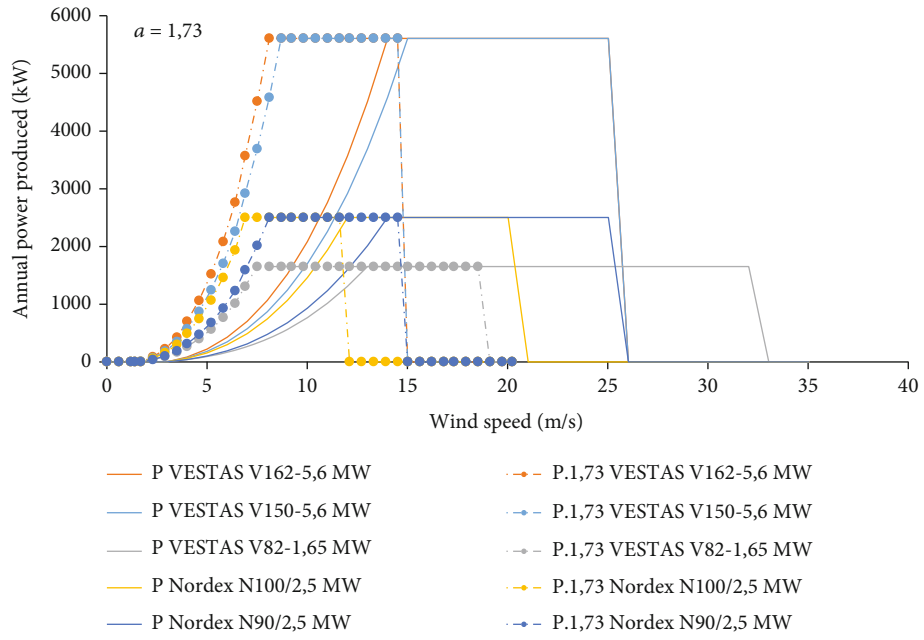


(e) Ngobo

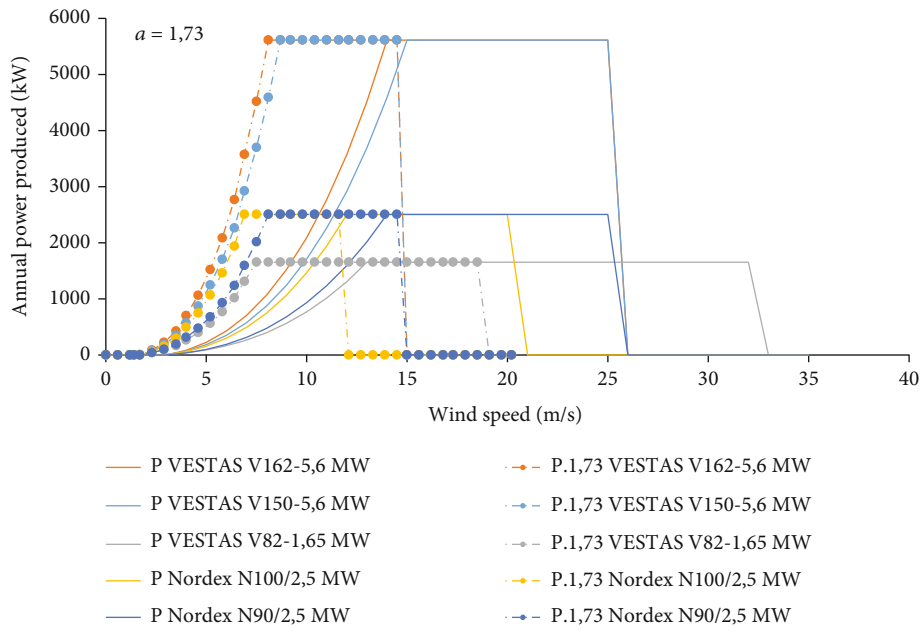


(f) Nkotabel

FIGURE 11: Continued.

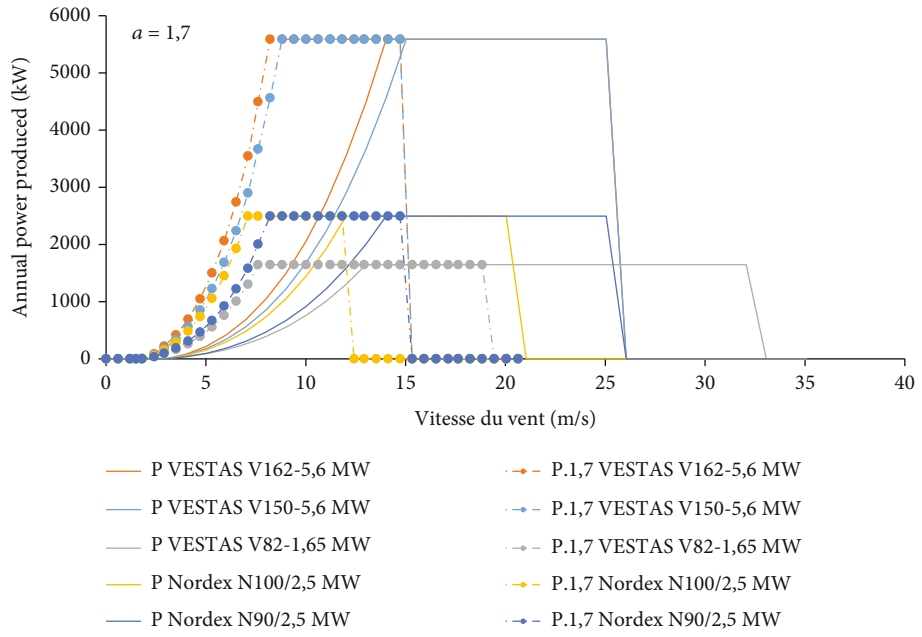


(g) Nkolkougda

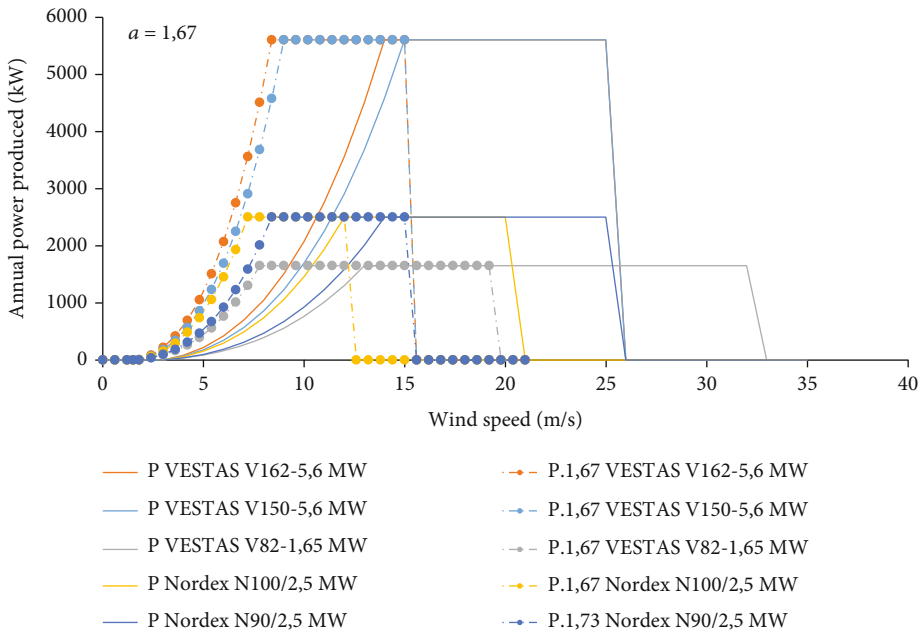


(h) Ayos

FIGURE 11: Continued.



(i) Etok



(j) Nloundou

FIGURE 11: Continued.

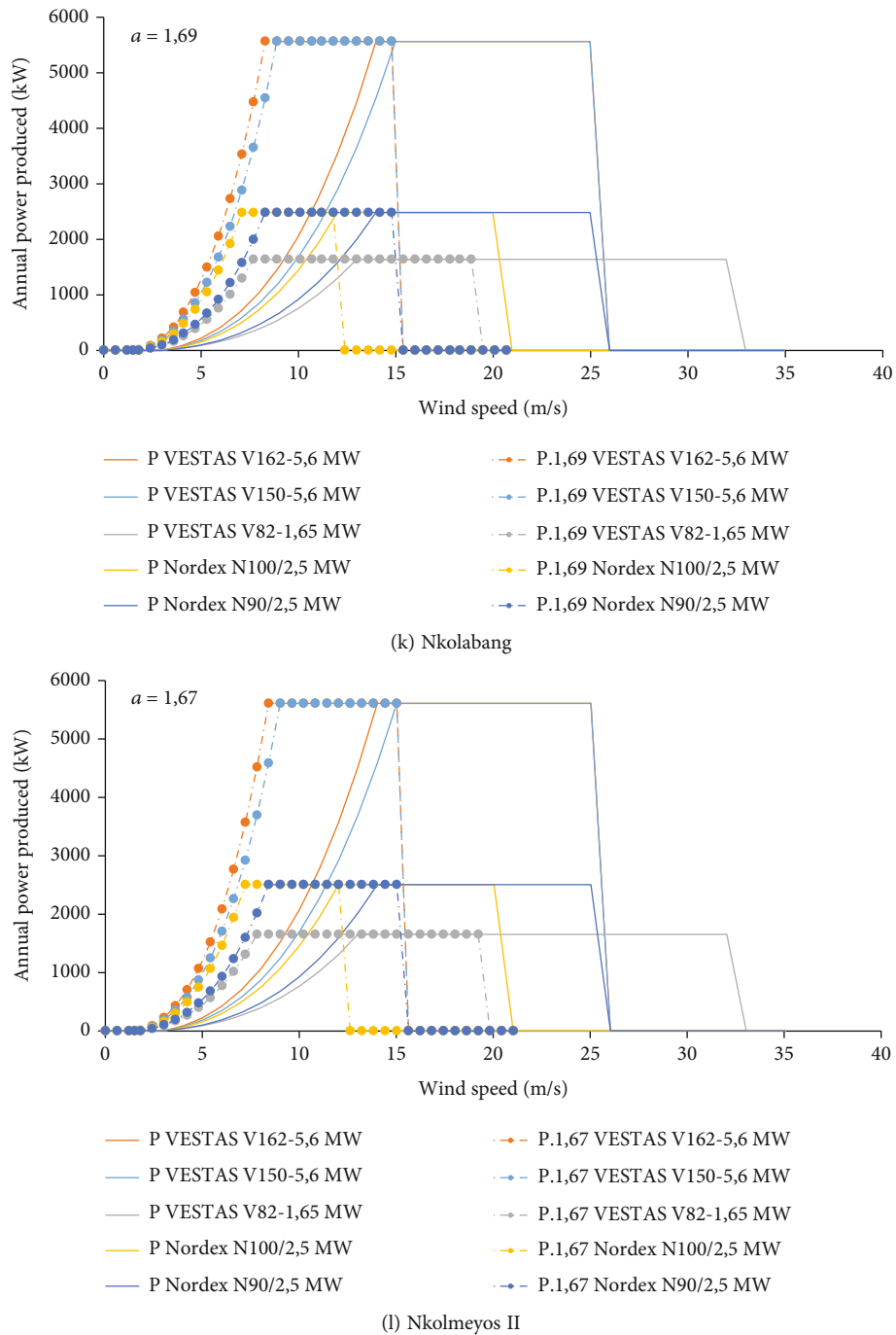


FIGURE 11: Strong line: classic annual power curves (quadratic model) of the selected wind turbines. Dotted line: annual adaptive power curves (modified quadratic model) of the wind turbines selected from the previous one by linear transformation equivalent to factor “ a ” selected locations.

19320.10361 h, obtained by the conventional method, or from 51270.00451 h to 51197.81828 h obtained by the uncertainty method, respectively, for the two aforementioned locations, which is superior to other wind turbine models. In addition, the VESTAS V150-5.6MW wind turbine model produces the lowest annual energy compared to other models and has the lowest capacity factor of 6.8%. This can be attributed to the higher rated speed and generation time of 7133.228008 h obtained by the conven-

tional method. In general, the capacity factor is greater for wind turbines with lower rated speed. This remark was observed both for large wind turbines and for small wind turbines. Moreover, Table 7 shows simulation results for a sample point in the domain. The AEP at each point was calculated by the conventional method. The total AEP of the wind farm with an installed capacity of 12.5MW of the NORDEX N100-2.5MW wind turbine of the twelve locations of the commune of Evdoula calculated from the

TABLE 7: Comparison between the two methods of calculating annual energy production, capacity factor, the number of production hours at rated power, and the total number of hours produced annually locations selected for the five wind turbines.

Wind turbines	Number of wind turbines (N_{wt})	Locations	CF (%)	Conventional method				Uncertainty method					
				Gross annual energy production AEP Gross (GWh) of a wind turbine	Net annual energy production AEP Net (GWh) of a wind turbine	Net annual energy production AEP Net produced by the fleet (GWh)/total energy produced (TEP)	Nhepn (number of production hours at nominal power)	Nh (total number of hours produced annually over the data collection period; its value is 8760 * 40	Gross annual energy production AEP Gross (GWh) of a wind turbine	Net annual energy production AEP Net (GWh) of a wind turbine	Net annual energy production AEP Net produced by the fleet (GWh)/total energy produced (TEP)	Nhepn (number of production hours at nominal power)	Nh (total number of hours produced annually over the data collection period; its value is 8760 * 40
VESTAS V162-5.6MW	5	Evodoula	11.4	223.4395183	67.0318555	335.1592775	11969.9742	663862.1392	685.8853562	205.7656069	1028.28034	-	-
		Ekol	11.7	229.0290554	68.70871661	343.543583	12269.41368	663590.1763	713.964415	214.1893245	1070.946622	-	-
		Ntounda	10	197.0015674	59.10047022	295.5023511	10553.6554	669585.8089	571.5539485	171.4661846	857.3309228	-	-
		Okok	11.7	229.9394475	68.98183425	344.9091713	12318.18469	663787.6111	717.1328017	215.1398405	1075.699202	-	-
		Ngofo	10.2	199.8824531	59.96473592	299.8236796	10707.98856	668583.3471	588.3693665	176.5108099	882.5540497	-	-
		Nkotabel	10.1	197.6070923	59.2821277	296.4106385	10586.09423	668590.7561	578.730364	173.6251092	868.1255461	-	-
		Nkolkougda	11.6	227.5695224	68.27085671	341.3542835	12191.22441	663304.9536	708.6998177	212.6099453	1063.049727	-	-
		Ayos	11.7	229.7258378	68.91775134	344.5887567	12306.74131	663795.7257	716.0620092	214.8186028	1074.093014	-	-
		Etok	9.9	194.7470152	58.42410455	292.1205227	10432.87581	668197.2009	568.6120048	170.5836014	852.9180072	-	-
		Nloundou	8.3	162.9702438	48.89107314	244.4553657	8730.548776	652465.036	440.1297427	132.0389228	660.1946141	-	-
VESTAS V150-5.6MW	5	Nkolabang	9.5	186.1161524	55.83484573	279.1742287	9970.508166	663380.0529	527.6808969	158.3042691	791.5213454	-	-
		Nkolmeyos II	8.5	166.7533057	50.0259917	250.1299585	8933.212803	652254.5403	455.8322486	136.7496746	683.7483728	-	-
		Evodoula	9.3	182.4940762	54.74822287	273.7411144	9776.46837	663862.1392	480.2654104	144.0796231	720.3981157	-	-
		Ekol	9.5	187.2356586	56.17069757	280.8534878	10030.48171	663590.1763	500.3979713	150.1193914	750.5969569	-	-
		Ntounda	8.2	161.2102412	48.36307235	241.8153618	8636.26292	669585.8089	400.9787555	120.2935726	601.4678632	-	-
		Okok	9.6	188.0587072	56.41761215	282.0880607	10074.5736	663787.6111	502.8292619	150.8487786	754.2438929	-	-
		Ngofo	8.3	163.5423306	49.06269919	245.3134959	8761.196283	668583.3471	412.7114882	123.8134464	619.0672322	-	-
		Nkotabel	8.2	161.571467	48.47144011	242.3572006	8655.614306	668590.7561	405.6901009	121.7070303	608.5351514	-	-
		Nkolkougda	9.5	185.9235746	55.77707239	278.885362	9960.191498	663304.9536	496.3907464	148.9172239	744.5861196	-	-
		Ayos	9.6	187.8768849	56.36306547	281.8153274	10064.83312	663795.7257	502.0594345	150.6178303	753.0891517	-	-
VESTAS V82-1.65MW	5	Etok	8.1	159.0308552	47.70925657	238.5462828	8519.510101	668197.2009	398.0774732	119.423242	597.1162098	-	-
		Nloundou	6.8	133.1535895	39.94607685	199.7303842	7133.228008	652465.036	308.294853	92.48845589	462.4422795	-	-
		Nkolabang	7.7	151.9996322	45.59988966	227.9994483	8142.837439	663380.0529	369.4629014	110.8388704	554.1943521	-	-
		Nkolmeyos II	6.9	136.3751711	40.91255133	204.5627566	7305.812737	652254.5403	319.6000925	95.88002774	479.4001387	-	-
		Evodoula	15	86.76500306	26.02950092	130.1475046	15775.4551	37593.17511	231.5987692	69.47963077	347.3981538	-	-
		Ekol	15.4	88.80189516	26.64056855	133.2028427	16145.79912	37610.64575	240.717872	72.21536159	361.076808	-	-
		Ntounda	13.3	77.07255794	23.12176738	115.6088369	14013.19235	37628.92428	194.440817	58.33224511	291.6612255	-	-
		Okok	15.4	89.13088692	26.73926608	133.6963304	16205.6158	37618.45035	241.721037	72.51631109	362.5815554	-	-
		Ngofo	13.5	78.12494417	23.43748325	117.1874163	14204.5353	37626.0177	199.9701714	59.99105142	299.9552571	-	-
		Nkotabel	13.4	77.29151846	23.18745554	115.9372777	14053.00336	37613.41251	196.8433309	59.05299926	295.2649963	-	-
VESTAS V82-1.65MW	5	Nkolkougda	15.3	88.27395651	26.48218695	132.4109348	16049.81027	37598.77924	239.0456978	71.71370935	358.5685468	-	-
		Ayos	15.4	89.05315453	26.71594636	133.5797318	16191.48264	37617.74393	241.3738476	72.41215427	362.0607714	-	-
		Etok	13.2	76.24197527	22.87259258	114.3629629	13862.17732	37589.85817	193.570633	58.0718991	290.3355946	-	-
		Nloundou	11.1	64.43548998	19.33064699	96.65323497	11715.54363	37599.83192	151.3204606	45.39613817	226.9806909	-	-
		Nkolabang	12.6	73.02083603	21.90625081	109.531254	13276.51564	37591.89872	180.0255821	54.00767462	270.0383731	-	-
		Nkolmeyos II	11.4	65.83334622	19.75000387	98.75001933	11969.69931	37617.65372	156.4864151	46.94592453	234.7296226	-	-

TABLE 7: Continued.

Wind turbines	Number of wind turbines (N_{wt})	Locations	CF (%)	Conventional method			Uncertainty method						
				Gross annual energy production (GWh) of a wind turbine	Net annual energy production (GWh) of a wind turbine	Nh (total number of hours produced annually over the data collection period; its value is 8760 * 40)	Gross annual energy production (GWh) of a wind turbine	Net annual energy production (GWh) of a wind turbine	Nh (total number of hours produced annually over the data collection period; its value is 8760 * 40)				
NORDEX N100-2.5MW	5	Evodoula	17.9	157.0606123	47.11818369	235.5909185	18847.27348	663862.1392	122.9649394	614.8246968	49185.97574	663862.1392	
		Ekol	18.3	160.648698	48.19460941	240.9730471	19277.84376	663590.1763	127.7278684	638.6393418	51091.14734	663590.1763	
		Ntouda	15.7	137.9015733	41.37047199	206.8523599	16548.1888	669585.8089	340.1402164	102.0420649	510.2103245	40816.82596	669585.8089
		Okok	18.4	161.1368208	48.34104623	241.7052312	19336.41849	663787.6111	427.2500376	128.1750113	640.8750564	51270.00451	663787.6111
		Ngobo	16	139.9646901	41.98940703	209.9470352	16795.76281	668583.3471	350.2636621	105.0790986	525.3954932	42031.63945	668583.3471
		Nkotabel	15.8	138.5794612	41.57383835	207.8691918	16629.53534	668590.7561	345.0554033	103.516621	517.583105	41406.6484	668590.7561
		Nkolkougda	18.2	159.8523903	47.95571708	239.7785854	19182.28683	663304.9536	423.2223287	126.9666986	634.8334931	50786.67945	663304.9536
		Ayos	18.4	161.0008634	48.30025902	241.5012951	19320.10361	663795.7257	426.6484857	127.9945457	639.9727285	51197.81828	663795.7257
		Etok	15.6	136.9591889	41.08775666	205.4387833	16435.10266	668197.2009	339.9676588	101.9902976	509.9514882	40796.11905	668197.2009
		Nloundou	13.1	114.4820601	34.34461803	171.7230901	13737.84721	652465.036	262.8518593	78.85555778	394.2777889	31542.22311	652465.036
		Nkolabang	14.9	130.8624915	39.25874745	196.2937372	15703.49898	663380.0529	315.4305155	94.62915465	473.1457732	37851.66186	663380.0529
		Nkolmeyos II	13.3	116.8911556	35.06734667	175.3367333	14026.93867	652254.5403	271.652347	81.4957041	407.4785205	32598.28164	652254.5403
		NORDEX N90-2.5MW	5	Evodoula	11.4	99.74978496	29.92493549	149.6246774	11969.9742	663862.1392	211.7020491	63.51061473	317.5530737
Ekol	11.7			102.245114	30.6735342	153.367671	19277.84376	663590.1763	220.3687953	66.11063858	330.5531929	663590.1763	
Ntouda	10			87.9471283	26.38413849	131.9206925	10553.6554	669585.8089	176.4130711	52.92392132	264.6196066	669585.8089	
Okok	11.7			102.6515391	30.79546172	153.9773086	12318.18469	663787.6111	221.3467341	66.40402024	332.0201012	663787.6111	
Ngobo	10.2			89.23323798	26.76997139	133.849857	10707.98856	668583.3471	181.6032364	54.48097093	272.408547	668583.3471	
Nkotabel	10.1			88.21745193	26.46523558	132.3261779	10586.09423	668590.7561	178.6342818	53.59028453	267.9514227	668590.7561	
Nkolkougda	11.6			101.5935368	30.47806103	152.3903051	12191.22441	663304.9536	218.7438502	65.62315506	328.1157753	663304.9536	
Ayos	11.7			102.5561776	30.76685328	153.8342664	12306.74131	663795.7257	221.0162285	66.30486856	331.5243428	663795.7257	
Etok	9.9			86.94063176	26.08218953	130.4109476	10432.87581	668197.2009	175.505025	52.65150749	263.2575375	668197.2009	
Nloundou	8.3			72.75457313	21.82637194	109.1318597	8730.548776	652465.036	135.8483128	40.75449383	203.7724692	652465.036	
Nkolabang	9.5			83.08756805	24.92627042	124.6313521	9970.508166	663380.0529	162.8714276	48.86142829	244.3071414	663380.0529	
Nkolmeyos II	8.5			74.44344003	22.33303201	111.66516	8933.212803	652254.5403	140.6949721	42.20849164	211.0424582	652254.5403	

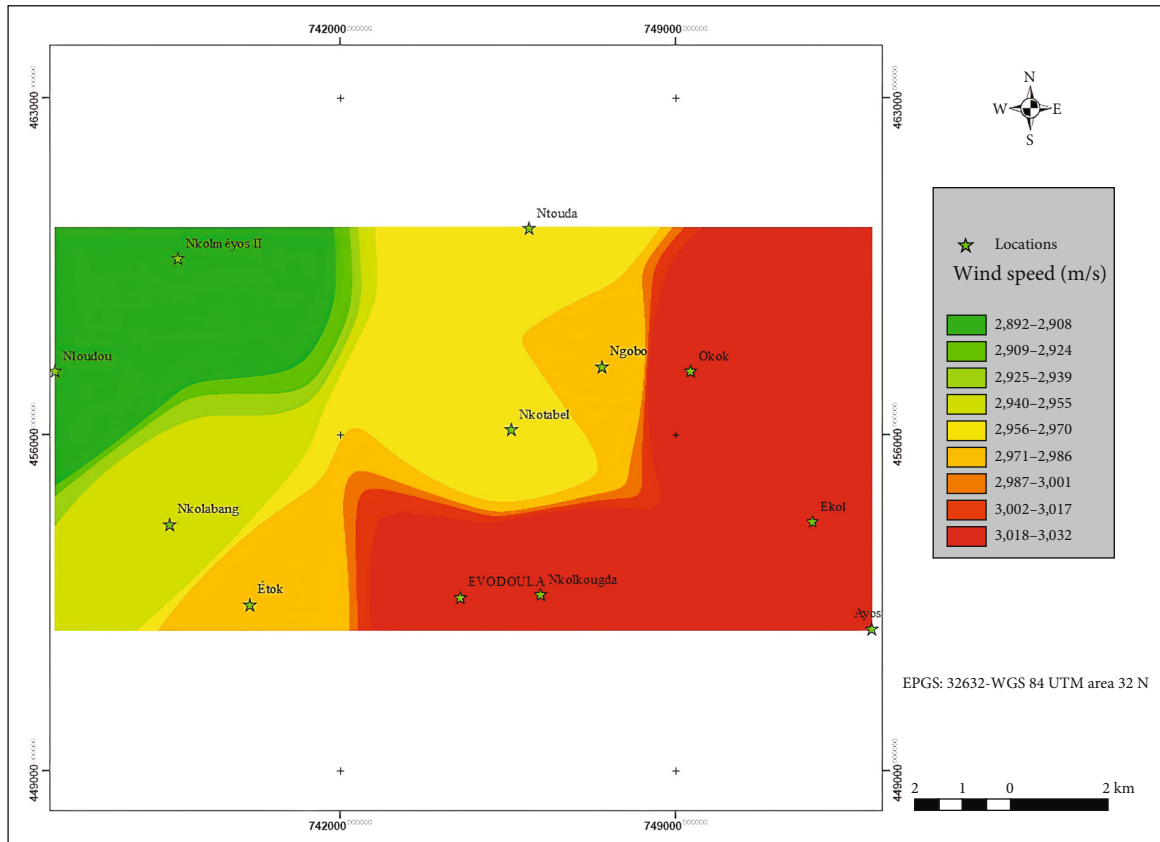
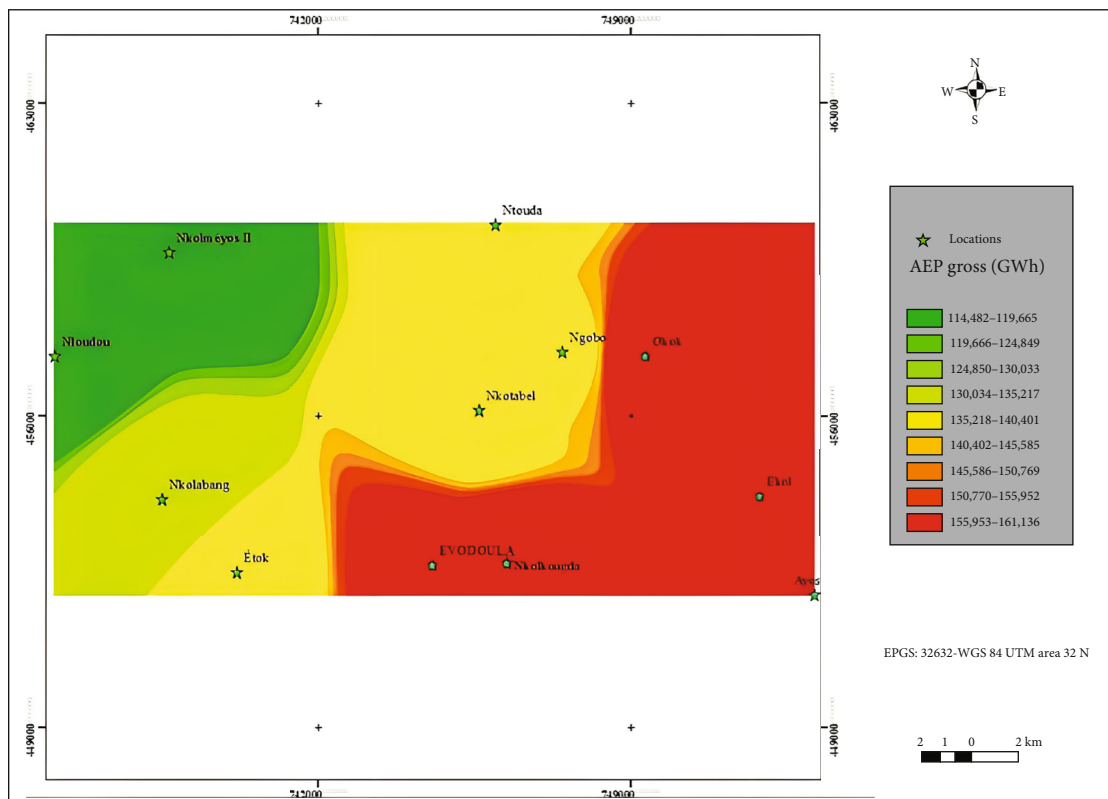


FIGURE 12: Horizontal interpolation of the wind speed at 100 m (AGL) in 2D in the EEZ of Evodoula over the study period 1980-2019.

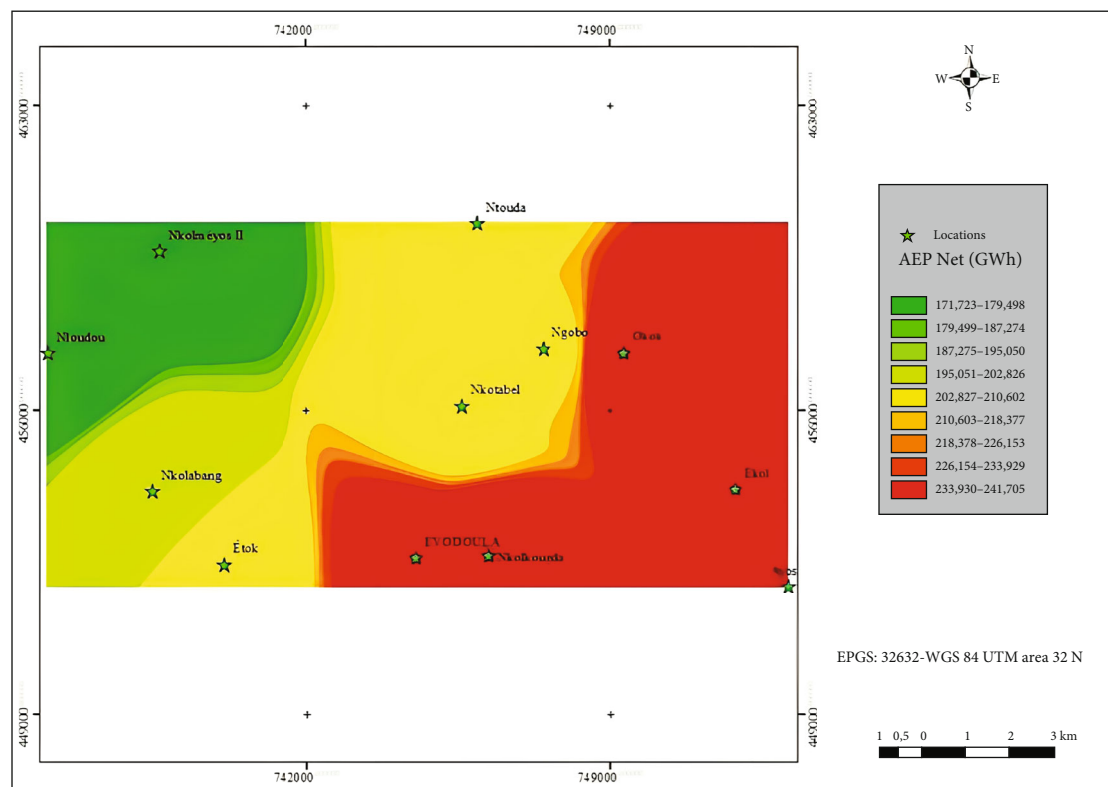
conventional method is 2573.010008 GWh. Or using the modified energy pattern factor method (MEPFM). Thus, the annual Weibull parameters of the twelve selected locations were estimated as indicated in Tables 2–5. The AEP at each point was calculated by the uncertainty method. The total AEP of the wind farm with an installed capacity of 12.5 MW of the NORDEX N100-2.5 MW wind turbine of the twelve locations of the municipality of Evodoula calculated from the uncertainty method is 6507.18781 GWh. Based on the capacity factor, it can be concluded that the NORDEX N100-2.5 MW turbine is cost-effective for Ayos and Okok locations and could be highly recommended for installation. Figure 12 shows the horizontal interpolation of the wind speed at 100 m above ground level (AGL). To show the combined effect of vertical extrapolation and horizontal interpolation of wind speeds, the mean wind speed atlas was plotted at 100 m using the corrected model of Justus and Mikhael [17] given to Eq. (6) and an inverse distance weighting (IDW) interpolation method proposed by the present study illustrated in Eq. (12). If the average annual wind speeds are known for certain places, we can develop a 2D wind resource map in the EEZ of Evodoula estimated at 100 m from the ground represented in Figure 12 which shows the average wind speed at these localities. The observation of this figure shows that favorable aggregated surfaces are available for important wind

energy development zones (ZDEE) of Evodoula EEZ. The determination of all these parameters allows us to identify the windiest areas and therefore the most suitable for the optimal installation of wind farms and to make the best choice for the types of wind turbine to be installed (large or small power), where the cost per kilowatt-hour produced is the least expensive. It can be seen that the best candidate locations for the production of wind energy are Evodoula, Ekol, Okok, Nkolkougda, and Ayos, all of which have an average speed exceeding 3 m/s. We conclude that the windiest and most optimal area is the place called Okok. Areas with a high wind resource are colored in red, located towards the extreme latitudes (452000 and 460500) for a range of variation of the average annual speed ranging from 3.018 m/s at 3.032 m/s, while the areas with low-wind resources are colored green, located towards the extreme latitudes (455000 and 460500) at the locations Nloundou and Nkolmeyes II when the wind speeds are reasonably low following a range of variation of the average wind speed ranging from 2.892 m/s to 2.908 m/s.

Figure 13 presents the average Gross and Net AEP resulting from the conventional method and the uncertainty on the Evodoula EEZ where the amount of AEP in the south-east zone of the EEZ was greater than in the other zones of the map resource. The AEP calculated from the uncertainty method followed a similar trend to the

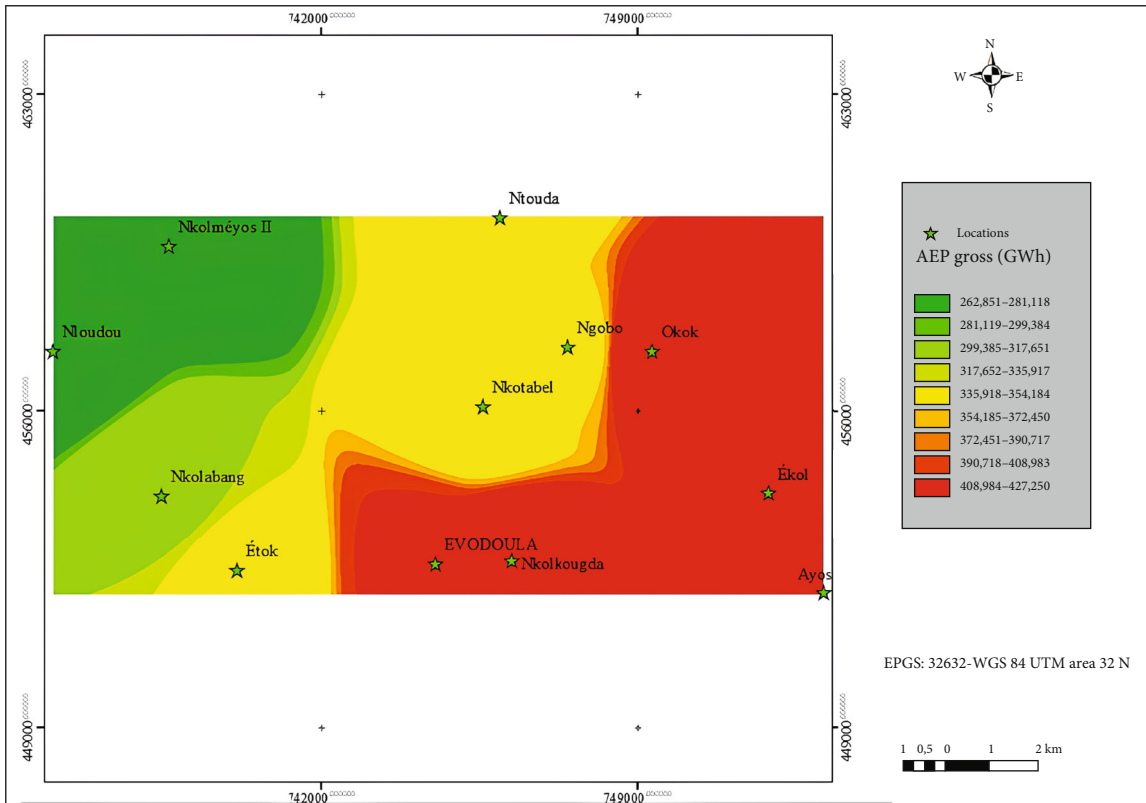


(a)

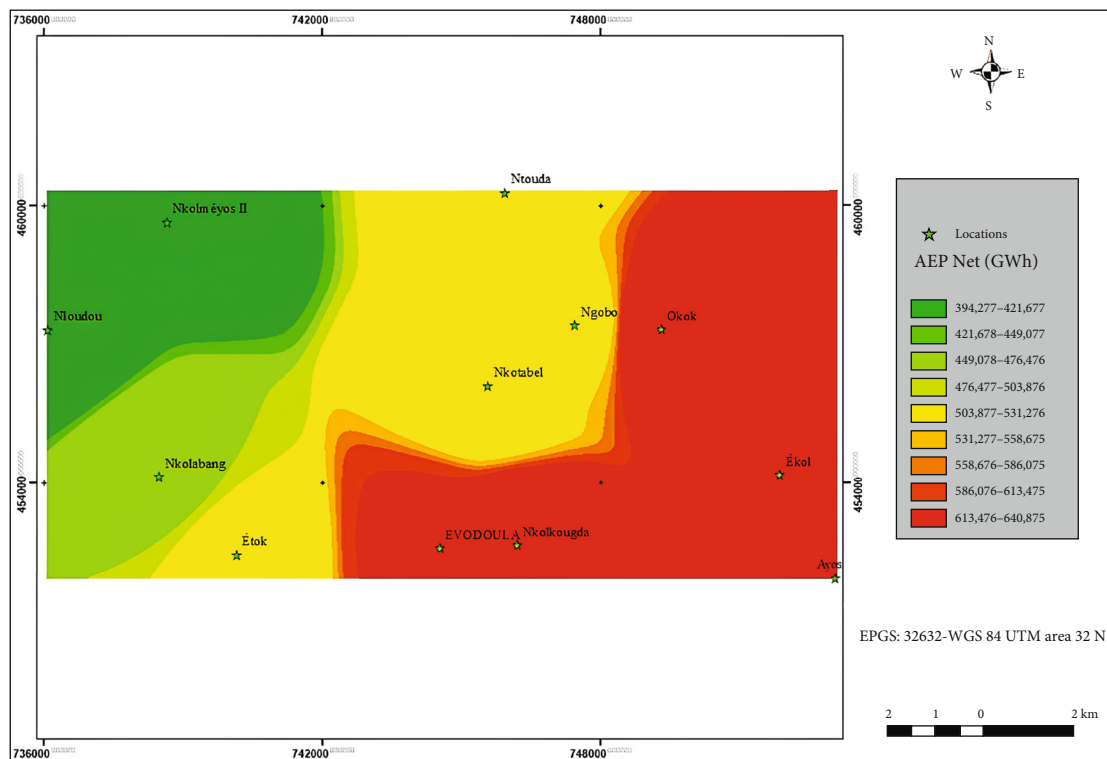


(b)

FIGURE 13: Continued.



(c)



(d)

FIGURE 13: Comparison of the resulting AEP Gross and Net in 2D in the EEZ of Evodoula over the study period of 1980-2019 of (a, b) the conventional method and (c, d) the uncertainty method.

TABLE 8: Specific cost of acquisition of wind turbines (\$/MW).

P_N (MW)	Minimum-maximum specific cost (\$/MW)	Mean specific cost (\$/MW)
<0.02	2.794-3.810	3.302
0.02-0.2	1.587-2.921	2.254
>0.2	0.889-2.032	1.4605

conventional method where the highest AEP values were found in the south-east zone of the EEZ; however, as noted earlier in Table 5, the uncertainty method resulted in sufficiently larger Gross and Net AEPs than the conventional method. The analysis showed that for the conventional method and the uncertainty method, in the north-west zone of the EEZ, the AEP level is low. On the north-east area, most of the time, the average Net AEP varies from 233.930 to 241.705 GWh by the conventional analysis, while by the uncertainty analysis, it almost reaches 613.476 to 640.875 GWh. Another important parameter for specifying the location of the appropriate place name is the stability of the AEP in the area. In addition, the results showed that, using the conventional method, gross AEP varies within a range of 114.482 to 119.665 GWh, in the case of sites Nloundou and Nkolmeyos II, where the amount of gross energy is low, compared to a range of 155.953 to 161.136 GWh in the case of sites Evodoula, Ekol, Nkolkougda, Okok, and Ayos, where the amount of energy is high. As a result, for the values resulting from the uncertainty method, gross AEP varies within a range of 262.851 to 281.118 GWh, in the case of the Nloundou and Nkolmeyos II localities, where the quantity of gross energy is low, versus a range of 408.984 to 427.250 GWh, in the case of the Evodoula, Ekol, Nkolkougda, Okok, and Ayos localities, where the quantity of gross energy is high. The interest of these figures leads to the conclusion that the most optimal area is the place called Okok.

4.3. Annual Estimate of the Cost Production Unitary (CPU) of Wind Electricity Produced per Kilowatt-Hour and the Present Value Cost (PVC). In order to obtain a techno-economic analysis of the energy produced, the costs per kilowatt-hour (kWh) produced by the five wind turbines installed on the selected locations are evaluated using Eqs. (32)–(38), taking into account the estimated annual energy production produced and the annual capacity factor previously assessed with the wind resources available in the twelve localities studied in the study area. This calculation is performed for the mean, minimum, and maximum values of the specific cost of wind turbines (see Table 8). In this table, we can see that the cost per megawatt decreases with the increase in the size of the wind turbine. For the above machine size of 0.2 MW, the mean cost of a wind turbine is around 1.4605 \$/MW, where the minimum cost is in the order of 0.889 \$/MW and the maximum cost is in the order of 2.032 \$/MW.

Figure 14 shows the estimate of the annual variation of the mean, minimum, and maximum cost production unitary of wind electricity produced per kilowatt-hour (CPU),

respectively, of the five wind turbines VESTAS V162-5.6MW, VESTAS V150-5.6MW, VESTAS V82-1.65MW, NORDEX N90-2.5MW, and NORDEX N100-2.5MW at selected locations. The analysis of the results obtained represented in this figure shows that the lowest value of the unit production cost of wind electricity produced per kilowatt-hour varies from $1.45E-04$ \$/kWh to $3.32E-04$ \$/kWh. This value is obtained for the NORDEX N100-2.5MW wind turbine with the wind resources of the place called Okok. The highest unit production cost of generated wind power ranges from $1.58E-03$ \$/kWh to $3.61E-03$ \$/kWh. This last value is obtained for the NORDEX N90-2 wind turbine, 5 MW with the wind resources of the place called Nloundou. Or comparatively, these results show that the lowest value of discounted annual PVC costs (\$ million) ranges from 0.035161181 (\$ million) to 0.080314208 (\$ million). This value is obtained for the NORDEX N100-2.5MW wind turbine with the wind resources of the place called Okok. The costs of the highest present values range from 0.257608306 (\$ million) at 0.588937316 (\$ million) and 0.172638508 (\$ million) at 0.394336161 (\$ million). These last values are obtained for the VESTAS V150-5.6MW and NORDEX N90-2.5MW wind turbines, respectively, with the wind resources of the location Nloundou.

In this study, the following estimates were made. The initial investment cost is equal to the sum of the component costs. The total investment cost is given by Eq. (33). The initial project investment is C_T , and the operation and maintenance cost is M_c , which is 15% of the initial investment. The estimated lifetime of the wind turbine is n to 20 years and a real interest rate is I of 12%. Table 9 represents the investment cost structure for a wind farm.

The PVC-levelized costs of the five wind turbines are estimated using Eq. (36). This calculation is performed for the minimum, mean, and maximum values of the costs of the wind farm, initiated using Eqs. (33) and (34) as indicated in Table 10.

Figure 15 presents the CPU of wind power generated per resulting kilowatt-hour calculated using conventional and uncertainty methods on the Evodoula EEZ where the amount of CPU in the south-east zone of the EEZ was lower than in the other zones of the resource map. The CPU calculated from the uncertainty method followed a similar trend to the conventional method where the lowest CPU values were found in the south-east zone of the EEZ; however, for the central zone of the EEZ, an opposite trend followed according to the two methods; however, as stated earlier since the average AEP calculated using the uncertainty method was higher than the conventional method, the most profitable locations are larger for the uncertainty method. The results showed that the total CPU of the twelve locations in the EEZ of the commune of Evodoula calculated from the conventional method was 0.004471219 CAD\$/kWh or 2.14 XAF/kWh, while that of the total CPU of the twelve locations in the EEZ of the municipality of Evodoula calculated from the uncertainty method was 0.000738888 CAD\$/kWh or 0.35 XAF/kWh. In addition, it can be seen that the lowest and highest values during the period studied (1980-2019) of the average annual

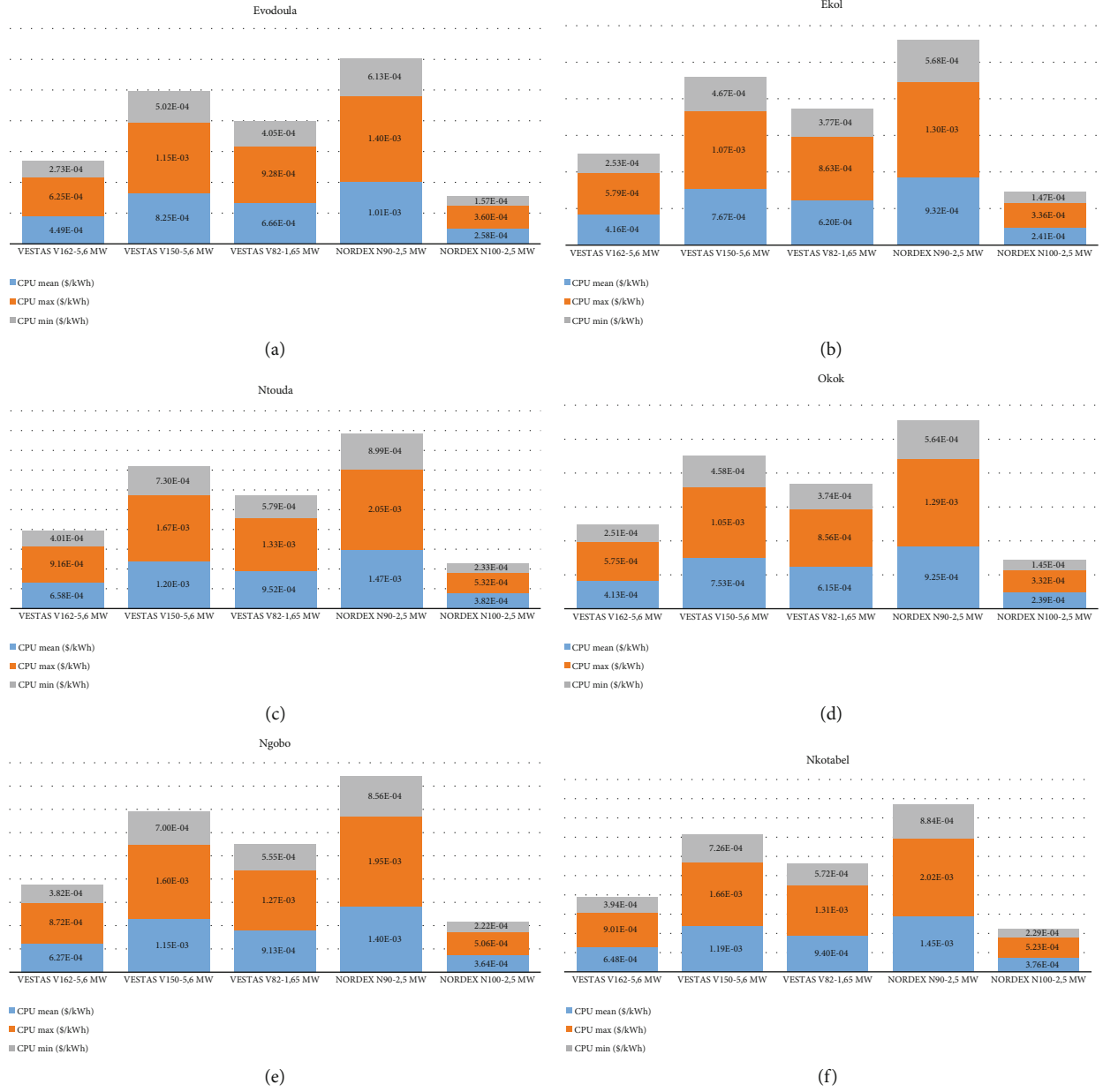


FIGURE 14: Continued.

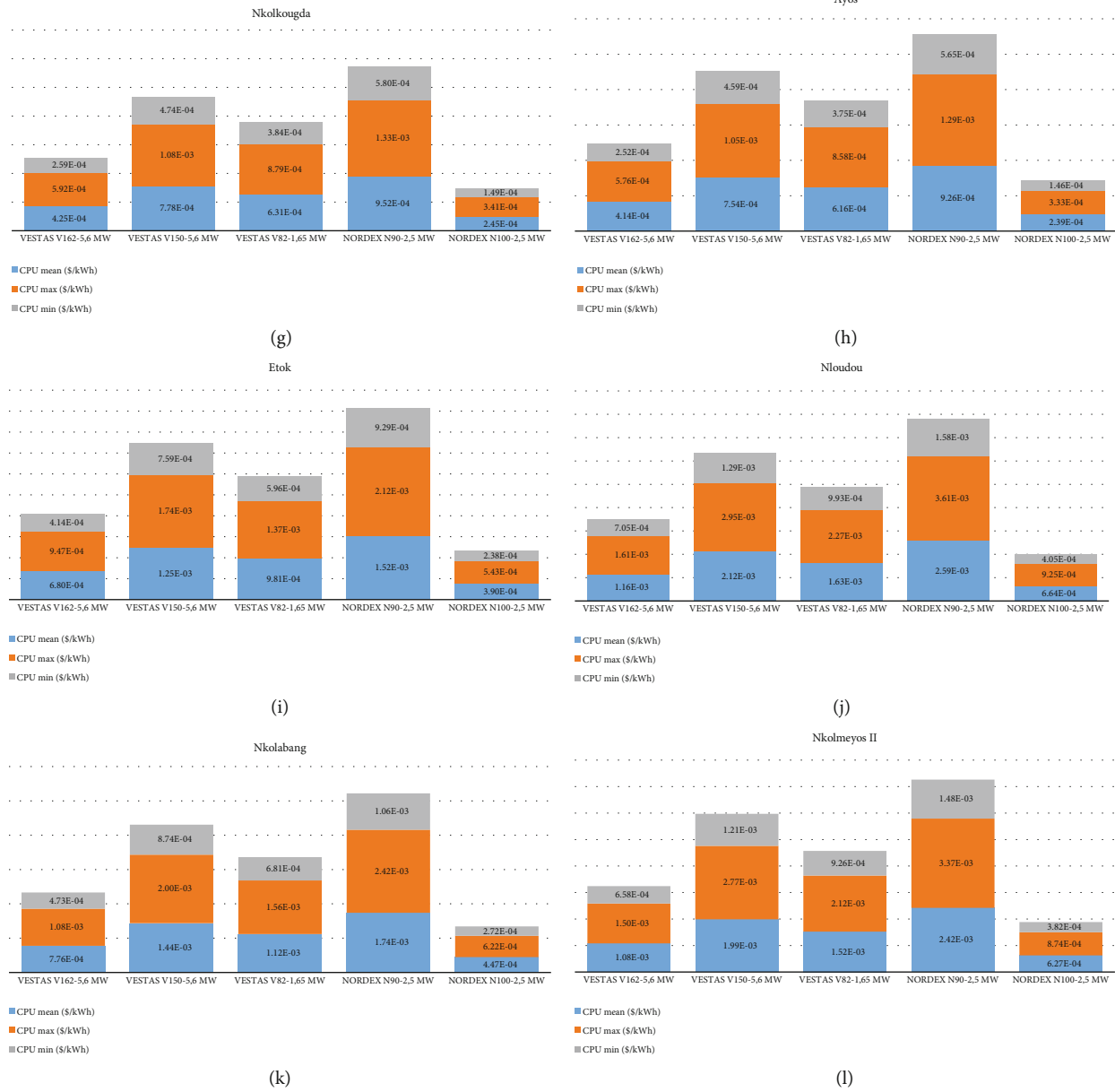


FIGURE 14: Continued.



FIGURE 14: Continued.

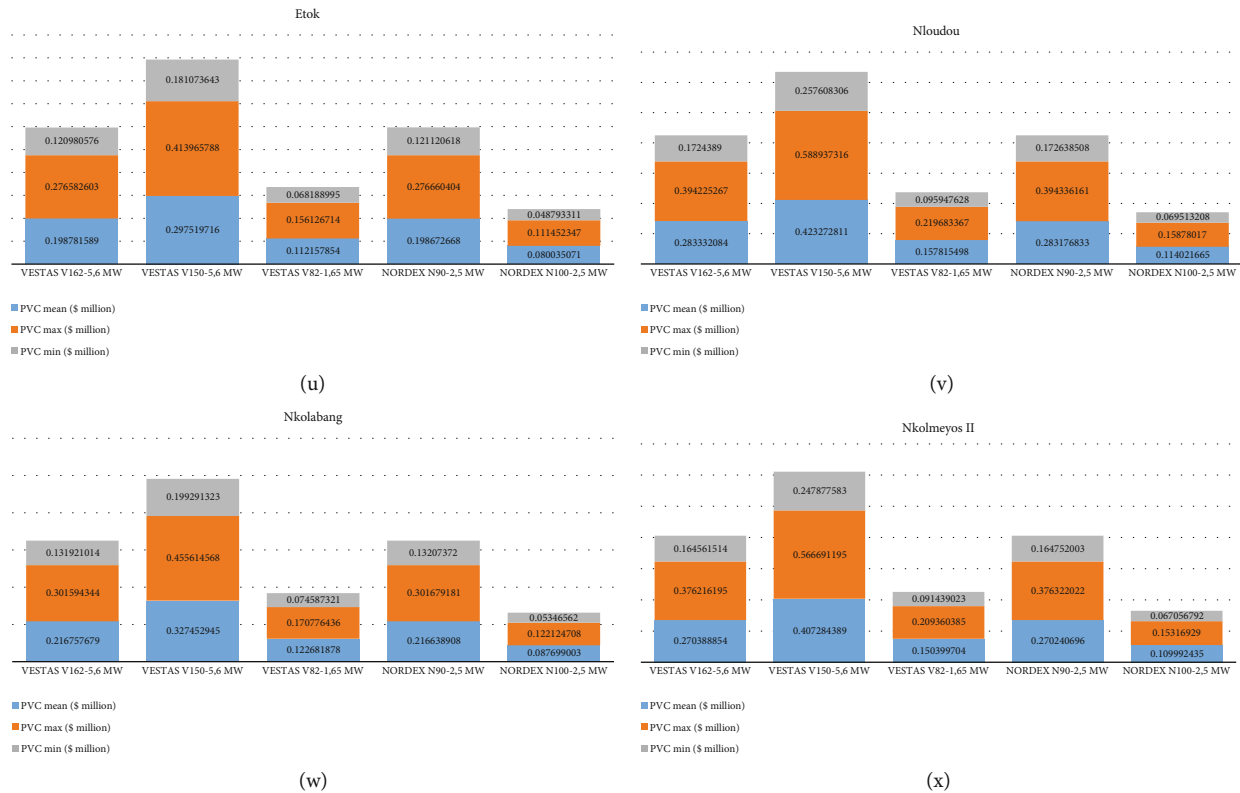


FIGURE 14: Comparison of annual estimates of cost production unitary per kilowatt-hour (CPU) and present value of costs (PVC) of the five wind turbines: V162-5.6MW, V150-5.6MW, VESTAS V82-1.65MW, NORDEX N90-2.5MW, and NORDEX N100-2.5MW: (a) CPU of Evodoula, (b) CPU of Ekol, (c) CPU of Ntouda, (d) CPU of Okok, (e) CPU of Ngobo, (f) CPU of Nkotabel, (g) CPU of Nkolkougda, (h) CPU of Ayos, (i) CPU of Etok, (j) CPU of Nloundou, (k) CPU of Nkolabang, (l) CPU of Nkolmeyos II, (m) PVC of Evodoula, (n) PVC of Ekol, (o) PVC of Ntouda, (p) PVC of Okok, (q) PVC of Ngobo, (r) PVC of Nkotabel, (s) PVC of Nkolkougda, (t) PVC of Ayos, (u) PVC of Etok, (v) PVC of Nloundou, (w) PVC of Nkolabang, and (x) PVC of Nkolmeyos II.

TABLE 9: Wind farm cost structure.

Wind turbines	75%
Transport/lifting	2%
Electrical connection	7%
Miscellaneous (telephone, terrain, markup)	1%
Preliminary studies and procedures	2%
Engineering	5%
Civil engineering	8%

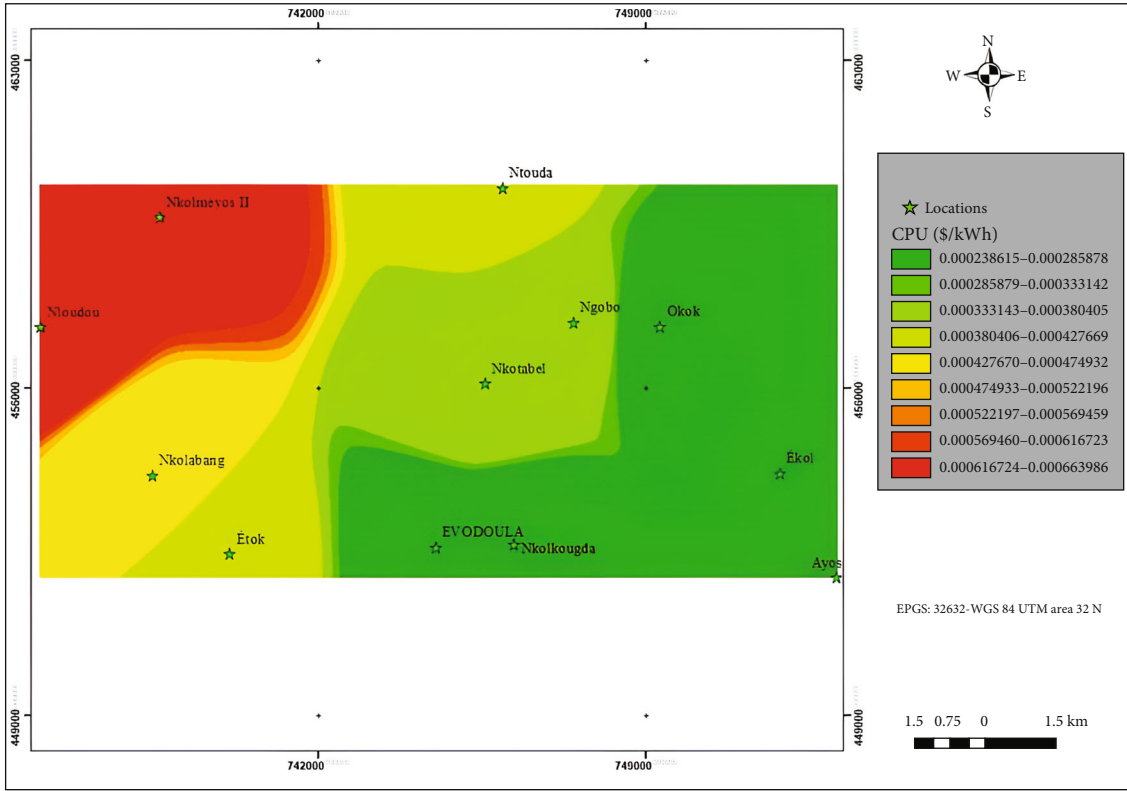
cost of electricity according to the conventional method are obtained at a location as 0.000238615 CAD\$/kWh, i.e., 0.11 XAF/kWh and 0.001159034 CAD\$/kWh, i.e., 0.55 XAF/kWh using NORDEX N100-2.5MW and VESTAS V150-5.6MW, respectively; based on the capacity factor, one can conclude that the NORDEX N100-2.5MW turbine is cost-effective for Okok and Ayos locations and could be highly recommended for installation. Assuming an interest rate of 12%, for the conventional and uncertainty methods, in the north-west zone of the EEZ, the CPU level is high. In the north-east zone, most of the time, for the two conventional and uncertainty methods, the average CPU varied from 0.000238615 to 0.000285878 CAD\$/kWh, i.e., 0.1 to 0.14

XAF/kWh, and from 0.000033941 to 0.000044165 CAD\$/kWh, i.e., 0.016 to 0.021 XAF/kWh, respectively. A small part of the south and north-west and a small part of the north shore have a fare mostly from 0.000380406 to 0.000427669 CAD\$/kWh, i.e., 0.18 to 0.20 XAF/kWh, obtained by the method conventional, while a small part of the south and south-east and a small part of the north shore have a tariff most of the time of 0.000054389 to 0.000064612 CAD\$/kWh or 0.026 to 0.031 XAF/kWh, obtained by the uncertainty method; however, compared to world electricity rates, the realization of an optimal onshore wind farm consisting of five 2.5 MW wind turbines with an installed capacity of 12.5 MW is reasonable with an interest rate of 12%. The interest of these figures shows the lowest average CPU higher wind resource in the north-east zone obtained by the uncertainty method (see Figure 15(b)). Thus, it is decided once again that the most suitable area for the installation is the place called Okok.

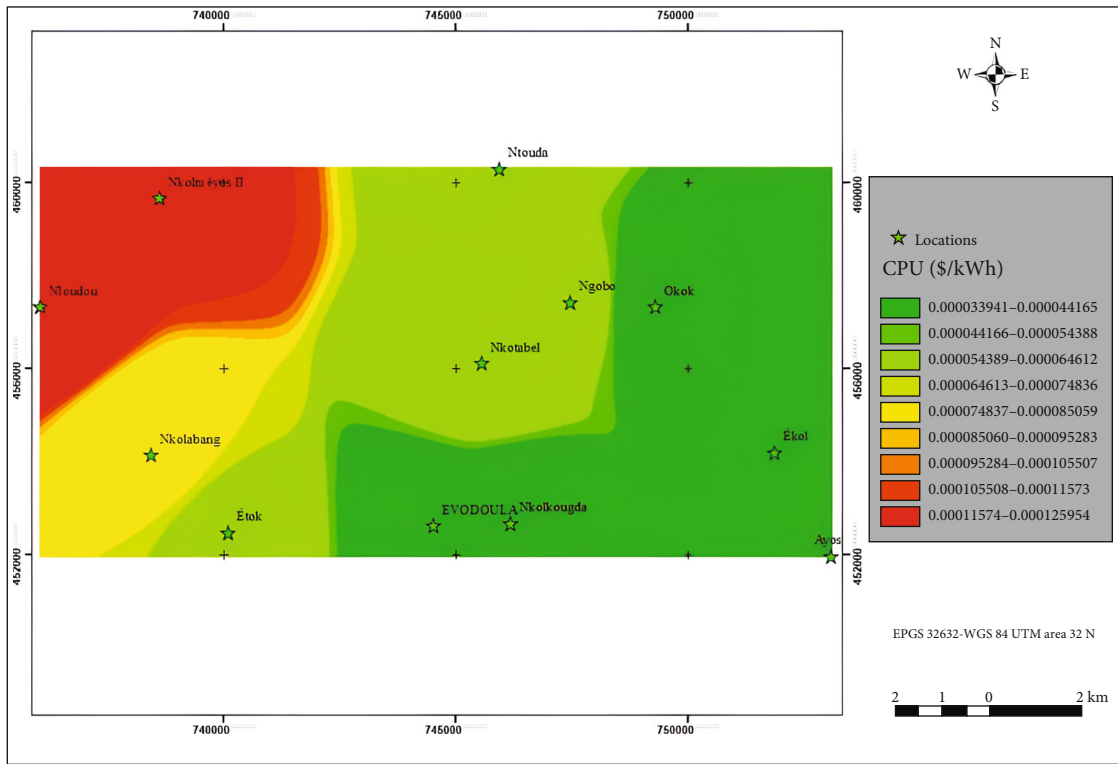
Table 11 shows the statistics for each wind turbine in the wind farm. The location of the 5 wind turbines on the location chosen with a higher wind resource that we deploy by synchronizing with Google Earth combined with a GIS to visualize the location of the wind farm according to the layout of the wind turbines on the maps of evolution of the wind speed, the gross and net annual energy production, and the

TABLE 10: The average, minimum, and maximum values of the costs of the wind farm.

Wind farm costs	Cost (\$ million)														
	Maximum cost values					Mean cost values					Minimum cost values				
	VESTAS V162-5.6MW	VESTAS V150-5.6MW	NORDEX N100-2.5MW	NORDEX N90-2.5MW	VESTAS V162-5.6MW	VESTAS V150-5.6MW	VESTAS V82-1.65MW	VESTAS V82-1.65MW	NORDEX N100-2.5MW	NORDEX N90-2.5MW	VESTAS V162-5.6MW	VESTAS V150-5.6MW	VESTAS V82-1.65MW	NORDEX N100-2.5MW	NORDEX N90-2.5MW
C_j	14.22	14.22	4.19	6.35	6.35	10.22	10.22	3.01	4.56	4.56	6.22	6.22	1.83	2.78	2.78
C_{Wt}	11.38	11.38	3.35	5.08	5.08	8.18	8.18	2.41	3.65	3.65	4.98	4.98	1.47	2.22	2.22
C_{Sg}	0.23	0.23	0.07	0.1	0.1	0.16	0.16	0.05	0.07	0.07	0.1	0.1	0.03	0.04	0.04
C_{Fin}	0.57	0.57	0.17	0.25	0.25	0.41	0.41	0.12	0.18	0.18	0.25	0.25	0.07	0.11	0.11
C_{Ci}	0.91	0.91	0.27	0.41	0.41	0.65	0.65	0.19	0.29	0.29	0.41	0.41	0.12	0.18	0.18
C_{Tr}	0.23	0.23	0.07	0.1	0.1	0.16	0.16	0.05	0.07	0.07	0.1	0.1	0.03	0.04	0.04
C_{El}	0.8	0.8	0.23	0.36	0.36	0.57	0.57	0.17	0.26	0.26	0.36	0.36	0.1	0.16	0.16
C_{Misc}	0.11	0.11	0.03	0.05	0.05	0.08	0.08	0.02	0.04	0.04	0.05	0.05	0.01	0.02	0.02



(a)

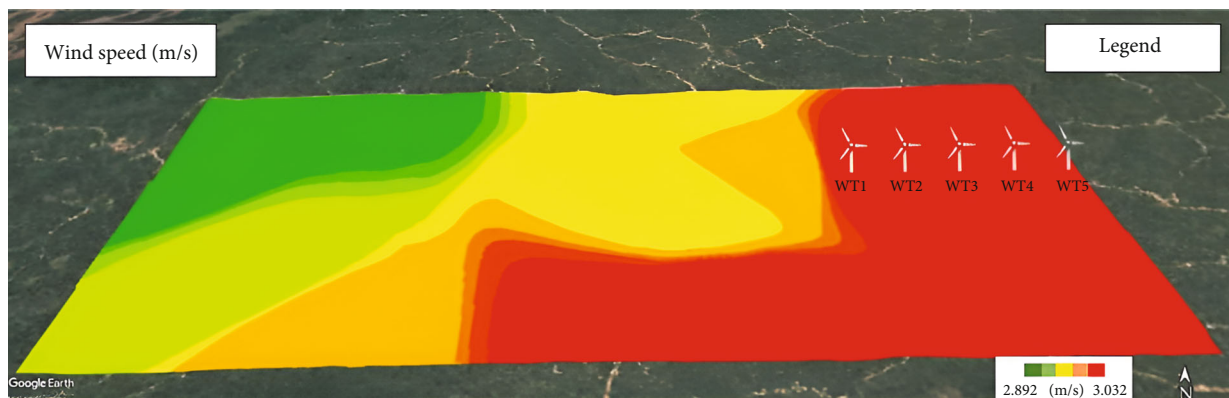


(b)

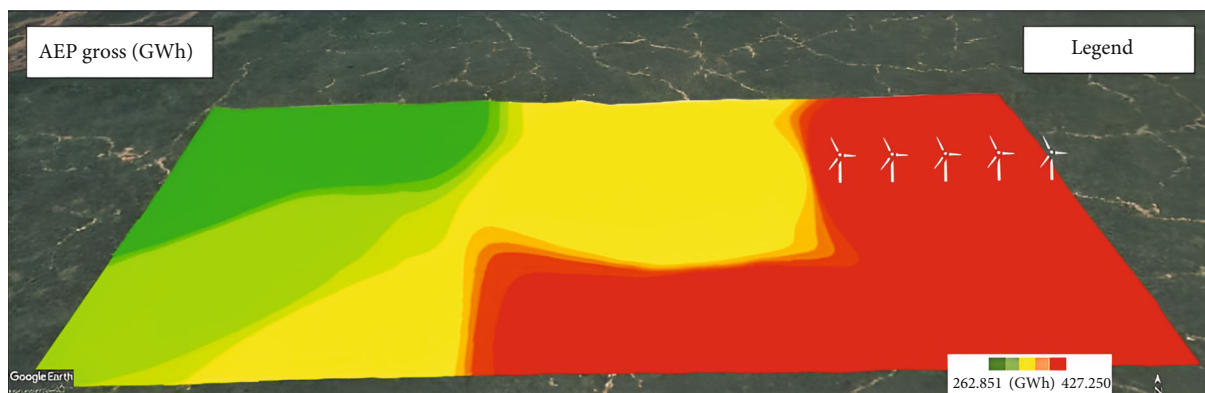
FIGURE 15: Comparison of the cost production unitary (CPU) of electricity produced per kilowatt-hour in 2D in the EEZ of Evodoula assuming a 12% interest over 40 years (1980-2019) for (a) the conventional method and (b) the uncertainty method.

TABLE 11: Summary of technical performance results, economic viability, and annual reduction of greenhouse gas (GHG) emissions at 100 m (AGL) using a single NORDEX N100-2.5MW wind turbine rated at 2.5 MW next to a configuration layout of one even row from $1 \times 10D$ to $4 \times 10D$ of an onshore wind farm with an installed capacity of 12.5 MW for the location of Okok.

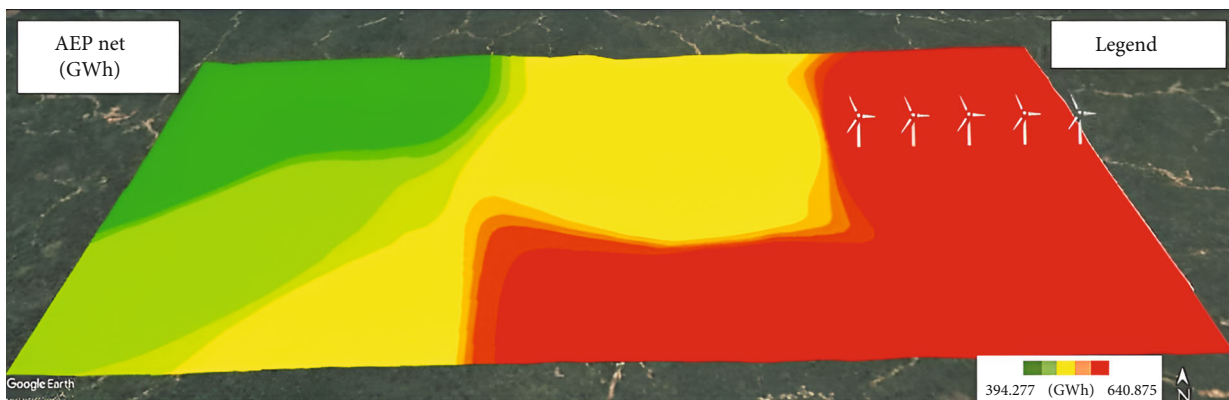
Locations where wind turbines are installed	Latitude Y (m)	Longitude X (m)	Elevation (m)	Wind speed, Vm (m/s)	AEP Gross (GWh/year)	AEP Net (GWh/year)	Loss rate proportional due to the effect wake (%)	Cost production unitary (CAD\$/kWh)	Present value cost (PVC) (CAD\$)	Net present value (NPV) (CAD\$)	Gross annual GHG emission reduction (tCO ₂ /year)	Net annual GHG emission reduction (tCO ₂ /year)
Wind turbine 1 (WT1)	457000.0445838217	749000.1076506755	487	3.031000	427.250000	640.875061	33.333339	0.000034	21789.752074	435795.04148	76940.248125	115410.38317
Wind turbine 2 (WT2)	457000.0445838217	750000.0476629087	495	3.031000	427.250000	640.875000	33.333333	0.000034	21789.750000	435795.00000	76940.248125	115410.37218
Wind turbine 3 (WT3)	457000.0445838217	751000.0013250716	500	3.030992	427.236816	640.854553	33.333263	0.000034	21789.054802	435781.09604	76937.873917	115406.69004
Wind turbine 4 (WT4)	457000.0445838217	751999.8819557157	501	3.031279	426.604553	639.913835	33.334063	0.000034	21757.070390	435141.40780	76824.014415	115237.28319
Wind turbine 5 (WT5)	457000.0445838217	752999.8807854662	509	3.031862	425.833923	638.755676	33.333833	0.000034	21717.692984	4343538.5968	76685.237438	115028.71902
Total annual energy production (AEP), annual wake loss rate (WLR), annual cost production unitary (CPU) per kilowatt-hour, present value of annual costs (PVC), annual net present value (NPV), and total annual reduction of greenhouse gas (GHG) emissions from the onshore wind farm by 12.5 MW over 1 year												
The 12.5 MW onshore wind farm	-	-	-	-	Total AEP Gross (GWh/year)	Total AEP Net (GWh/year)	Rate losses due to the effect wake (%)	Total cost production unitary (CAD\$/kWh)	Total present value cost (PVC) (CAD\$)	Total net present value (NPV) (CAD\$)	Total Gross annual GHG emission reduction (tCO ₂ /year)	Total Net annual GHG emission reduction (tCO ₂ /year)
Total energy production (TEP), total wake loss rate (WLR), total cost production unitary (CPU) per kilowatt-hour, present value of total costs (PVC), total net present value (NPV), and reduction of total greenhouse gas emissions (GHG) of the onshore wind farm by 12.5 MW over 20 years	-	-	-	-	2134.175292	3201.274125	33.333566	0.00017	544216.60125	10884332.025	384327.62202159	576493.44761531
The 12.5 MW onshore wind farm	-	-	-	-	TEP Gross (TWh)	TEP Net (TWh)	Rate losses of to the effect of wake (%)	Cost production unitary (CAD\$/kWh)	Present value cost (PVC) (CAD\$ million)	Net present value (NPV) (CAD\$ million)	Gross annual GHG emission reduction (million tCO ₂)	Net annual GHG emission reduction (million tCO ₂)
	-	-	-	-	42.68350584	64.0254825	33.3335663	0.0034	10884332.025	217686640.5	7686552.4404318	11529868.952306



(a)

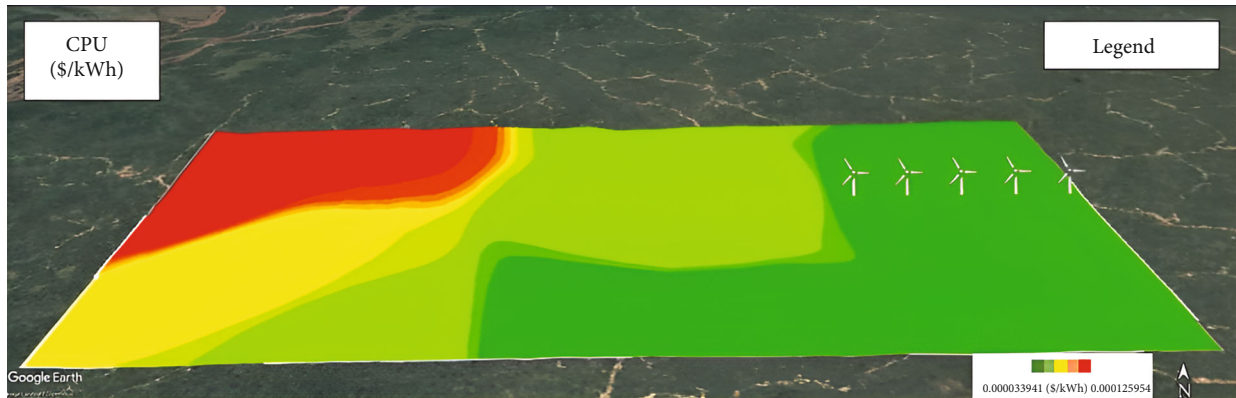


(b)



(c)

FIGURE 16: Continued.



(d)

FIGURE 16: Maps of potential wind resources obtained by synchronizing the location of wind power sites with Google Earth, indicating the optimal onshore wind farm (5×NORDEX N100-2.5MW) away from $1 \times 10D$ to $4 \times 10D$, superimposed on the location Okok at 100 m for (a) projection of the wind turbines (5×N100-2.5MW) on the surfaces of the 2D wind speed map, (b) projection of wind turbines (5×N100-2.5MW) on the surfaces of the AEP Gross map in 2D, (c) projection of the wind turbines (5×N100-2.5MW) on the surfaces of the AEP Net 2D map, and (d) projection of the wind turbines (5×N100-2.5MW) on the surfaces of the CPU board in 2D.

unit production cost of the NORDEX N100-2.5MW wind turbine and the topography of the land is shown in Figure 16) while respecting the layout of the wind turbines ($1 \times 10D$ to $4 \times 10D$). We thus notice that at the entrance of the 5 wind turbines, the average annual speed varies from 3.030992 to 3.031862 m/s, and as for the gross annual energy production, it varies from 425.833923 to 427.250000 GWh/year. The loss rate due to the wake effect shows that the maximum was suffered by the wind turbine (WT4) with 33.334063%, while the lowest loss is around 33.333263%. Thus, it is noted that the net energy production, without losses due to the wake effect, varies from 638.755676 to 640.875061 GWh/year. Furthermore, the superimposition in Table 11 indicates that the total annual energy production of the optimal wind farm composed of five 2.5 MW turbines gives a total loss rate because the wake effect is 33.333566%, thus inducing a gross total annual energy production of 2134.175292 GWh/year to a total net annual energy production of 3201.274125 GWh/year. According to statistics from Our World in Data, annual (CO_2) emissions from Cameroon's average national electricity generation mix amounted to 180.0825 g/kWh [67]. The production of such wind farms could thus make it possible to reduce gross total annual CO_2 emissions by 384327.62202159 t CO_2 /year and reduce total net annual CO_2 emissions by 576493.44761531 t CO_2 /year. In Table 12, the results are obtained after having simulated the gross and net annual energy production of the wind farm with a rated power of 12.5 MW on the heights of the municipality studied at the proven optimal place, and we establish the economic study of this project which relates to the calculation of the cost per kilowatt-hour generated from the onshore wind farm. This economic study was carried out using the PVC (present value cost) method, the NPV (net present value) method, and the CPU (cost production unitary) method described in the Section 3.3.13, for estimating the financial return of our work. Thus, the results of the economic study obtained by the uncertainty method are summa-

rized on Table 12, which gives a cost of 0.0034 CAD\$/kWh for the kilowatt-hour produced, relating to a project which would have cost a total of nearly 11 million CAD\$ and a total net discounted cost of nearly 218 million CAD\$ with an over a period of 20 years. Furthermore, the eventual installation of the present onshore wind farm with a capacity of 12.5 MW would have produced nearly 64.0254825 TWh during this period of 20 years. The annual profit generated (PVB) from the wind farm would have produced more than CAD\$6 billion. Now that we know how much the onshore wind farm (of 5 wind turbines) brings in 20 years, we have estimated a return on investment (ROI) of 2880.882%. This seemed like a very large number for a return on investment. This means that for every million dollars spent on the project, an average annual cash flow (net profit) valued at almost CAD\$30 million has been achieved. Thanks to this very high ROI, we can start to establish a budget for a more substantial expenditure over the next 20 years. The expansion of the onshore wind farm will continue to boost energy over time, thus ensuring an even higher ROI in the future. In another important number, the return time has been determined for a 20-year life, and the product will have to work for more than 7 years before being paid. Based on the two methods proposed (the conventional method and the uncertainty method) and the emphasis placed on the cost production unitary per kilowatt-hour of electricity by parsimony. These results show that the construction of a 12.5 MW onshore wind farm at a place called Okok can be considered economically viable and parsimonious, especially if we consider the uncertainty method whose cost is the lowest. In comparison with the current sale price of electricity from public service companies in Cameroon, according to the Electricity Sector Regulatory Agency (ARSEL), the price per kilowatt-hour of electricity of conventional origin for domestic or residential sold to individuals (households) varies from 50 to 99 XAF/kWh, i.e., 0.10475 to 0.2079 CAD\$/kWh (at low voltage level) [70].

TABLE 12: Estimation of the financial return of the 12.5 MW Onshore wind farm consisting of five NORDEX N100-2.5MW wind turbines over 20 years on the aggregated surfaces at the location Okok.

Financial cost of the 12.5 MW onshore wind farm	CPU _{selling price} (CAD\$/kWh)	CPU _{cost per kWh of the wind farm} (CAD\$/kWh)	Net TEP (TWh)	PVB (CAD\$ billion)	Average annual cash flow (CAD\$ million)	PVC (CAD\$ million)	NPV (CAD\$ million)	ROI (%)	PBP (Yr)
	0.10475-0.2079	0.0034	64.0254825	6.488982651375	29808823.5294	10884332.025	217686640.5	2880.882	7.3

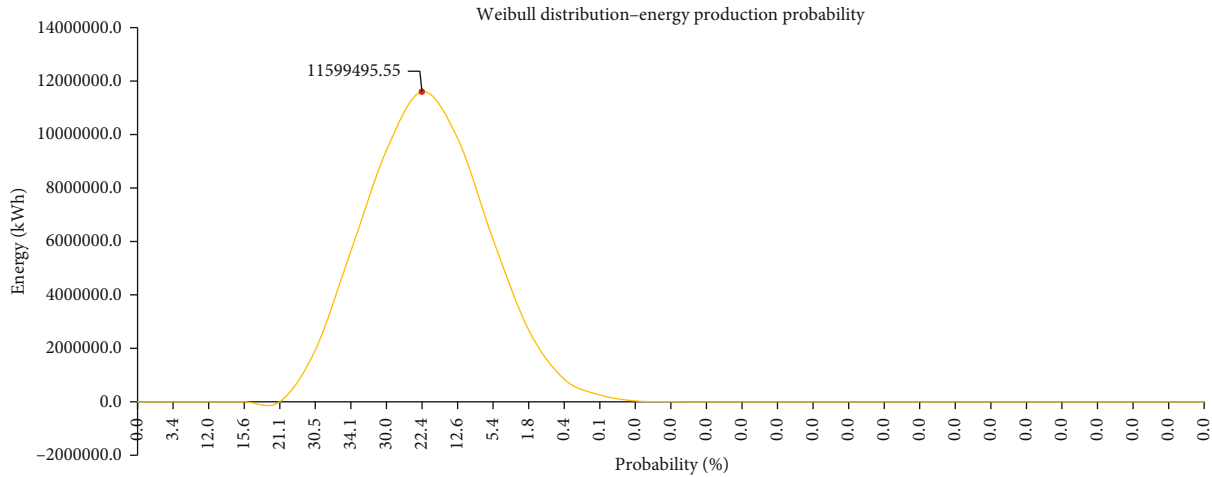


FIGURE 17: Variation energy production based on of the Weibull distribution probability.

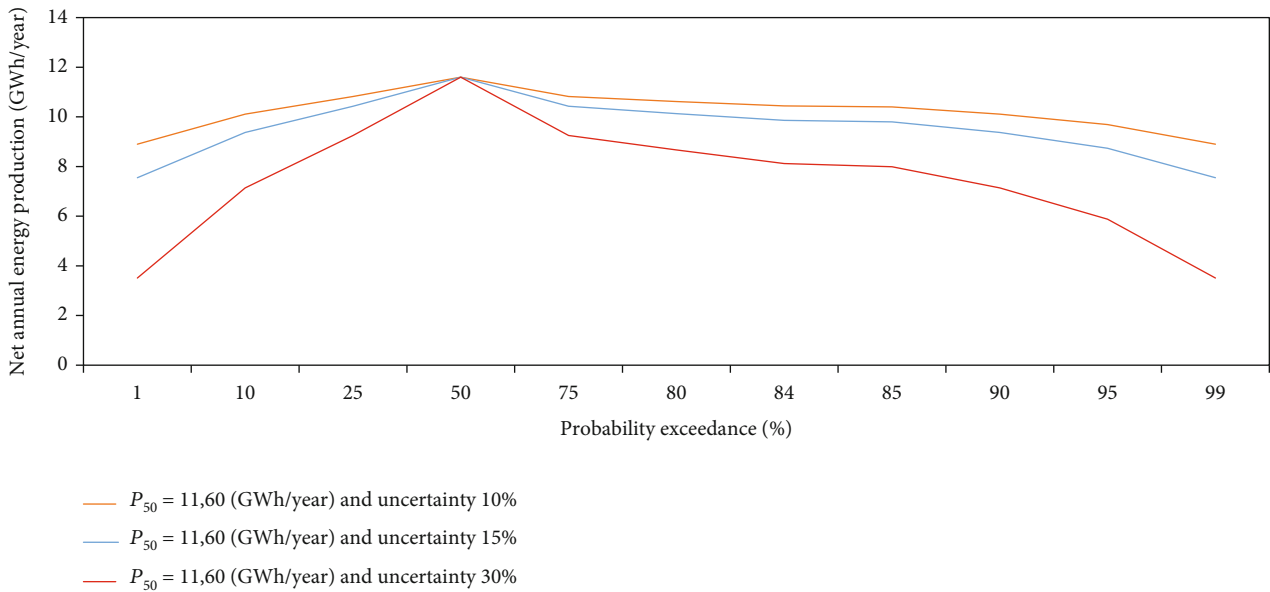


FIGURE 18: Variations of the different levels of probability of exceedance: P_{50} of 11.60 GWh and uncertainty of 10%, 15%, and 30%.

To optimize the implementation of the onshore wind farm, stochastic or modulating systems are essential to adapt and adjust the wind speed data linked to the use of an adaptive power curve, obtained by a semiempirical approach of the parametrized powers (physical and modified) of a wind power generation system based on the determination of a modulation factor “ a ” before they are put into operation in order to optimize the use of the bandwidth and minimize the disturbances. In this regard, observed parameters that are important for wind resource assessment are fitted to establish probability models. These models can help in the analysis of the uncertainty of the annual energy productions (AEP Gross and AEP Net) and of the cost production unitary (CPU). With regard to wind speed uncertainty, it is commonly taken into account in various studies, such as the determination of wind energy potentials for specific locations [34, 71, 72], assessment of structural reliability levels [73–75], or economic and financial estimates [76–78]. The results

obtained were conducted to find the optimal locations for wind power installations. The reviewed literature shows in this study how the interest of the combinations of horizontal and vertical interpolation techniques for wind resource mapping using software tools (GIS), with detailed multicriteria decision-making (MCDM) methodologies (Section 3.2), shown in Figure 4, successfully solved the problem of identifying optimal locations. In addition, the results obtained from the uncertainty method were compared with those from the conventional method. The resulting differences from conventional analysis and uncertainty can be used for more accurate decision-making in renewable energy projects. The small difference between conventional analysis and uncertainty analysis will result in a large difference in the generated (adjusted) power. In order to show the accuracy of the results obtained, the applications and importance of GIS for wind resource assessment have been explored in several case studies. Cheng et al. [79] used a GIS system to

TABLE 13: P_{50} from 11.60 GWh/year and total uncertainty 10%, 15%, and 30%.

P_{50} (GWh/year)	P_{75} (GWh/year)	P_{90} (GWh/year)	$\sigma 1$	P_{75} (GWh/year)	P_{90} (GWh/year)	$\sigma 2$	P_{75} (GWh/year)	P_{90} (GWh/year)	$\sigma 3$	
11.60	10.82	10.11	1.74	10.43	9.37	1.16	9.25	7.14	3.48	
	-6.72%	-12.84%		-10.08%	-19.22%		-20.26%	-38.45%		
	10%			15%			30%			
	σ is the absolute standard deviation of the energy production estimate Uncertainty Difference from P_{50}									

perform a wind resource assessment in Bolivia, while the wind characterization and uncertainty analysis is performed by Amirinia et al. [34] for Persian Gulf. Similarly, the evaluation of the wind resource to determine the opportunity to deploy wind farms is studied by Tercan et al. [80], Liu et al. [81], Gil-García et al. [82], and Pakere et al. [83] for Turkey, China, the USA, and Latvia, respectively. Indeed, geographic information systems (GIS) are used to assess possible sites for the installation of offshore wind farms based on wind potential and LCOE assessment [34, 84–86]. GIS implementations are used to study the economic feasibility of exploiting offshore wind resources in the UK, India, the Persian Gulf, and Africa. From this point of view, the results obtained on this paper present a potential interest, a technical, economic, and environmental value. It focuses mainly on the missing areas covered by this study and considers twelve specific cases that show the applicability of the work relying on a geographic information system (GIS) tool to identify possible sites for the installation of onshore wind farms based on the annual energy production (AEP); the evaluation of the cost production unitary (CPU); the economic aspects having been analyzed using financial parameters, namely, PVB, AACF, PVC, NPV, ROI, and PBP; and the environmental aspects resulting from the qualitative analysis of the reduction of greenhouse gas emissions. This geographic information system (GIS) tool was used to present the results and discuss the feasibility, sustainability, raising the energy deficit, strengthening of the energy mix, and reduction of the drop in the energy bill of renewable energies in the municipality under study. That said, mastering this software allows us to effectively analyze and interpret complex data sets, leading to meaningful insights and impactful solutions.

To finance a wind project, the bank requires the investor to submit the uncertainties related to the estimate of the AEP wind farm, in order to limit errors and make the project more reliable. Proper assessment of uncertainties is essential in determining the feasibility and risks of developing a wind energy project. This step is important for a correct analysis of the economic viability of the project. Figure 17 shows the variation of the energy production probability indicating a value close to 11.60 GWh/year with a probability of 22.4%. The calculated net AEP is the value of energy production called P_{50} , which corresponds to the production estimation center energy in normal Gaussian distribution. This represents an energy value with a 50% chance of being exceeded. Figure 18 shows different levels of exceedance probability depending on the net annual energy production (Net AEP). This figure shows the same amount of energy in P_{50} , but with different values for the total uncertainty as indicated in Table 13. This painting shows a project with an energy P_{50} equal to 11.60 GWh/year and total uncertainty of 10%, 15%, and 30%. Energy values within P_{75} and P_{90} (75% and 90% probability of overshoot) are used to show the impact caused by global uncertainty. It is recommended that the total project uncertainty be around 15%. The energy values in P_{75} and P_{90} are respectively 10.08% and 19.22% lower than the energy value in P_{50} , with an absolute standard deviation of energy production estimate σ_2 equal to 1.16. It can be seen that the higher the value of the total uncertainty,

the greater the difference between P_{50} and the other levels of probability of exceedance.

5. Conclusions and Perspectives

In this study, the technoeconomic analysis of the wind potential and evaluation of the cost of production of electricity of wind origin, the case of the twelve locations of the commune of Evodoula in Cameroon was investigated, by estimating the shape and scale parameters of the Weibull distribution function using the energy pattern factor method (EPFM) and by comparing two methods, the conventional method and the method of uncertainty, taking into account a spatiotemporal comparative approach combined with geographic information system (GIS) tools proposed in this work. It appears that the research theme of this work related to a double problem devoted firstly to the development of maps of potential wind resources and secondly to the appropriate optimal design of an onshore wind farm for the selected locations in this locality in Cameroon. This work is a tool for decision support, development, and popularization of research, enabling the technoeconomic analysis of wind energy potential and the evaluation of electricity production costs. The wind energy potential in the Evodoula EEZ is of interest for the parsimonious production of energy and the cost of producing wind-generated electricity on the aggregated surfaces of the wind energy development zones (ZDEE) in the EEZ. Thus, the use of a (GIS) to make wind energy viable and parsimonious is the only environment that allows an aggregate annual energy production (AEP) and an aggregate electricity cost production unitary (CPU) per the spatial interpolation procedure using the inverse distance weighting (IDW) method. Since then, the principal objective was approached in the content of this study, based on wind speed data from forty years (1980-2019) of monthly measurements, taken 10 m above the ground in the twelve locations of the EEZ of Evodoula in Cameroon having been used efficiently to perform detailed statistical analysis of wind speed data. The frequency distributions of the wind speed, the average wind speed, and the two parameters of the Weibull distribution function at a defined latitude and longitude were calculated at different time scales: four-decadal, decadal, interannual, annual, and monthly. The modified power law method is used to extrapolate wind speed at a defined latitude and longitude to heights greater than 10 m above ground level (AGL). After estimating the wind map which was established by numerical wind simulation and GIS exclusion analysis, annual energy production maps (AEP Gross and AEP Net) were drawn, but also the maps of cost production unitary (CPU) of electricity have been developed. The different models of wind turbines for the production of electricity at these locations are proposed for the possibility of installing wind farms on these locations. Using current wind turbine technologies, the discounted minimum cost production unitary is estimated, and the financial return of the onshore wind farm is assessed for the proven optimal location. The analysis of the results obtained gave the conclusions and prescribed the following recommendations:

- (i) Monthly temporal variations in wind speed over the 40-year period of the twelve locations in the Evodoula EEZ reveal that the windy months present a maximum of the average monthly wind speed during the periods from July to August, August being the windiest month. As for the minimum, it occurs during the period of the month of November
- (ii) The horizontal wind profiles of the twelve locations correspond closely to the Weibull distribution function
- (iii) At 100 m height, the wind rose showed a prevalence of the wind direction with the average speed varying between 2.7 and 3.3 m/s most significant from north (N) to north-east (NE)
- (iv) The location Okok has the most optimal average annual wind potential of 847.333 W/m² compared to other locations with an average annual wind speed of 2.971 m/s and a wind speed greater than or equal at 3 m/s for about 33.92% of time. The place called Ayos is the second in terms of annual average wind potential of 846.854 W/m² with an average annual wind speed of 2.974 m/s and a wind speed greater than 3 m/s for about 34.23% of the time. It should also be noted that the highest monthly average wind potential of 2067.827 W/m² is reached in August with an average monthly wind speed of 4.440 m/s, although the place called Nkolmeyos II has the lowest average annual wind potential of 75.663 W/m², with an average annual wind speed of 1.108 m/s, and the wind blows at more than 2.844 m/s for 34.87% of the time
- (v) The wind potential of the ZIDEE wind energy development interest areas (Evodoula, Ekol, Ayos, Okok, and Nkolkougda) in the EEZ is stable and corresponds to the exceptional class with a wind speed class of seven during the annual cycle of period studied
- (vi) Based on its superior performance compared to the other four, the NORDEX N100-2.5MW wind turbine, motivated by its scalable adaptability performance factor "*a*," is adaptive preferred for large community power generation local, because it has the highest capacity factor and the lowest cost production unitary per kilowatt-hour
- (vii) The annual comparison results from simulations of the performance of the two models indicated a modulating factor *a* of between 1.67 and 1.73 over the twelve locations (see Figure 11). It can be seen that for locations Evodoula, Ekol, Okok, Nkolkougda, and Ayos, an identical modulating factor *a* = 1.73 (very windy locations) was indicated, and for locations Etok, Ngobo, Ntouda, and Nkotel, an identical modulating factor *a* = 1.7 (less windy locations) was shown. However, location Nkolabang showed a different modulating factor *a* = 1.69 (little windy location), and as for locations Nloundou and Nkolmeyos II, an identical modulating factor *a* = 1.67 (slightly windy locations) was shown
- (viii) The highest capacity factor of 18.4% was almost identical in the locations Okok and Ayos with NORDEX N100-2.5MW. This can be attributed to the rated speed of 12 m/s and the generation time of 19336.41849 h and 19320.10361 h, obtained by the conventional method, or from 51270.00451 h and 51197.81828 h obtained by the uncertainty method, respectively, for the two aforementioned locations. However, the VESTAS V150-5.6MW wind turbine model produced the lowest annual energy compared to other models and resulted in the lowest capacity factor of 6.8%. This can be attributed to the higher rated speed and generation time of 7133.228008 h obtained by the conventional method
- (ix) The total AEP of the wind farm with an installed capacity of 12.5 MW of the NORDEX N100-2.5MW wind turbine of the twelve locations calculated from the conventional method was 2573.010008 GWh. However, the total AEP of the farm at each point calculated by the uncertainty method was 6507.18781 GWh
- (x) Based on the comparison of the annual energy production and the cost production minimum discounted unitary by the two methods (the conventional method and the uncertainty method), the study of the 12.5 MW onshore wind farm at Okok shows the possibility of producing electricity at a parsimonious updated cost per kilowatt-hour for the entire duration of the installations of 0.0034 CAD\$/kWh or 1.62 XAF/kWh. In comparison with the current sale price of the public service agency (ARSEL) in Cameroon (at the low voltage level), this research concludes that the energy cost of the proposed onshore wind farm in Okok is much cheaper by more than 98% than the utility price
- (xi) The onshore wind farm built will have the effect of avoiding the emission of CO₂ by more than 11 million tons equivalent per year (MtCO_{2,eq}/Yr) since the energy produced comes from the atmosphere. The farm will have to achieve an average annual cash flow valued at nearly CAD\$30 million after 20 years of operation. These savings would allow the installation of CO₂ capture systems in conventional power plants
- (xii) The proposed onshore wind farm would have cost a total of almost CAD\$11 million and a total net present cost of almost CAD\$218 million over a 20-year period

- (xiii) The onshore wind farm with a capacity of 12.5 MW would have produced nearly 64.0254825 TWh during this relative 20-year period. The annual profit generated (PVB) from the wind farm would have produced more than CAD\$6 billion. The return on investment (ROI) or the break-even point of the project was estimated at 2880.882%
- (xiv) Payback time has been estimated at over 7 years before being paid for over a 20-year lifespan
- (xv) Uncertainties and risks have been identified and quantified to estimate the confidence levels of the results related to the development of the project. We recommend that the total project uncertainty be around 15%. The energy values in P_{75} and P_{90} are respectively 10.08% and 19.22% lower than the energy value in P_{50} equal to 11.60 GWh/year

Recommendations to designers are the following:

- (i) When analyzing and comparing the offers submitted by the manufacturers, we recommend updating the production calculations if necessary to take into account the latest technical information characteristics of wind turbines. It deserves to be taken into account to assess performance available on the power curves in the selected location
- (ii) The configuration of the onshore wind farm must be controlled at the level of the interdistances between wind turbines. These must be sufficiently spaced from each other to prevent the turbulence induced by the wind farm from exceeding the load limits used during the design of the wind turbine. If exceeded, it may be necessary to implement a sector management system to protect the wind turbine when turbulence levels are critical
- (iii) The location and numbering of the wind turbines are indicated on the map of Figure 16(a). This deserves to be taken into account when configuring the wind farm while respecting the minimum separation distance between wind turbine and orientation of 10 times the diameter of the rotor placed horizontally on a row of 5 wind turbines at the axis of the dominant winds
- (iv) For normative reasons, in order to avoid the influence of the rated speed on the capacity factor, the installation height must be 100 m above the ground. It will be worth it during the process of implementations to ensure better recovery of stable and optimal energy production successfully and at a lower cost production unitary per kilowatt-hour

This work constitutes in this regard a decision support tool, development, and popularization of research making it possible to demonstrate the technoeconomic analysis of wind potential and evaluation of the cost of electricity production; the wind origin in the Evodoula EEZ is interesting

for parsimonious energy production and cost of wind electricity production on the aggregated surfaces of the wind energy development zones (ZDEE) in the EEZ. The analysis approach developed is highly interesting for ideal sites where the technoeconomic studies and evaluation of the cost of wind electricity production are not known. Indeed, the spatial distribution of the wind energy potential and the cost of wind electricity production at 100 m above the ground of the twelve locations considered, in the surrounding areas but also in certain places allows us to have a global view of all the extent of the EEZ considered, in order to guide policy makers and national and international investors on the wind energy development interest areas (ZIDEE) in the EEZ to plan and operationalize an Onshore wind farm project in Evodoula. On the other hand, this work is relevant, because it concerns the production of electricity by wind energy conversion technologies. This production system is able of supplying electricity on demand. Our deep interest in the development of a mathematical model makes it possible to find a realistic capacity factor which sequentially gives a better result in the evaluation of the wind resource and thus indicates the choice of the performance criteria of the wind turbines.

This is why to deal with the evaluation of wind resources and the development of a wind atlas in the EEZ of Evodoula, the laws of probability according to a spatiotemporal analysis combined with a geographic information system (GIS) were proposed in this work, due to the absence of a reliable and precise wind atlas in Cameroon in general and in particular in this area of Evodoula. Thus, the use of a GIS to make renewable energy viable, including wind energy, constitutes the only environment-allowing aggregate production by the spatial interpolation procedure. This powerful technique allows the generation of a continuous surface or regular grid at a controlled resolution and is a better solution for identifying, visualizing, assisting, deciding, quantifying, modeling, storing, monitoring, mitigating, and analyzing spatial reference data when developing renewable energy atlases on existing and promising renewable energy possibilities in any municipality or area of Evodoula.

It is concluded that the location Okok has the potential to install utility wind turbines to produce energy at the lowest electricity production cost per kilowatt-hour at a recommended height of 100 m. Wind-generated electricity production would be profitable and suitable for electrical and mechanical applications not connected to the public distribution network. Indeed, in rural areas where the electricity network is not available, the use of autonomous wind systems with battery and storage and water pumping wind turbines (domestic uses and irrigation of large agricultural farms with larger scale and battery charging) is more cost-effective than diesel generators. Obviously, the implementation of the research results obtained can be verified by comparing them to the potential of other countries by identifying the windiest areas and therefore the most favorable for the optimal implementation of wind farms and to make the best choice for the types of wind turbines to be installed (large or small power).

The perspectives of this work are aimed for, on the one hand, a more complete evaluation of the extractable wind

potential by the use of modified power models and an evaluation of the cost production unitary in the Department of Lekie that would be of great importance to analyze spatial variations and identify the best eligible and favorable sites for the installation of wind farms and, on the other hand, a comparison of the mapping of the wind resource using GIS software between the municipalities of the Lekie Department, in order to show the quality and impact of simulations using other methods of horizontal interpolation.

Abbreviations

GIS:	Geographic information system
Esri:	Environmental Systems Research Institute
mm:	Millimeter
°C:	Degree Celsius
UTM:	Universal Transverse Mercator
WGS 84:	World Geodetic System 1984
EEZ:	Exclusive economic zone
ZIDEE:	Wind energy development area of interest
ZDEE:	Zones of development of wind energy
AGL:	Above ground level
WT:	Wind turbine
CAD\$:	Canadian dollars
USD:	US dollars
CF:	Capacity factor
WECS:	Wind energy conversion system
WRA:	Assessment of wind resources
NRoC:	North Region Cameroon
O&M:	Operations and maintenance
LCOE:	Levelized cost of electricity
COE:	Cost of energy
Nh:	Number of operating hours
Nhepn:	Equivalent number of hours at nominal power
ROI:	Return on investment
PBP:	Payback, return, or break-even period
G:	Annual reduction of GHG emissions
IDW:	Inverse distance weighting
P_{50} :	Median net production obtained or energy value with a 50% probability of being exceeded
P_{75} :	Energy production at 75%, so we are sure to reach or energy value with a 75% probability of being exceeded
P_{90} :	Energy production at 90%, so we are sure to exceed or energy value with a 90% probability of being exceeded
C_{10} :	Weibull scale parameter at 10 m (m/s)
K_{10} :	Weibull shape parameter at 10 m
I :	Interest rate (%)
MCDM:	Multicriteria decision-making
NPV:	Net present of values
PVB:	Present value of benefits
AEP:	Annual energy production
TEP:	Total energy production
AEP Net:	Net annual energy production
AEP Gross:	Gross annual energy production
TEP Net:	Net total energy production
TEP Gross:	Gross total energy production
PT(t):	Total power

WLR:	Rate of losses due to the wake effect
GHG:	Emissions of greenhouse gases
"a":	Adjustable adaptability performance factor
p :	Power parameter
D :	Diameter
2D:	Dimension two
3D:	Dimension three
CO ₂ :	Carbon dioxide
ARSEL:	Electricity Sector Regulatory Agency
NCDT:	National Committee for Development of Technologies
MINRESI:	Ministry of Scientific Research and Innovation.

Nomenclature

Lists of Symbols

$f(V_{Lat,Lon})$:	Frequency of occurrence of wind speeds (not cumulative) at a defined latitude and longitude (%)
$F(V_{Lat,Lon})$:	Wind speed frequencies (cumulative) at a defined latitude and longitude (%)
$P(V_{Lat,Lon})$:	Available instantaneous power given at speed V by the turbine (W)
$p(v_{Lat,Lon})$:	Average power density available on the site (W/m ²)
NASA:	National Aeronautic Space and Administration
MERRA-2:	Modern-Era Retrospective Analysis for Research and Applications, version 2
\bar{P} :	Average theoretical incident power (P) per unit area (W/m ²)
z_0 :	Soil roughness
$V_{Lat,Lon}$:	Wind speed at a defined latitude and longitude (m/s)
$\bar{V}_{Lat,Lon}$:	Mean value of the wind speed at a defined latitude and longitude (m/s)
x :	Point to interpolate
x_i :	Interpolation point (known)
V_{Lat,Lon_j} :	Known values at a defined latitude and longitude of the function $\hat{V}_{Lat,Lon}$
$\hat{V}_{Lat,Lon}$:	Represents the entire report that gives an estimate of the known value at the point of interest at a latitude and longitude at the point x_i
$w_i(x)$:	Simple weighting function
d :	Given distance from each point of interest of the interpolation point x_i to the point to be interpolated x
n :	Total number of known points used in the interpolation
$V_{Lat,Lon}(z_1)$:	Reference speed measured at 10 m from the ground at a defined latitude and longitude (m/s)
$\hat{V}_{Lat,Lon}(z_2)$:	Speed calculated at values greater than 10 m at a defined latitude and longitude (m/s)
z_1 :	Reference height equal to 10 (m)
z_2 :	Desired height at variable values greater than 10 (m)
WPD:	Wind power density (W/m ²)

WED:	Wind energy density (MWh/m ²)
WPD _{Lat,Lon} (z ₂):	Wind power density at a defined latitude and longitude (W/m ²)
WED _{Lat,Lon} (z ₂):	Wind energy density at a defined latitude and longitude (MWh/m ²)
PDF:	Probability density function
CDF:	Cumulative distribution function
EPFM:	Energy pattern factor method
MEPFM:	Modified energy pattern factor method
MK _e :	Modified energy pattern factor method
K:	Weibull form parameter (-)
C:	Weibull scale parameter (m/s)
T:	Time
h:	Hour
\bar{Z} :	Geometric mean between two heights
S:	Surface (m ²)
MWh:	Megawatt hour
GWh:	Gigawatt hour
TWh:	Terawatt hour
kWh:	Kilowatt-hour
CSV:	Values separated by commas
CPU:	Cost production unitary of the electricity produced (CAD\$/kWh)
PVC:	Present value of costs (CAD\$)
MW:	Megawatt
Wh:	Watt-hour
kW:	Kilowatt
W:	Watts
Yr:	Year.

Lists of Greek Letters

$\rho_{Lat,Lon}$:	Air density at a defined latitude and longitude (kg/m ³)
$\Gamma()$:	Gamma function
α :	Roughness coefficient.

Data Availability

All data created during this research is openly available from Global Modeling and Assimilation Office, MERRA-2 tavg1_2d_slv_Nx:2d, 1-Hourly, Time-Averaged, Single-Level, Assimilation, Single-Level Diagnostics V5.12.4, Greenbelt, MD, USA, Goddard Earth Sciences Data and Information Services Center (GES DISC), consulté [June 23, 2021] DOI: 10.5067/VJAFPLI1CSIV.

Conflicts of Interest

The authors have declared no potential conflict of interest with respect to research authorship and/or publication of this article.

Authors' Contributions

Vincent De Paul Igor Essouma Koung conceptualized and designed the study, prepared the material, collected the data, and analyzed and/or interpreted the wind data provided by MERRA-2, developed the maps of potential wind resources, and modeled the power law indices and adopted a rigorous, methodical approach inspired by scientific research that has

led to the drafting of an original article. Francis Daniel Menga, an associate researcher at NCDT/MINRESI, read the content of our article, and his remarks have indeed improved the quality of the project. Beguide Bonoma, a professor at the University of Yaounde I, conceptualized the project. Jean Luc Nsouandele, a professor at the University of Maroua, read the content of our article, and his remarks and his revision have effectively improved the quality of the project. Ruben Martin Mouangue, a professor at the University of Douala, read the content of our article, and his conceptualization, his supervision, his always judicious remarks, and his careful proofreading have greatly improved the quality of the formal analysis and brought the necessary observations of the project. The authors have read and accepted the published version of the manuscript.

Acknowledgments

The authors of this paper would first like to sincerely thank the National Aeronautics and Space Administration (NASA)/Goddard Space Flight Center (GSFC) for making available to them the wind speed and wind direction data that were used in carrying out this work. In addition, the authors wish to sincerely thank the team of the Laboratory of Energy and Environment of the Faculty of Sciences, in particular, the Department of Physics of the University of Yaoundé I, for their constant support, their encouragement, and their wise advice and experience in this job.

References

- [1] V. G. Gormo, D. K. Kidmo, B. P. Ngoussandou, B. Bogno, D. Raidandi, and M. Aillerie, "Wind power as an alternative to sustain the energy needs in Garoua and Guider, North Region of Cameroon," *Energy Reports*, vol. 7, pp. 814–829, 2021.
- [2] D. K. Kidmo, B. Bogno, M. Aillerie, and K. Deli, "Technical and economic potentialities of the development of electric wind pumping systems in the North Region of Cameroon," *International Association of Energy, Environment and Economy*, vol. 2, no. 1, 2021 <http://globalpublisher.org/journals-1006/>.
- [3] D. K. Kidmo, B. Bogno, K. Deli, M. Aillerie, and B. P. Ngoussandou, "Economic assessment of WECS for water pumping systems in the North Region of Cameroon," *Renewable Energy Environmental Sustainability*, vol. 6, no. 6, 2021.
- [4] N. A. Arreyndip, J. Eboenow, and D. Afungchui, "Wind energy potential assessment of Cameroon's coastal regions for the installation of an onshore wind farm," *Heliyon*, vol. 2, p. 187, 2016.
- [5] M. Y. Kazet, R. M. Mouangue, A. Kuitche, and J. M. Ndjaka, "Wind energy resource assessment in Ngaoundere locality. Africa-EU Renewable Energy Research and Innovation Symposium, RERIS 2016, 8-10 March 2016, Tlemcen, Algeria," *Energy Procedia*, vol. 93, pp. 74–81, 2016.
- [6] M. Dawoua, A. Sadam, and B. Miguiri, "Estimation and technico-economic analysis of the wind power potential in North of Cameroon," *Review of Materials and Renewable Energies*, vol. 5, no. 2, pp. 1–6, 2021.

- [7] D. K. Kidmo, K. Deli, D. Raidandi, and S. D. Yamigno, "Wind energy for electricity generation in the far north region of Cameroon. Africa-EU Renewable Energy Research and Innovation Symposium, RERIS 2016, 8-10 March 2016, Tlemcen, Algeria," *Energy Procedia*, vol. 93, pp. 66–77, 2016.
- [8] D. K. Kidmo, B. Bogno, M. Aillerie et al., "Assessment of wind energy potential and cost estimation of wind-generated electricity at hilltops surrounding the city of Maroua in Cameroon," *Technologies and Materials for Renewable Energy, Environment and Sustainability*, vol. 1758, no. 1, article 020012, 2016.
- [9] S. Gaddada and S. P. K. Kodicherla, "Wind energy potential and cost estimation of wind energy conversion systems (WECSs) for electricity generation in the eight selected locations of Tigray region (Ethiopia)," *Renewables: Wind, Water and Solar*, vol. 3, p. 10, 2016.
- [10] A. Gungor, M. Gokcek, H. Uçar, E. Arabaci, and A. Akyuz, "Analysis of wind energy potential and Weibull parameter estimation methods: a case study from Turkey," *International Journal of Environmental Science and Technology*, vol. 17, pp. 1011–1020, 2020.
- [11] M. Adnan, J. Ahmad, F. S. Ali, and M. Imran, "A techno-economic analysis for power generation through wind energy: a case study of Pakistan," *Energy Reports*, vol. 7, pp. 1424–1443, 2021.
- [12] S. A. Kaboli and R. Nazmabadi, "Techno-economic analysis and modeling of the feasibility of wind energy in Kuwait," *Renewable Energy Environment Sustainable*, vol. 7, no. 9, 2022.
- [13] M. A. Abdelrahman, R. H. Abdel-Hamid, M. A. A. Adma, and M. Daowd, "Techno-economic analysis to develop the first wind farm in the Egyptian Western desert at Elkharga Oasis," *Clean Energy*, vol. 6, pp. 211–225, 2022.
- [14] M. Jeutho Gouajio, P. Tiam Kapen, and D. Yemele, "Comparison of numerical methods in estimating Weibull parameters to install a sustainable wind farm in mount Bamboutos, Cameroon," *International Journal of Energy Sector Management*, vol. 15, no. 6, pp. 1033–1049, 2021.
- [15] R. M. Mouangue, M. Y. Kazet, D. Lissouck, A. Kuitche, and J. M. Ndjaka, "Potential of wind energy development for water pumping in Ngaoundere," *Journal of Fundamentals of Renewable Energy and Applications*, vol. 6, no. 198, 2015.
- [16] R. M. Mouangue, M. Y. Kazet, A. Kuitche, and J. M. Ndjaka, "Influence of the determination methods of K and C parameters on the ability of Weibull distribution to suitably estimate wind potential and electric energy," *International Journal of Renewable Energy Development*, vol. 3, no. 2, p. 145, 2014.
- [17] J. L. Nsouandele, D. K. Kidmo, S. M. Djetouda, and N. Djongyang, "Statistical estimation of wind data from the Weibull distribution for the prediction of the production of electrical energy of wind origin on Mount Tinguelin in Garoua in North Cameroon," *Journal of Renewable Energies*, vol. 19, no. 2, pp. 291–301, 2016.
- [18] R. H. Tonsie Djiela, P. Tiam Kapen, and G. Tchien, "Wind energy of Cameroon by determining Weibull parameters: potential of an environmentally friendly energy," *International Journal of Environmental Science and Technology*, vol. 18, no. 8, pp. 2251–2270, 2021.
- [19] P. Tiam Kapen, M. Jeutho Gouajio, and D. Yemele, "Analysis and efficient comparison of ten numerical methods in estimating Weibull parameters for wind energy potential: applications to the city of Bafoussam, Cameroon," *Renewable Energy*, vol. 159, pp. 1188–1198, 2020.
- [20] J. Feng, L. Feng, J. Wang, and C. W. King, "Evaluation of the onshore wind energy potential in mainland China-based on GIS modeling and EROI analysis," *Resources, Conservation and Recycling*, vol. 152, article 104484, 2020.
- [21] M. A. Baseer, S. Rehman, J. P. Meyer, and M. M. Alam, "GIS-based site suitability analysis for wind farm development in Saudi Arabia," *Energy*, vol. 141, pp. 1166–1176, 2017.
- [22] J. Xu, X. Song, Y. Wu, and Z. Zeng, "GIS-modelling based coal-fired power plant site identification and selection," *Applied Energy*, vol. 159, pp. 520–539, 2015.
- [23] K. Atici, A. Simsek, A. Ulucan, and M. Tosun, "A GIS-based multiple criteria decision analysis approach for wind power plant site selection," *Utilities Policy*, vol. 37, pp. 86–96, 2015.
- [24] D. Latinopoulos and K. Kechagia, "A GIS-based multi-criteria evaluation for wind farm site selection. A regional scale application in Greece," *Renewable Energy*, vol. 78, pp. 550–560, 2015.
- [25] S. H. Siyal, U. Mörtberg, D. Mentis, M. Welsch, I. Babelon, and M. Howells, "Wind energy assessment considering geographic and environmental restrictions in Sweden: a GIS-based approach," *Energy*, vol. 83, pp. 447–461, 2015.
- [26] O. A. Omitaomu, B. R. Blevins, W. C. Jochem et al., "Adapting a GIS-based multicriteria decision analysis approach for evaluating new power generating sites," *Applied Energy*, vol. 96, pp. 292–301, 2012.
- [27] S. M. Ali, A. S. Mahdi, and A. H. Shaban, "Wind speed estimation for Iraq using several spatial interpolation methods," *British Journal of Science*, vol. 7, no. 2, pp. 48–55, 2012.
- [28] R. Van Haaren and V. Fthenakis, "GIS-based wind farm site selection using spatial multi-criteria analysis (SMCA): evaluating the case for New York State," *Renewable and Sustainable Energy Reviews*, vol. 15, no. 7, pp. 3332–3340, 2011.
- [29] B. Sliz-Szkliniarz and J. Vogt, "GIS-based approach for the evaluation of wind energy potential: a case study for the Kujawsko-Pomorskie Voivodeship," *Renewable and Sustainable Energy Reviews*, vol. 15, no. 3, pp. 1696–1707, 2011.
- [30] J. Hossain, V. Sinha, and V. V. N. Kishore, "A GIS based assessment of potential for windfarms in India," *Renewable Energy*, vol. 36, no. 12, pp. 3257–3267, 2011.
- [31] J. R. Janke, "Multicriteria GIS modelling of wind and solar farms in Colorado," *Renewable Energy*, vol. 35, no. 10, pp. 2228–2234, 2010.
- [32] N. Aydin, E. Kentel, and S. Duzgun, "GIS-based environmental assessment of wind energy systems for spatial planning: a case study from Western Turkey," *Renewable and Sustainable Energy Reviews*, vol. 14, no. 1, pp. 364–373, 2010.
- [33] S. M. J. Baban and T. Parry, "Developing and applying a GIS-assisted approach to locating wind farms in the UK," *Renewable Energy*, vol. 24, no. 1, pp. 59–71, 2001.
- [34] G. Aminiria, S. Mafi, and S. Mazaheri, "Offshore wind resource assessment of Persian Gulf using uncertainty analysis and GIS," *Renewable Energy*, vol. 113, pp. 915–929, 2017.
- [35] D. K. Kidmo, R. Danwe, N. Njongyang, and S. Y. Doka, "Comparison of five numerical methods for estimating Weibull parameters for wind energy applications in the district of Kousseri, Cameroon," *Asian Journal Natural Applied Science*, vol. 3, no. 1, pp. 72–87, 2014.
- [36] D. K. Kidmo, R. Danwe, S. Y. Doka, and N. Njongyang, "Statistical analysis of wind speed distribution based on six Weibull methods for wind power evaluation in Garoua, Cameroon," *Renewable Energy Review*, vol. 18, no. 1, pp. 105–125, 2015.

- [37] O. S. Ohunakin, "Assessment of wind energy resources for electricity generation using WECS in North-Central region, Nigeria," *Renewable and Sustainable Energy Reviews*, vol. 15, no. 4, pp. 1968–1976, 2011.
- [38] O. S. Ohumakin, M. S. Adaramola, and O. M. Oyewola, "Wind energy evaluation for electricity generation using WECS in seven selected locations in Nigeria," *Applied Energy*, vol. 88, no. 9, pp. 3197–3206, 2011.
- [39] R. Gelaro, W. McCarty, M. J. Suárez et al., "MERRA-2 overview: the modern-era retrospective analysis for research and applications, Version 2 (MERRA2)," *Journal of Climate*, vol. 30, no. 14, pp. 5419–5454, 2017.
- [40] A. Albani and M. Ibrahim, "Wind energy potential and power law indexes assessment for selected near-coastal sites in Malaysia," *Energy*, vol. 10, no. 3, p. 307, 2017.
- [41] V. M. Aboobacker, P. R. Shanass, S. Veerasingam, E. M. Al-Ansari, F. N. Sadooni, and P. Vethamony, "Long term assessment of onshore and offshore wind energy potentials of Qatar," *Energies*, vol. 14, no. 4, p. 1178, 2021.
- [42] D. K. Kidmo, B. Bogno, K. Deli, and D. Goron, "Seasonal wind characteristics and prospects of wind energy conversion systems for water production in the Far North Region of Cameroon," *Smart Grid and Renewable Energy*, vol. 11, no. 9, pp. 127–164, 2020.
- [43] M. H. Soulouknga, S. Y. Doka, N. Revanna, N. Djongyang, and T. C. Kofane, "Analysis of wind speed data and wind energy potential in Faya-Largeau, Chad, using Weibull distribution," *Renewable Energy*, vol. 121, pp. 1–8, 2018.
- [44] M. D. Dogara, H. O. Aboh, P. M. Gyuk, and M. K. O. Onwumere, "The use of energy pattern factor (EPF) in estimating wind power density," *Science World Journal*, vol. 11, no. 3, pp. 27–30, 2016, <http://www.scienceworldjournal.org/>.
- [45] J. A. Guarienti, A. Kaufmann Almeida, A. Menegati Neto, A. R. de Oliveira Ferreira, J. P. Ottonelli, and I. de Almeida Kaufmann, "Performance analysis of numerical methods for determining Weibull distribution parameters applied to wind speed in Mato Grosso do Sul, Brazil," *Sustainable Energy Technology Assessments*, vol. 42, article 100854, 2020.
- [46] H. G. Kim, J. Y. Kim, and Y. H. Kang, "Comparative evaluation of the third generation reanalysis data for wind resource assessment of the Southwestern offshore in South Korea," *Atmosphere Journal*, vol. 9, no. 2, p. 73, 2018.
- [47] G. I. S. Geography, "Inverse distance weighting (IDW) interpolation," 2020, (<https://gisgeography.com/inverse-distance-weighting-idw-interpolation/>), last access [August 10, 2022].
- [48] D. Shepard, "A two-dimensional interpolation function for irregularly-spaced data," in *Proceedings of the 1968 23rd ACM national conference*, New York, 1968.
- [49] D. Duplyakin, S. Zisman, C. Phillips, and H. Tinneland, *Bias characterization, vertical interpolation, and horizontal interpolation for distributed wind siting using mesoscale wind resource estimates*, National Renewable Energy Laboratory, Golden, CO (United States), 2021, NREL/TP-2C00-78412, available at: (<https://www.nrel.gov/docs/fy21osti/78412.pdf>), lastaccess [April 30, 2022].
- [50] M. Irwanto, N. Gomesh, M. R. Mamat, and Y. M. Yusoff, "Assessment of wind power generation potential in Perils, Malaysia," *Renewable and Sustainable Energy Reviews*, vol. 38, pp. 296–308, 2014.
- [51] S. A. Akdağ and A. Dinler, "A new method to estimate Weibull parameters for wind energy applications," *Energy Conversion and Management*, vol. 50, no. 7, pp. 1761–1766, 2009.
- [52] NOAA, "Wind Energy Resource Atlas of the United States," 1976, http://rredc.nrel.gov/wind/pubs/atlas/appendix_A.html (8 of 24).
- [53] L. Lu, H. Yang, and J. Burnett, "Investigation on wind power potential on Hong Kong Islands—an analysis of wind power and wind turbine characteristics," *Renewable Energy*, vol. 27, no. 1, pp. 1–12, 2002.
- [54] A. G. Lira, P. A. C. Rosas, A. M. Arajo, and N. J. Castro, "Uncertainties in the estimate of wind energy production," in *Proceedings of the Energy Economics Iberian Conference—EEIC*, Lisboa, Portugal, 2012.
- [55] T. R. Ayodele, A. A. Jimoh, J. L. Munda, and J. T. Agee, "Viability and economic analysis of wind energy resource for power generation in Johannesburg, South Africa," *International Journal of Sustainable Energy*, vol. 33, no. 2, pp. 284–303, 2013.
- [56] H. Faïda, J. Saadi, M. Khaider, S. El Alami, and M. Monkade, "Study and analysis of wind data in order to size a wind energy production system: case of a site in Northern Morocco," *Journal of Renewable Energies*, vol. 13, no. 3, pp. 477–483, 2010.
- [57] Z. H. Hulio, W. Jiang, and S. Rehman, "Technical and economic assessment of wind power potential of Nooriabad, Pakistan," *Energy Sustainability and Society*, vol. 7, no. 1, p. 35, 2017.
- [58] K. Sukkiramathi and C. V. Seshaiyah, "Analysis of wind power potential by the three parameter Weibull distribution to install a wind turbine," *Energy Exploration and Exploitation*, vol. 38, no. 1, pp. 158–174, 2020.
- [59] A. Mostafaeipour, A. Sedaghat, A. Dehghanniri, and V. Kalantar, "Wind energy feasibility study for City of Shahrabak in Iran," *Renewable and Sustainable Energy Reviews*, vol. 15, no. 6, pp. 2545–2556, 2011.
- [60] J. F. Touafio Ngbara, S. Oumarou, S. Malenguiza, M. Y. Kazet, J. M' Boliguipa, and R. M. Mouangue, "Analysis of a wind turbine project in the city of Bouar (Central African Republic)," *Scientific African*, vol. 8, p. 354, 2020.
- [61] H. A. Moria, S. Salehin, M. N. Alghamdi, and A. K. M. Sadrul Islam, "Assessment of Wind Characteristics and Electricity Generation Potential for Yanbu, Saudi Arabia," *Assessment*, vol. 8, no. 11, 2014.
- [62] Y. Kassem, H. Gökçekuş, and H. Çamur, "Effects of climate characteristics on wind power potential and economic evaluation in Salamis Region, Northern Cyprus," *International Journal of Applied Environmental Sciences*, vol. 13, no. 3, pp. 287–307, 2018.
- [63] Y. Kassem, H. Çamur, and S. M. Alhuoti, "Solar energy technology for Northern Cyprus: assessment, statistical analysis, and feasibility study," *Energies*, vol. 13, no. 4, p. 940, 2020.
- [64] S. Diaf, G. Notton, and D. Diaf, "Technical and economic assessment of wind farm power generation at Adrar in Southern Algeria," *Energy Procedia*, vol. 42, pp. 53–62, 2013.
- [65] M. S. Adaramola, O. M. Oyewola, O. S. Ohumakin, and O. O. Akinnawonu, "Performance evaluation of wind turbines for energy generation in Niger Delta, Nigeria," *Sustainable Energy Technologies and Assessments*, vol. 6, pp. 75–85, 2014.
- [66] M. Jamil, S. Parsa, and M. Majidi, "Wind power statistics and an evaluation of wind energy density," *Renewable Energy*, vol. 6, no. 5–6, pp. 623–638, 1995.
- [67] H. Ritchie, M. Roser, and P. Rosado, "Cameroon : CO₂ country profile: CO₂ and greenhouse gas emissions. Cameroon:

- Carbon Intensity: How Much Carbon Does It Emit per Unit of Energy ?. Our World in Data,” 2020, <https://ourworldindata.org/co2-and-other-greenhouse-gas-emissions>.
- [68] R. Pallabazzer, “Evaluation of wind-generator potentiality,” *Solar Energy*, vol. 55, no. 1, pp. 49–59, 1995.
- [69] R. Pallabazzer and A. A. Gabow, “Wind generator potentiality in Somalia,” *International Journal of Renewable Energy*, vol. 2, no. 4-5, pp. 353–361, 1992.
- [70] “Decision N°_0096_/ARSEL/DG/DCEC/SDCT DU_28 may 2012_ fixing the sales tariffs excluding electricity taxes applicable by the Company Eneo Cameroon from the Year 2012,” <https://www.eneocameroon.cm/index.php/fr/prepaye.pdf>.
- [71] G. Aminiria, B. Kamranzad, and S. Mafi, “Wind and wave energy potential in Southern Caspian Sea using uncertainty analysis,” *Energy*, vol. 120, pp. 332–345, 2017.
- [72] P. Quan and T. Leephakpreeda, “Assessment of wind energy potential for selecting wind turbines: an application to Thailand,” *Sustainable Energy Technologies and Assessments*, vol. 11, pp. 17–26, 2015.
- [73] C. Hubler, W. Weijtjens, R. Rolfes, and C. Devriendt, “Reliability analysis of fatigue damage extrapolations of wind turbines using offshore strain measurements,” *Journal of Physics: Conference Series*, vol. 1037, article 032035, 2018.
- [74] H. S. Toft, L. Svenningsen, J. D. Sørensen, W. Moser, and M. L. Thøgersen, “Uncertainty in wind climate parameters and their influence on wind turbine fatigue loads,” *Renewable Energy*, vol. 90, pp. 352–361, 2016.
- [75] L. Ziegler, S. Schafhirt, M. Scheu, and M. Muskulus, “Effect of load sequence and weather seasonality on fatigue crack growth for monopile-based offshore wind turbines,” *Energy Procedia*, vol. 94, pp. 115–123, 2016.
- [76] A. Kavousi-Fard, M.-R. Akbari-Zadeh, F. Kavousi-Fard, and M.-A. Rostami, “Effect of wind turbine on the economic load dispatch problem considering the wind speed uncertainty,” *Journal of intelligent & Fuzzy Systems*, vol. 28, no. 2, pp. 693–705, 2015.
- [77] E. B. Mora, J. Spelling, A. H. Van der Weijde, and E.-M. Pavageau, “The effects of mean wind speed uncertainty on project finance debt sizing for offshore wind farms,” *Applied Energy*, vol. 252, article 113419, 2019.
- [78] P. Rotela Junior, E. Fischetti, V. G. Araújo et al., “Wind power economic feasibility under uncertainty and the application of ANN in sensitivity analysis,” *Energies*, vol. 12, no. 12, p. 2281, 2019.
- [79] C. Cheng, N. P. Gutierrez, A. Blakers, and M. Stocks, “GIS-based solar and wind resource assessment and least-cost 100% renewable electricity modelling for Bolivia,” *Energy for Sustainable Development*, vol. 69, no. 1, pp. 134–149, 2022.
- [80] E. Tercan, “Land suitability assessment for wind farms through best-worst method and GIS in Balıkesir province of Turkey,” *Sustainable Energy Technologies and Assessments*, vol. 47, no. 7, article 101491, 2021.
- [81] X. Liu, B. Huang, R. Li et al., “Wind environment assessment and planning of urban natural ventilation corridors using GIS: Shenzhen as a case study,” *Urban Climate*, vol. 42, article 101091, 2022.
- [82] I. C. Gil-Garcia, A. Ramos-Escudero, M. S. Garcia-Cascales, H. Dagher, and A. Molina-Garcia, “Fuzzy GIS-based MCDM solution for the optimal offshore wind site selection: the Gulf of Marine case,” *Renewable Energy*, vol. 188, pp. 130–147, 2022.
- [83] I. Pakere, M. Kacare, A. Grāvelsiņš, R. Freimanis, and A. Blumberga, “Spatial analyses of smart energy system implementation through system dynamics and GIS modelling. Wind power case study in Latvia,” *Smart Energy*, vol. 7, no. 22, article 100081, 2022.
- [84] S. Cavazzi and A. G. Datton, “An offshore wind energy geographic information system (OWE-GIS) for assessment of the UK’s offshore wind energy potential,” *Renewable Energy*, vol. 87, pp. 212–228, 2016.
- [85] P. Elsner, “Continental-scale assessment of the African offshore wind energy potential: spatial analysis of an underappreciated renewable energy resource,” *Renewable and Sustainable Energy Reviews*, vol. 104, pp. 394–407, 2019.
- [86] S. Gadad and P. C. Deka, “Offshore wind power resource assessment using Oceansat-2 scatterometer data at a regional scale,” *Applied Energy*, vol. 176, pp. 157–170, 2016.